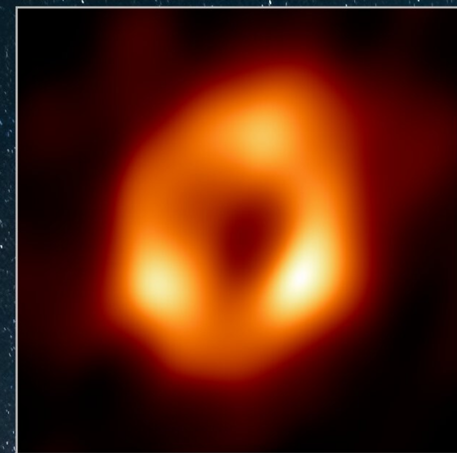

Detecting Dark Matter with the Multi-Messenger Observations of Supermassive Black Holes

Guan-Wen Yuan (袁官文)

Department of Physics, University of Trento;
Trento Institute for Fundamental Physics and Applications (TIFPA) - *INFN*.

July/8/2025@ICRANet, Pescara

Outline

- Part I: Detecting WIMP Annihilation and ALP Polarization Oscillation with EHT Observation
  - Searching for the signal of WIMP annihilation in the shadow of M87*.*[JHEP(2022)]*
  - Detecting the ALP induced polarization oscillation with the observations of Sagittarius A*. *[JCAP(2021)]*

- Part II: Searching for ULDM and WIMP Spike with S-star Kinematics Observed by Keck/VLT
  - Constraining properties of ULDM with Keck Observations of S2's Orbit. *[PRD(2022)]*
  - Exploring WIMP-spike distribution around GC with S-stars. *[MNRAS(2024)]*

- Part III: Rapidly Growing PBHs seeded the massive Galaxies in high-redshift Observations. *[SCPMA(2024)]*

- Part IV: Exploring DM distribution with nanohertz stochastic gravitational wave background. *[PDU(2025)]*

Motivation:

when a strong gravitational field is present around an SMBH, dark matter with gravitational interactions can congregate and create an environment that is far more dense than it would be in other regions.

Observational Evidences of Dark Matter in Astronomy/Cosmology

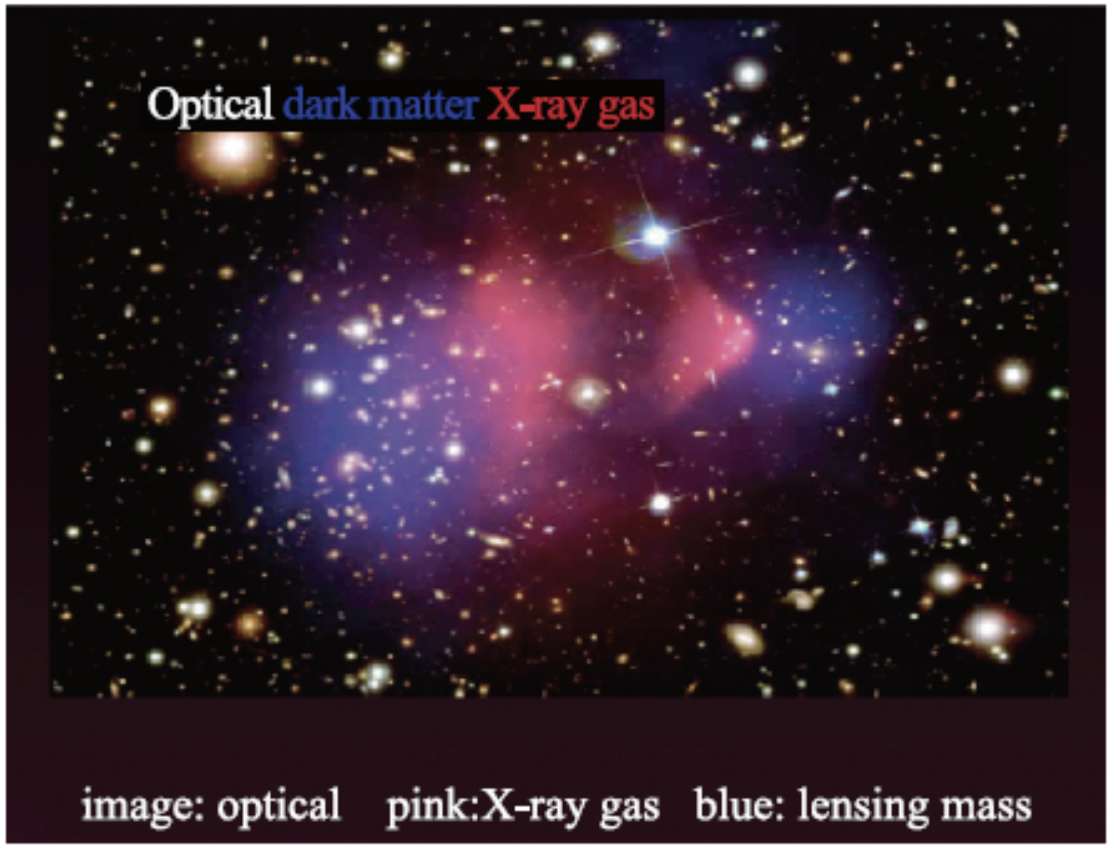

Collisions of Galaxy Clusters

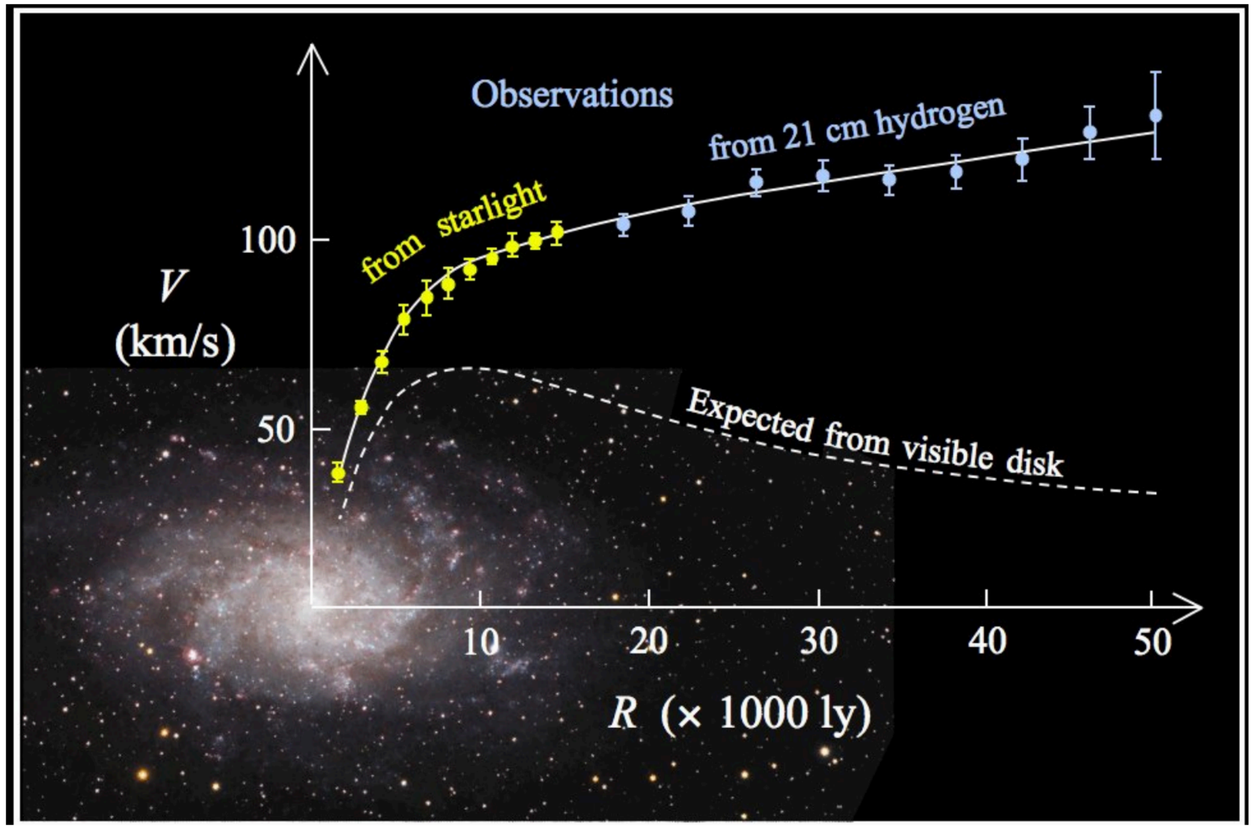

Galactic Rotation Curve

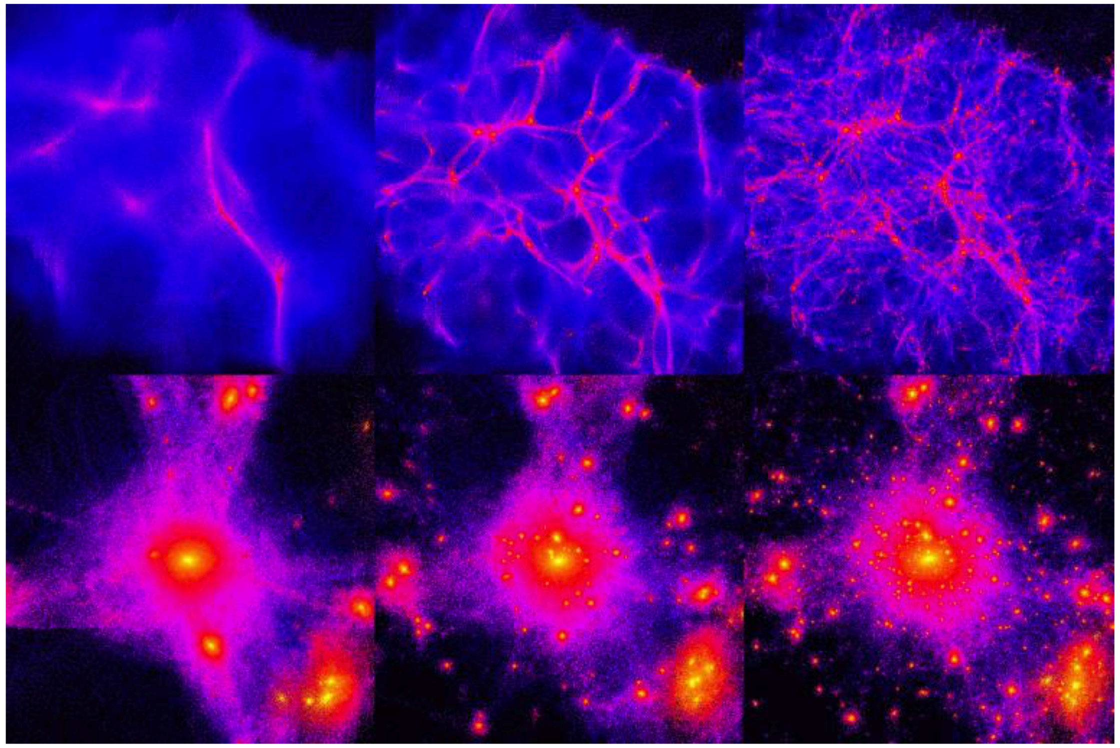

Large Scale Structure

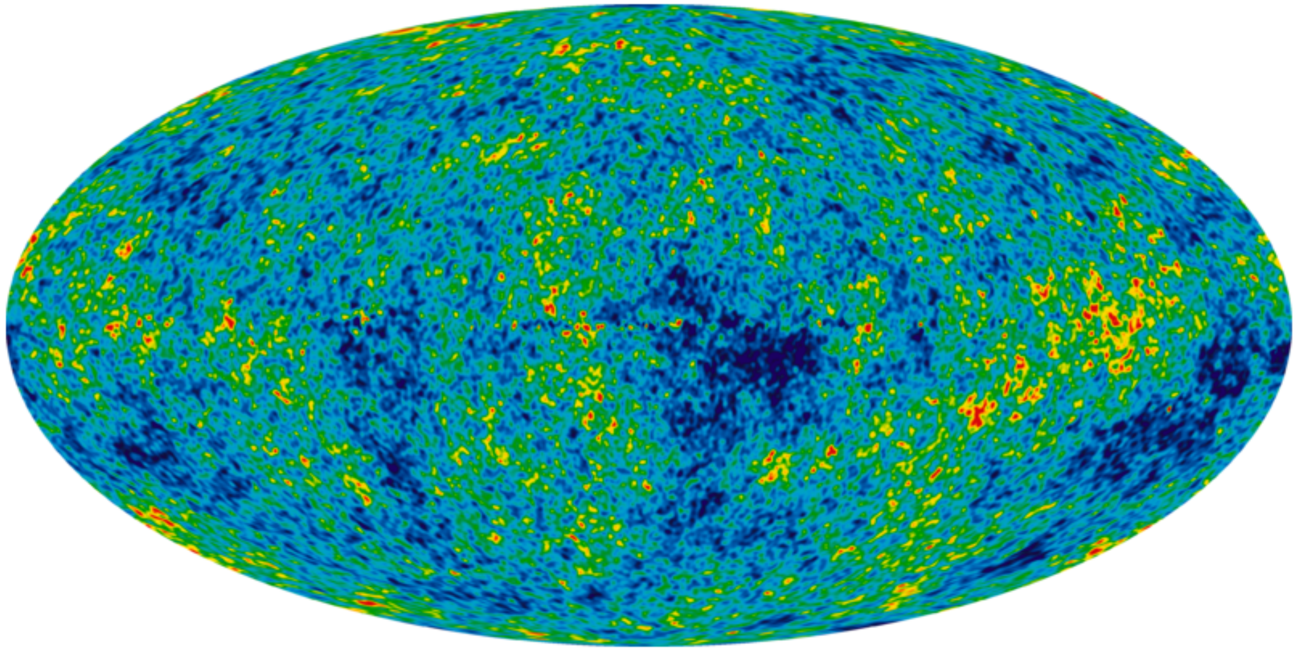

Cosmic Microwave Background

“Classical” Dark Matter Candidates and Their Observational Effect

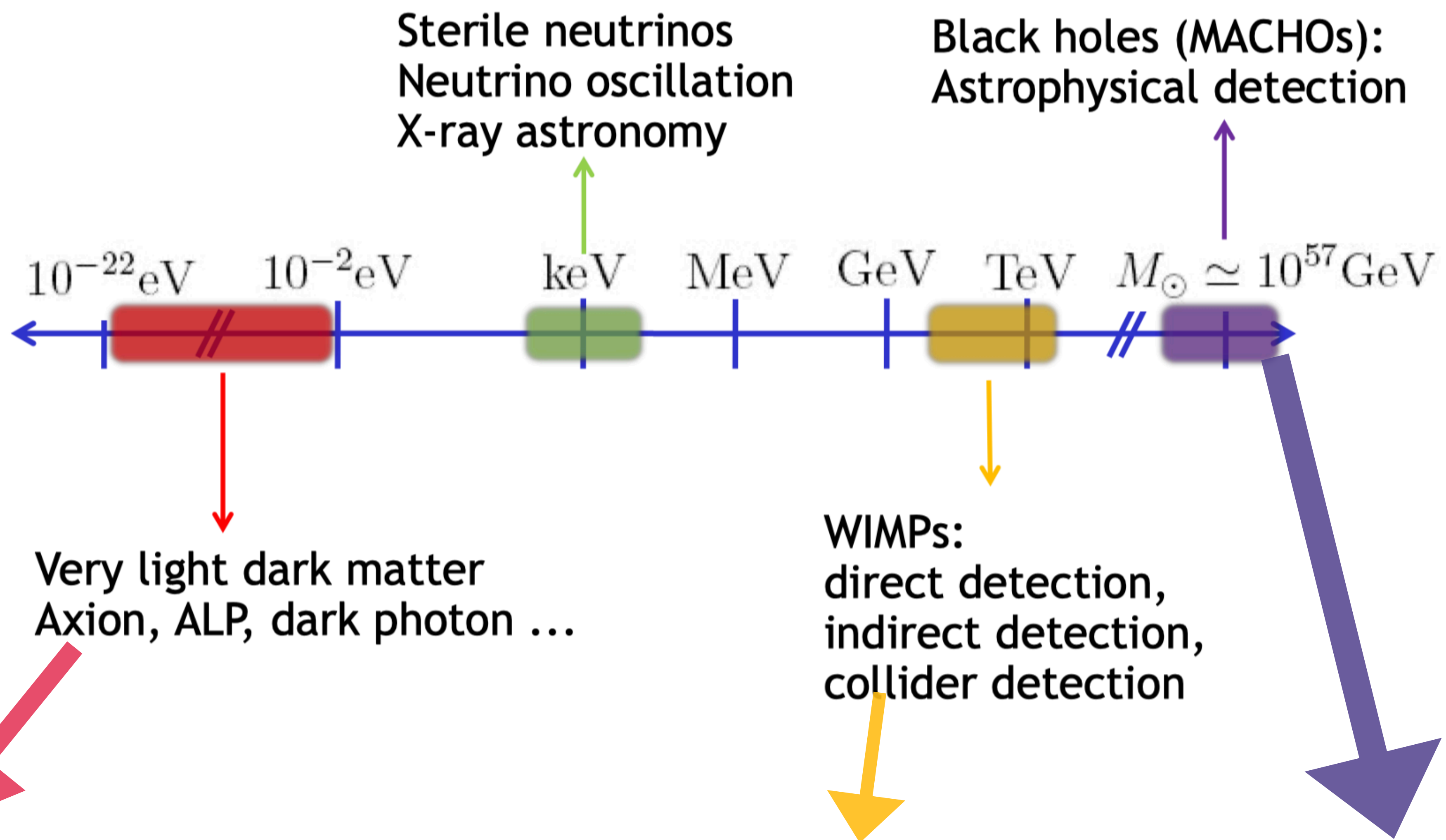

(a) Light dark matter exists in the form of waves, and is expected to form structures such as soliton core, super-radiance around SMBH.
(b) It may affect polarization observations, orbit kinematics, atomic spectrum and so on.

(a) The numerical simulation does not take into account the strong gravitation induced by SMBH in small scales, which will accrete dark matter particles to form ‘spikes’.
(b) The dense WIMPs annihilate into e^+e^- and generate synchrotron radiation, and modulate spectrum energy distribution(SED).

(a) The distribution of primordial black holes that formed in the early universe is different from that of produced by astrophysical processes.
(b) JWST high redshift galaxy observations and gravitational wave observations provide a new way to study PBH.

Part I: Detecting WIMP Annihilation and ALP Polarization Oscillation with EHT Observation

- Searching for the Signal of WIMP Annihilation in the Shadow of M87*
  A. The Distribution of WIMP Around SMBH
  B. Propagation and Radiation of Electron Around SMBH
  C. M87* Limitation for Different WIMP Annihilation Channels
- Detecting the ALP induced polarization oscillation with the observations of Sagittarius A*
  D. Axion/ALP Birefringence Effect
  E. Soliton Core+NFW Dark Matter Profile
  F. Data Analysis and Results

Event Horizon Telescope (EHT)

A Global Network of Radio Telescopes

2018 Observatories

- **ALMA** — Atacama Large Millimeter/submillimeter Array, CHAJNANTOR PLATEAU, CHILE
- **APEX** — Atacama Pathfinder EXperiment, CHAJNANTOR PLATEAU, CHILE
- **30-M** — IRAM 30-M Telescope, PICO VELETA, SPAIN
- **JCMT** — James Clerk Maxwell Telescope, MAUNAKEA, HAWAII
- **LMT** — Large Millimeter Telescope, SIERRA NEGRA, MEXICO
- **SMA** — Submillimeter Array, MAUNAKEA, HAWAII
- **SMT** — Submillimeter Telescope, MOUNT GRAHAM, ARIZONA
- **SPT** — South Pole Telescope, SOUTH POLE STATION
- **GLT** — The Greenland Telescope, THULE AIR BASE, GREENLAND, DENMARK

Observing in 2020

- **Kitt Peak** — Kitt Peak 12-meter Telescope, KITT PEAK, ARIZONA, USA
- **NOEMA** — NOEMA Observatory, PLATEAU DE BURE, FRANCE

Milestone Results of Event Horizon Telescope

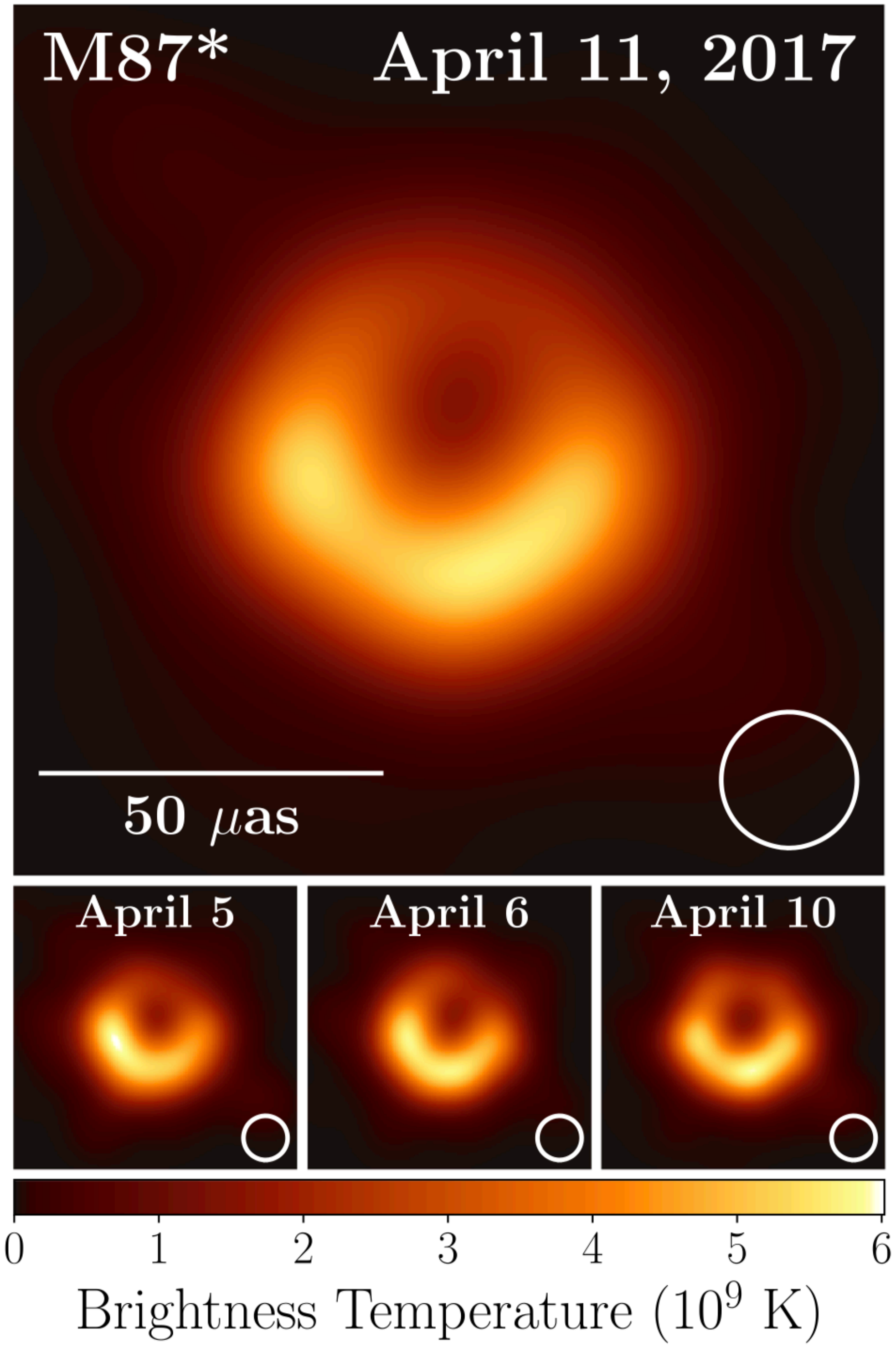

EHTC+2019

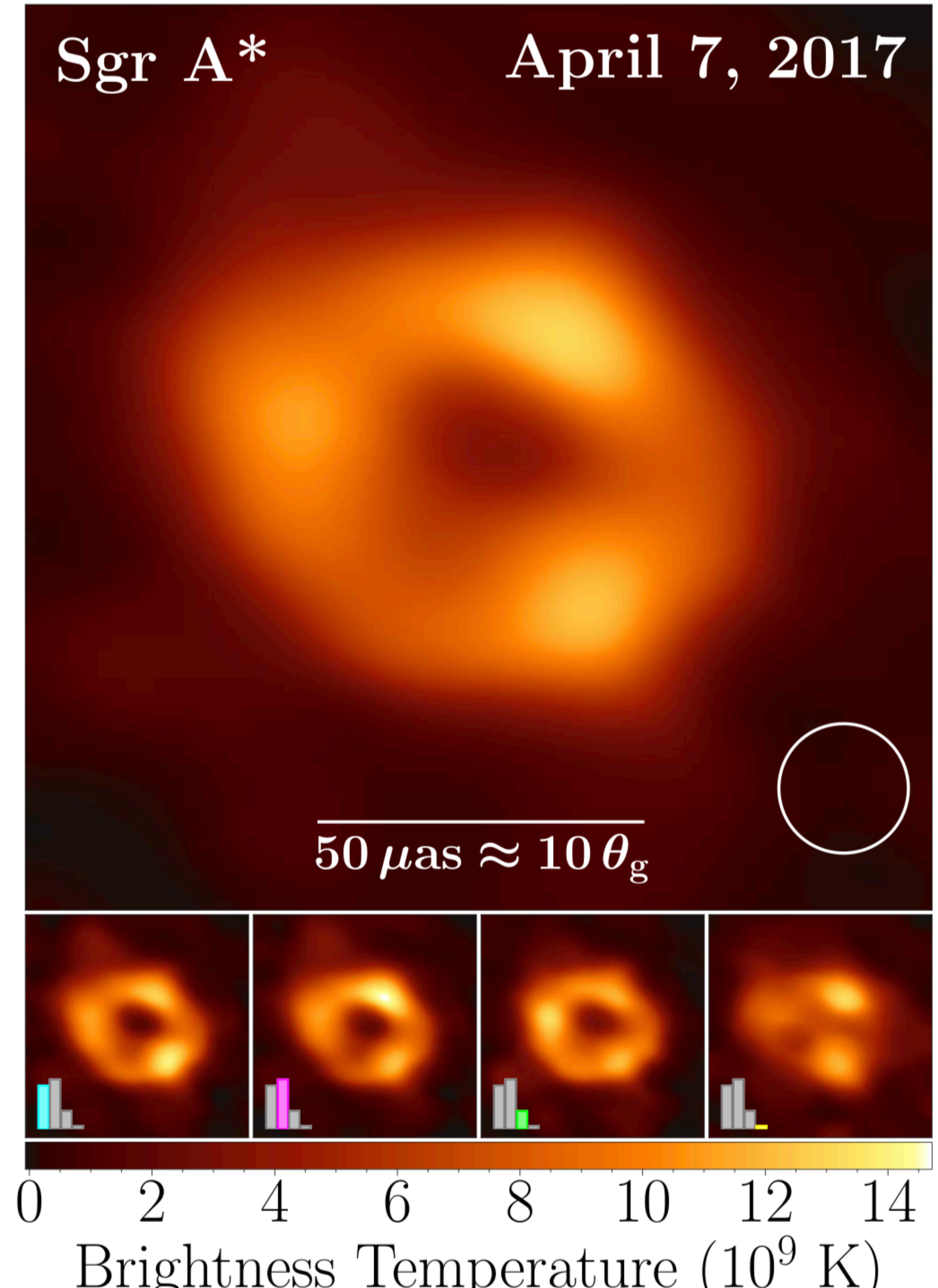

EHTC+2022

We could estimate their mass, distance, magnetic field, temperature, flux, polarization, size…..

Project1—Propagation and Radiation of Electron Around SMBH

WIMP-induced electron/positron (e^+e^-) synchrotron radiation around SMBH:

source function come from WIMP annihilation

$$q_i(r,p) = \frac{c}{4\pi p^2} Q_i(r,E) = \frac{c}{4\pi p^2} \frac{\langle \sigma v \rangle_i \rho^2(r)}{2m_\chi^2} \frac{\mathrm{d}N_{ann}}{\mathrm{d}E}(E)$$

spatial diffusion

injection term

$$-\frac{1}{r^2}\frac{\partial}{\partial r}\left[r^2 D \frac{\partial f_e}{\partial r}\right] + \boxed{v\frac{\partial f_e}{\partial r} - \frac{1}{3r^2}\frac{\partial}{\partial r}\left(r^2 v\right) p \frac{\partial f_e}{\partial p}} + \frac{1}{p^2}\frac{\partial}{\partial p}\left(\dot{p} p^2 f_e\right) = q(r,p)$$

advection current and energy gain
due to the adiabatic compression

radiative losses

Then, we have the solution of the e^+e^- propagation equation around SMBH:

$$p_{\mathrm{inj}}\left(R_{\mathrm{inj}}; r, p\right) = p\left[\frac{k_0 R_{\mathrm{Sch}}^{-\frac{1}{2}}}{c} R_{\mathrm{inj}}^{\frac{3}{2}} p \left(\frac{r}{R_{\mathrm{inj}}} - 1\right) + \left(\frac{R_{\mathrm{inj}}}{r}\right)^{\frac{1}{2}}\right]^{-1}$$

$$n_i(r,p) = \int_r^{r_{\mathrm{acc}}} \frac{Q_i\left(R_{\mathrm{inj}}, p_{\mathrm{inj}}\right)}{v(R_{inj})} \left(\frac{R_{\mathrm{inj}}}{R_{\mathrm{S}}}\right)^{\frac{5}{2}} \left(\frac{p_{\mathrm{inj}}}{p}\right)^4 \mathrm{d}R_{\mathrm{inj}}$$

Roberto Aloisio etc, Neutralino annihilation at the galactic center revisited, JCAP(2004).
Marco Regis, Piero Ullio, Multi-wavelength signals of dark matter annihilation at the Galactic center, PRD(2008).

The Distribution of WIMP Around SMBH

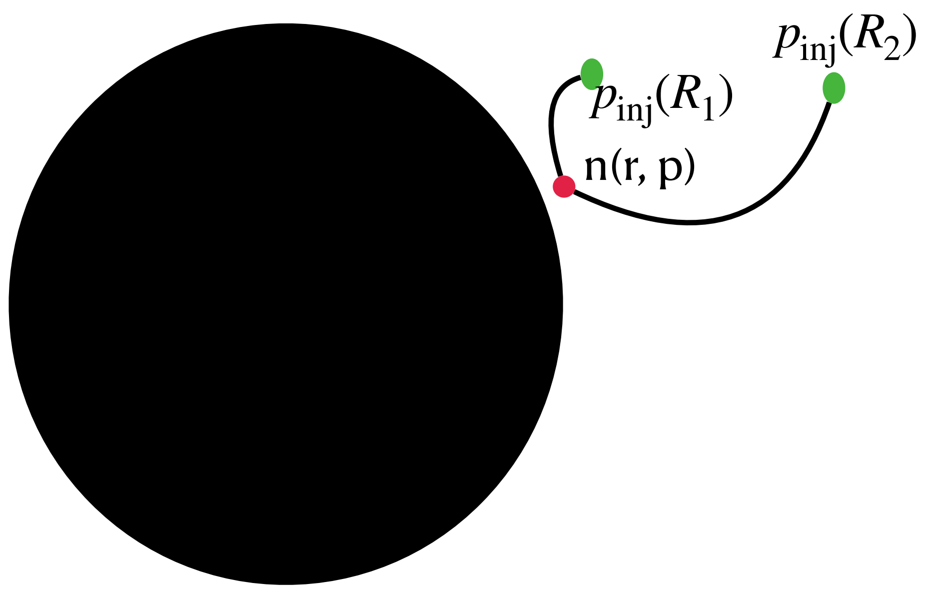

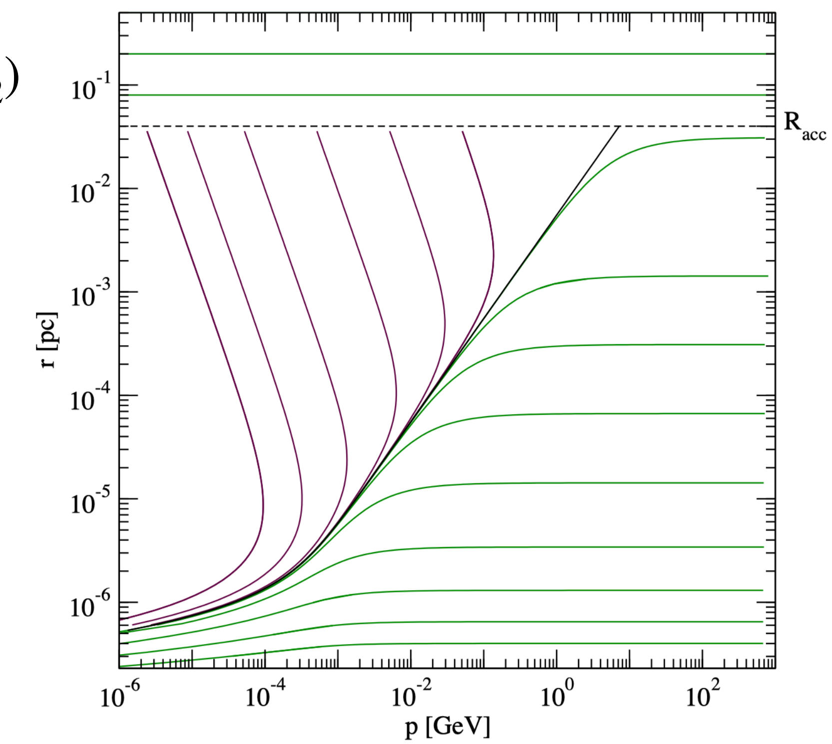

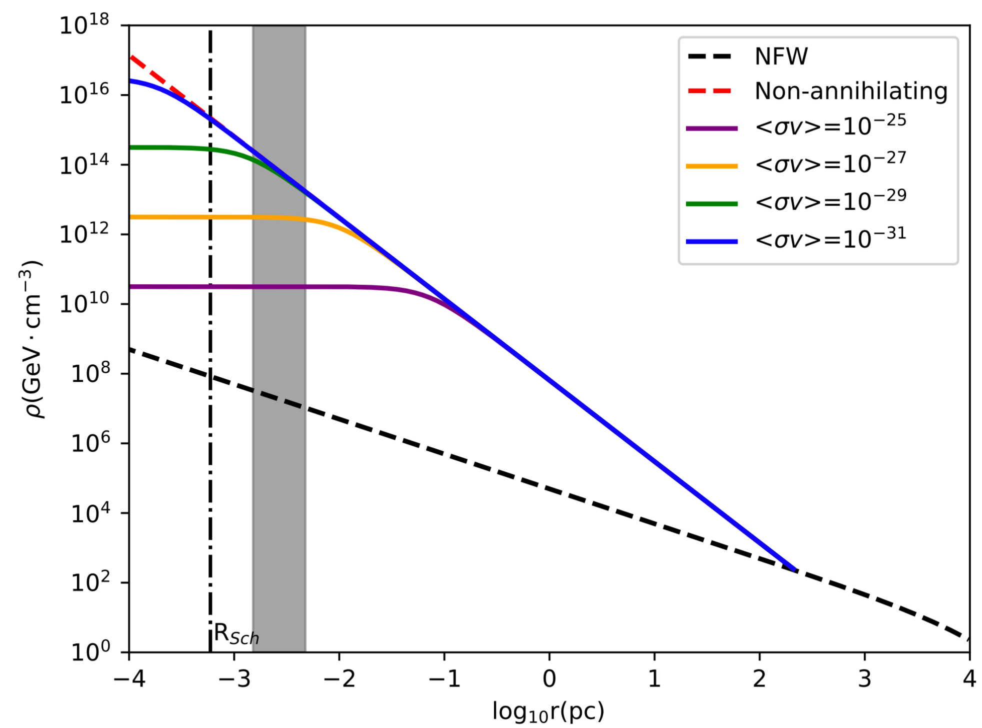

As the plasma flow onto the central BH, there are two competitive physical processes take place:
(a) the particles' momentum loss due to radiative processes;
(b) the particles gain energy in the adiabatic compression.

Due to the balance of WIMP accretion and annihilation around SMBH, we have the WIMP 'spike' distribution:

$$\rho(r) = \begin{cases} 0 & r < R_{Sch} \\ \dfrac{\rho_{sp}(r)\rho_{\rm sat}}{\rho_{\rm sp}(r)+\rho_{\rm sat}} & R_{Sch} \le r < R_{\rm sp} \\ \dfrac{\rho_0}{(r/r_0)(1+r/r_0)^2} & r \ge R_{\rm sp} \end{cases}$$

Paolo Gondolo, Joseph Silk, Dark Matter annihilation at the galactic center, PRL(1999)
Thomas Lacroix, etc, Unique probe of dark matter in the core of M87 with EHT, PRD(2017)

Flux Predicted by WIMP Annihilation

The synchrotron emissivity annihilated from WIMP per unit frequency at ν by an electron of energy E_e present in a magnetic field B is

$$P_{\rm syn}(\nu, E_e, B, \theta) = \frac{\sqrt{3} e^3 B \sin\theta}{m_{\rm e} c^2} \frac{\nu}{\nu_c} \int_{\nu/\nu_c}^{\infty} dy K_{5/3}(y) \,.$$

$$j_{\rm syn}(\nu, r) = 2 \int_{m_e}^{M_\chi} dE \langle P_{\rm syn} \rangle (\nu, E, B) n_e(r, E)$$

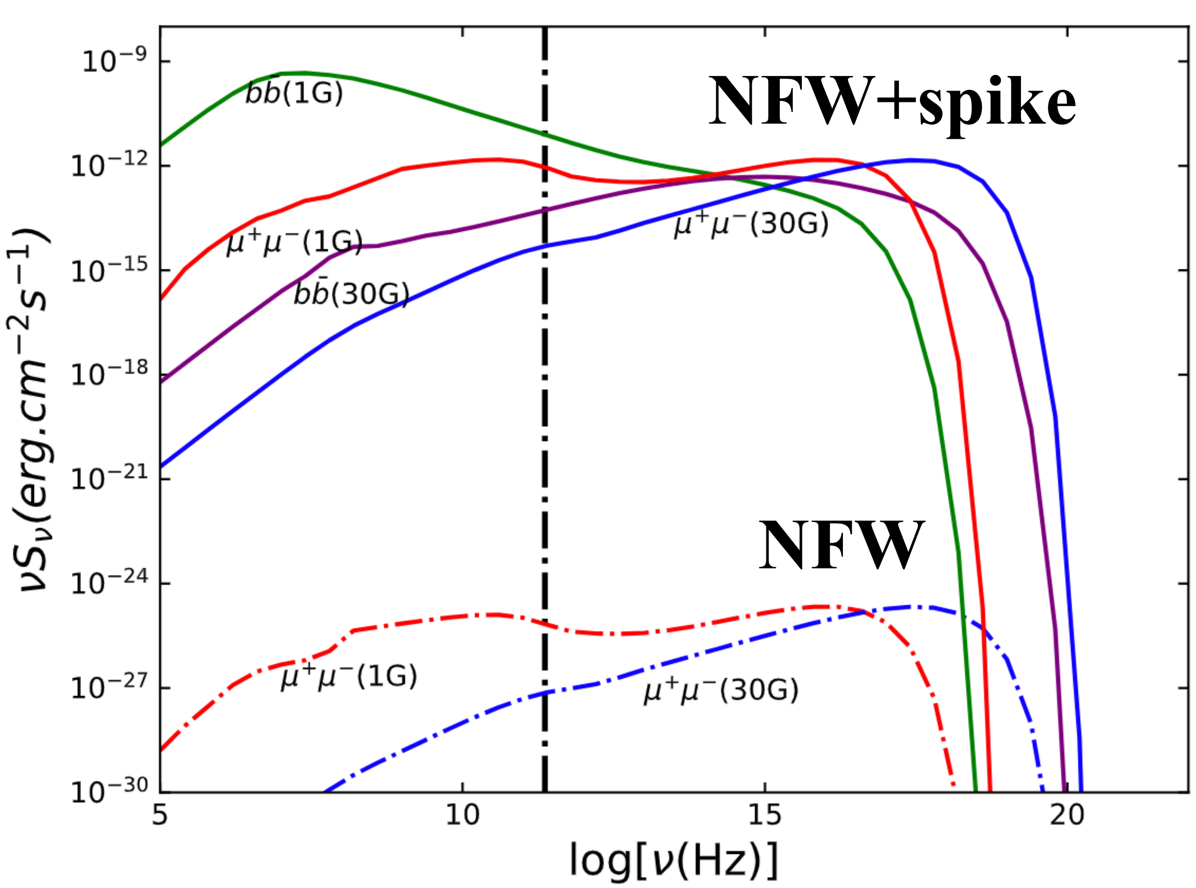

Spectra of synchrotron emission

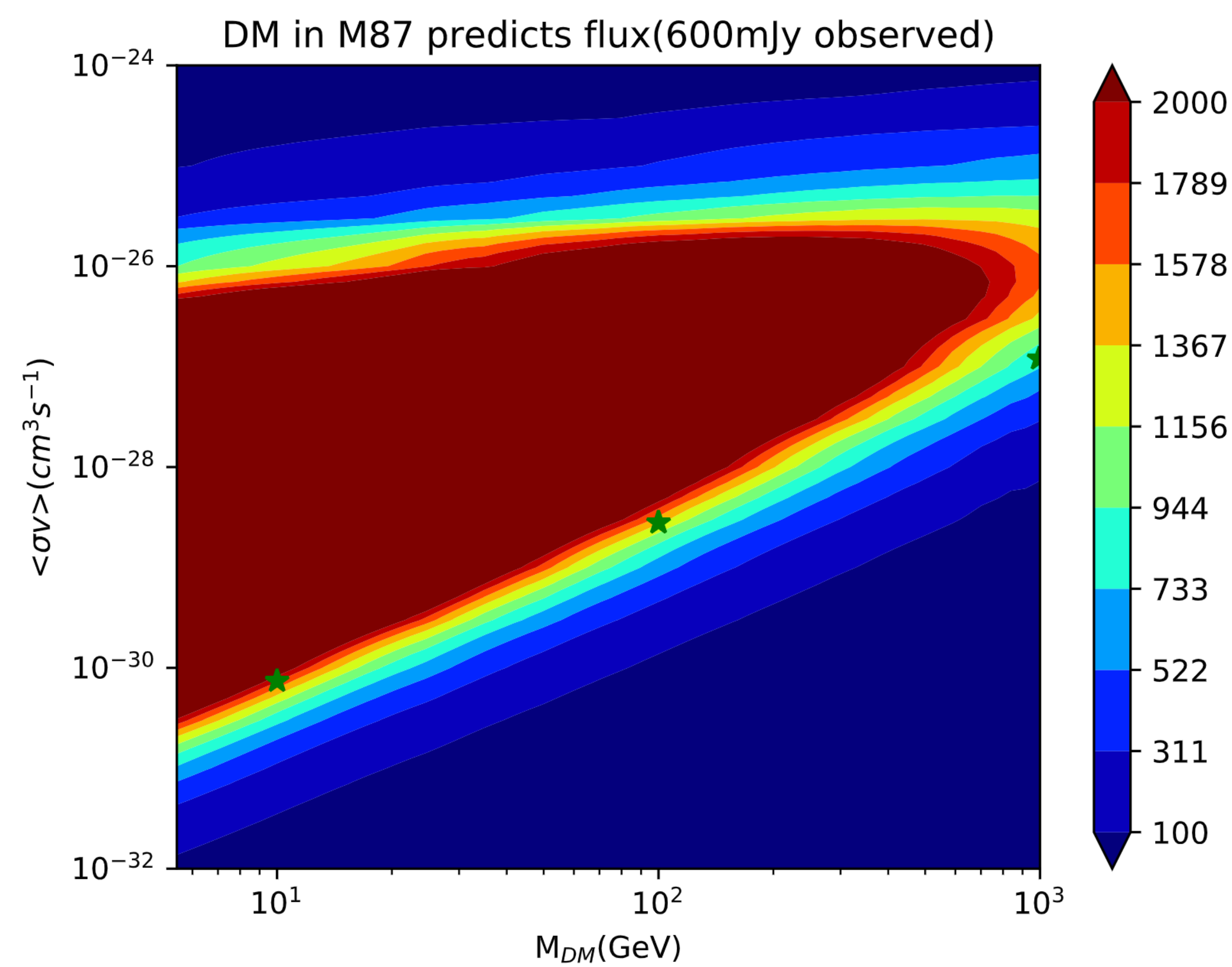

Flux predicted by WIMP annihilation around M87*

M87* Limitation for Different WIMP Annihilation Channels

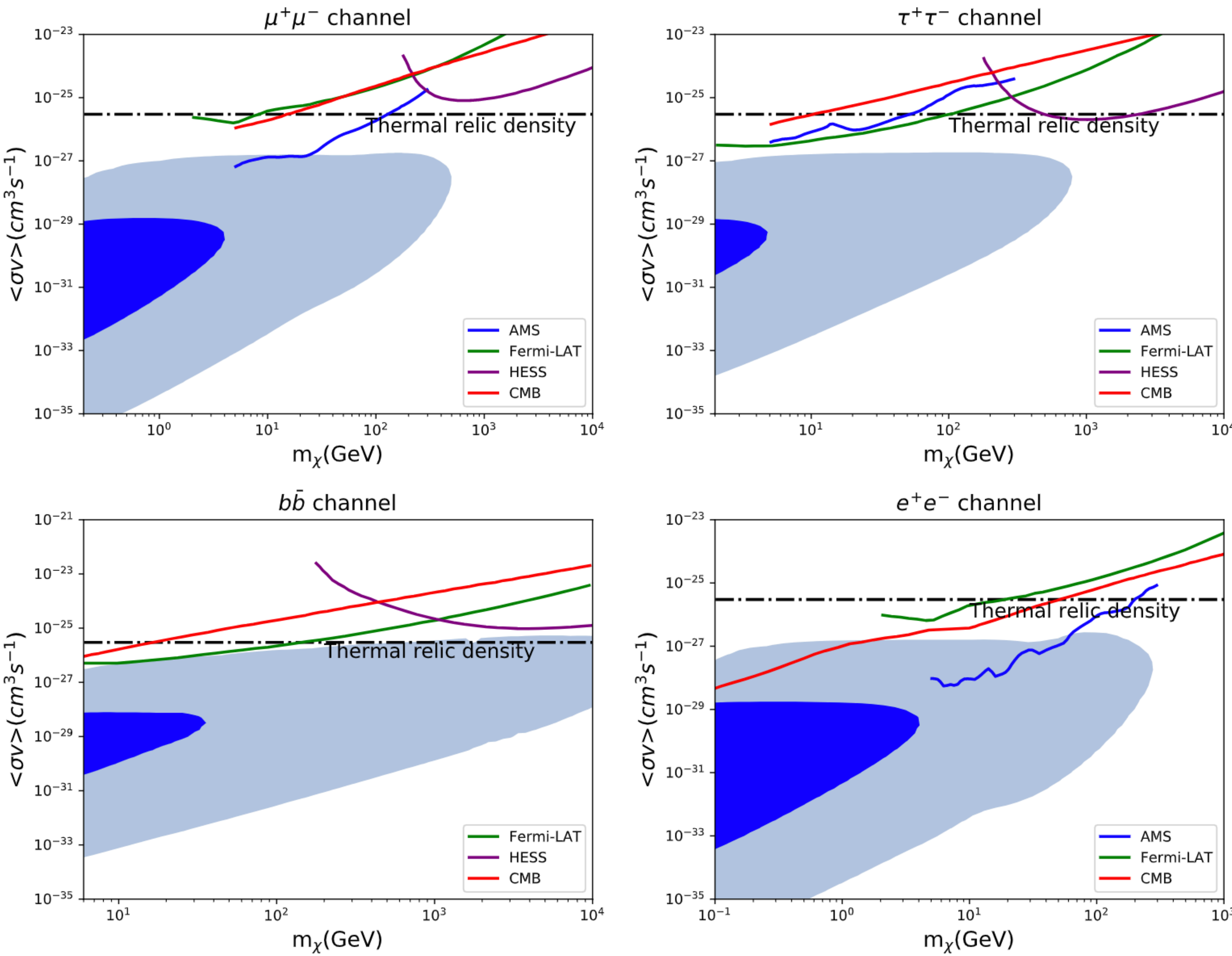

dark blue contour(30G)
light blue contour(1G)

Guan-Wen Yuan, et al, Constraints on Dark Matter Annihilation from the Event Horizon Telescope Observations of M87*, JHEP 04(2022) 018, [arXiv: 2106.05901]

Project2—Axion/ALP Birefringence Effect

The axion or axion-like particle (ALP) field can interact with the electromagnetic field and give rise to a rotation effect on the photon polarization, which is called the birefringence effect. The relevant Lagrangian terms include

$$\mathscr{L} = -\frac{1}{4}F_{\mu\nu}F^{\mu\nu} + \frac{1}{2}\left(\partial_\mu a \partial^\mu a - m^2 a^2\right) + \frac{g_{a\gamma}}{4} a F_{\mu\nu}\tilde{F}^{\mu\nu}$$

The dispersion relation of EoM induce two polarization states propagate:

$$w_\pm = k\sqrt{1 \pm \frac{g_{a\gamma}(\dot{a} + \hat{\boldsymbol{k}} \cdot \nabla a)}{k}} \approx k \boxed{\pm \frac{1}{2} g_{a\gamma} \partial_0 a}$$

The difference between the frequencies of the two polarization components is translated into the change of the polarization angle for a linearly polarized emission:

$$\Delta\phi = \frac{1}{2}\int_{t_{emit}}^{t_{obs}} \left(w_+ - w_-\right) dt = \frac{1}{2} g_{a\gamma} \int_{t_{emit}}^{t_{obs}} \partial_0 a dt = \frac{1}{2} g_{a\gamma} \left[a\left(t_{obs}, \boldsymbol{x}_{obs}\right) - a\left(t_{emit}, \boldsymbol{x}_{emit}\right)\right]$$

Where the $a(t_{obs}, \mathbf{x}_{obs})$ and $a(t_{emit}, \mathbf{x}_{emit})$ are the ALP amplitude in observation and emission points, respectively.

Soliton Core+NFW Dark Matter Profile

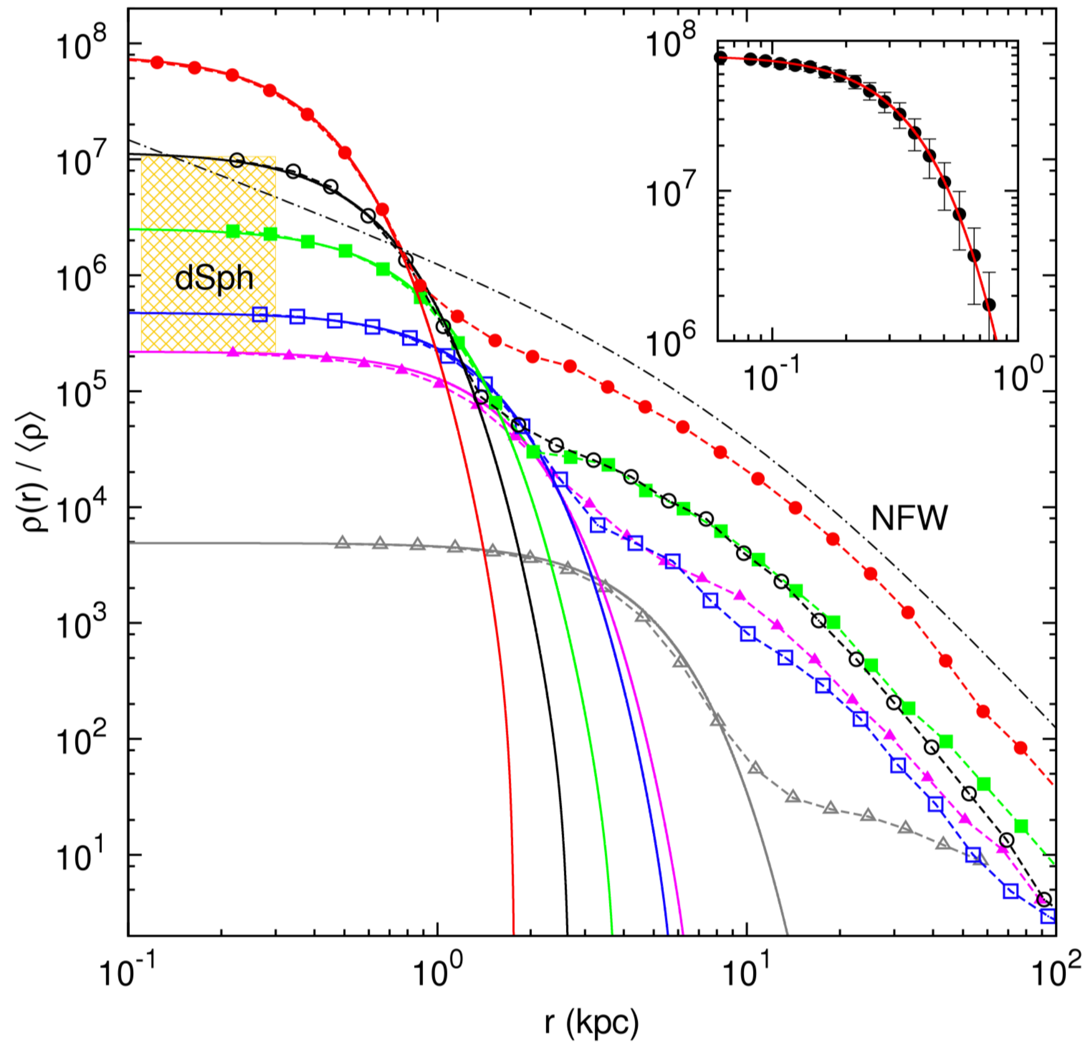

$$i\left(\partial_t + \frac{3}{2}\frac{\dot{a}}{a}\right)\psi = \left(-\frac{1}{2m}\nabla^2 + m\Psi\right)\psi$$

$$i\partial_t\psi = \left(-\frac{1}{2m}\nabla^2 + m\Psi\right)\psi, \quad \nabla^2\Psi = 4\pi G\delta\rho$$

Soliton core for ultralight ALP

$$\rho_{\rm DM} = \begin{cases} 190 \times \left(\frac{m_a}{10^{-18}\ \mathrm{eV}}\right)^{-2}\left(\frac{r_c}{1\ \mathrm{pc}}\right)^{-4} M_\odot\ \mathrm{pc}^{-3}, & \text{for } r < r_c \\ \frac{\rho_0}{r/R_g(1+r/R_g)^2}, & \text{for } r > r_c \end{cases}$$

$$\Delta\phi \simeq 5^\circ \sin\left(2\pi\frac{t}{T} + \delta(\boldsymbol{x})\right)\left(\frac{\rho_{\rm DM}}{2\times 10^9\mathrm{GeV/cm^3}}\right)^{\frac{1}{2}}\left(\frac{g_{a\gamma}}{10^{-12}\mathrm{GeV}^{-1}}\right)\left(\frac{m}{10^{-18}\mathrm{eV}}\right)^{-1}$$

Hsi-Yu Schive, et al, *Nature Physics*, 2014, 10(7) :496-499
Hsi-Yu Schive, et al, *Physical Review Letters*, 113, 261302 (2014)

Data Analysis

The least χ^2 fitting $\chi^2 = \sum_{i=1}^{N} \frac{(\phi_{\mathrm{obs},i} - \phi(t_i))^2}{\sigma_i^2},$ with $\phi(t) = \Delta\phi(t) + \phi_{\mathrm{bkg}}$

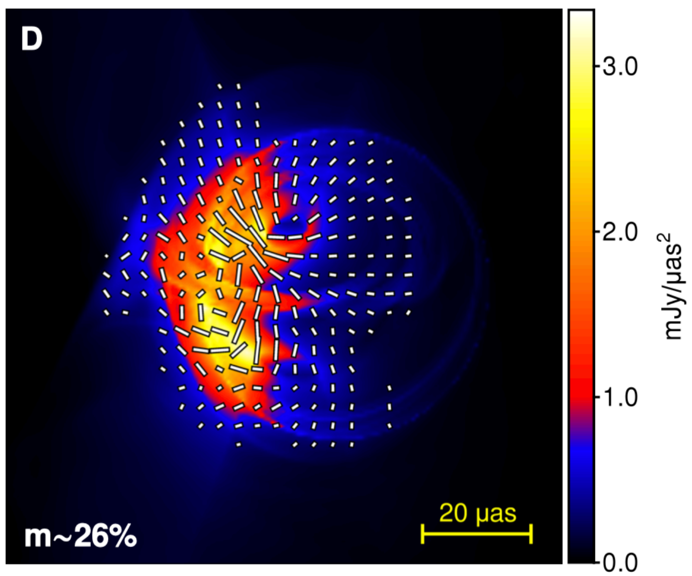

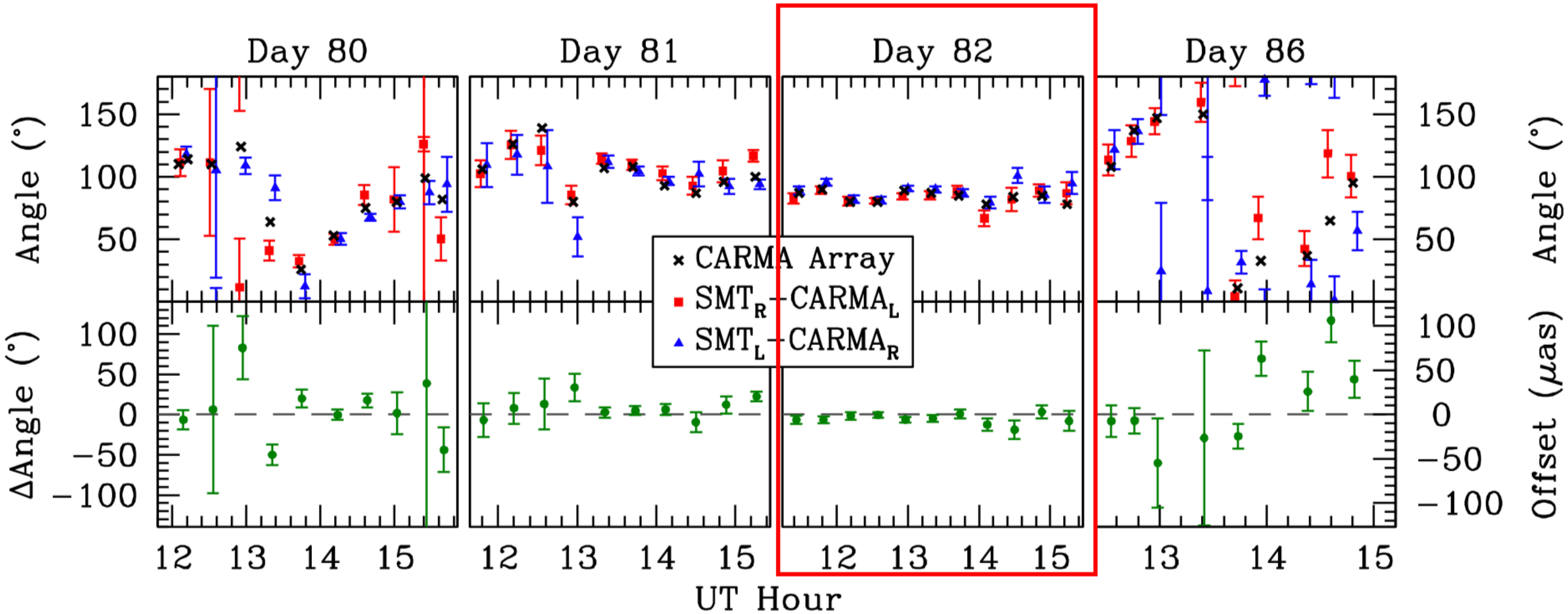

Polarization Data from M.Johnson et al. Fig 3 and Fig.S8

According to the axion typical oscillation period $T = \frac{2\pi}{m_a} \simeq 4 \times 10^3 (\frac{10^{-18}\mathrm{eV}}{m_a})$sec, we could get the experimental sensitivity mass range $(2.9 \sim 29.2) \times 10^{-19}$eV.

M.Johnson, et al, Science,2015, 350(6265):1242-1245

Results

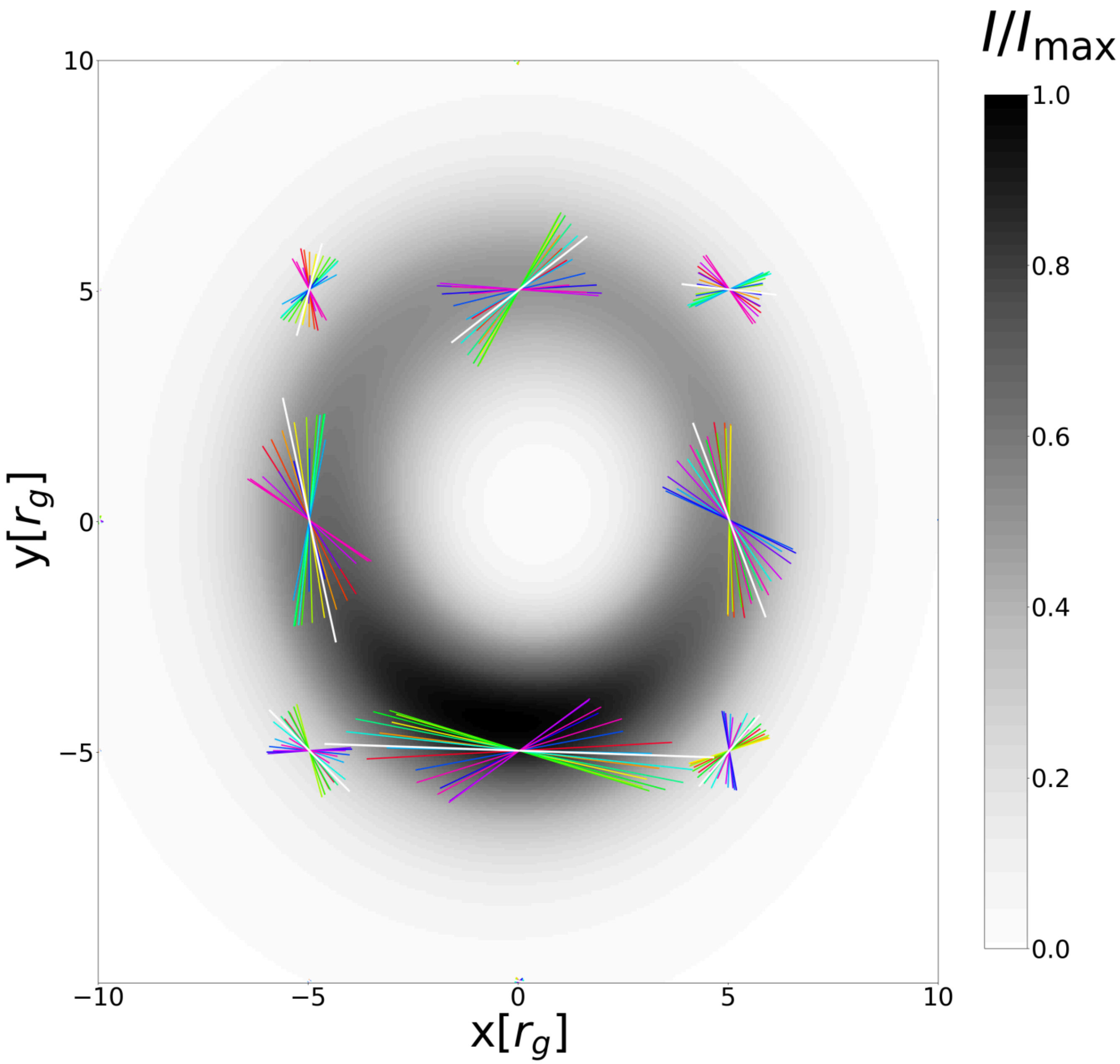

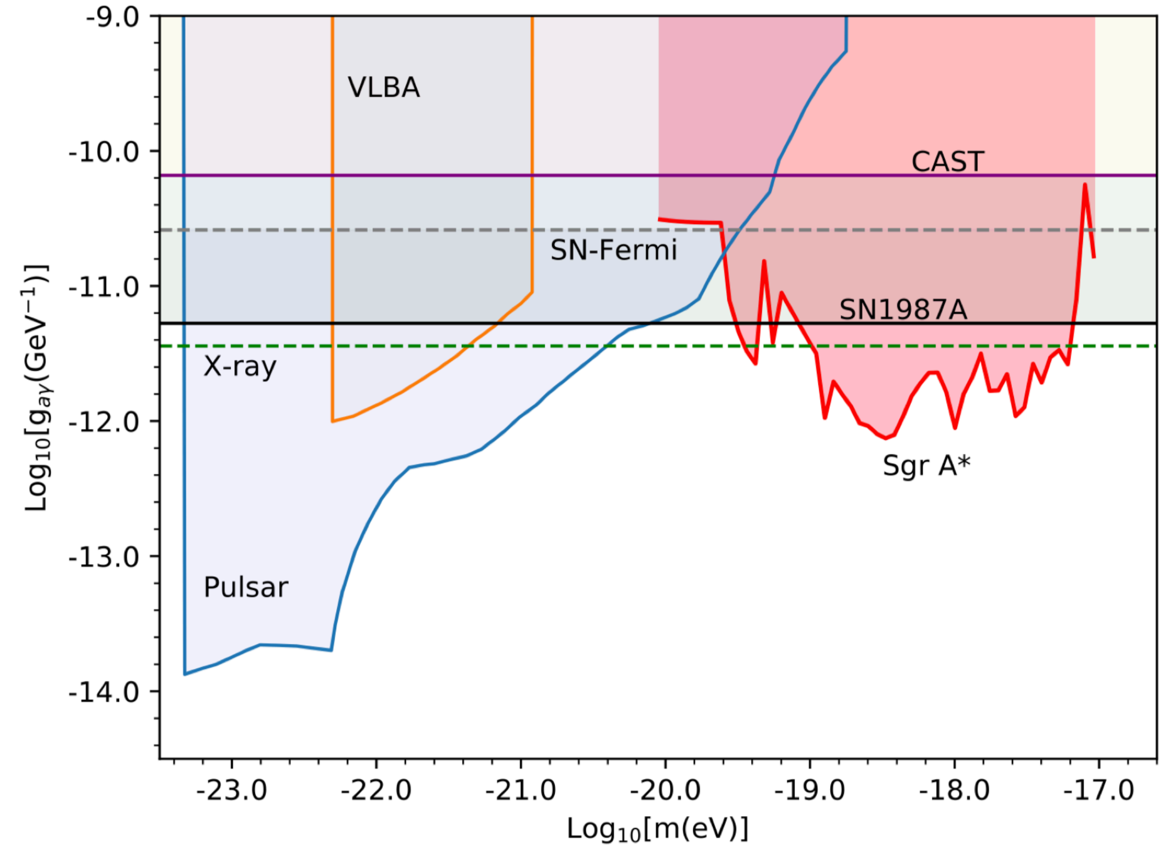

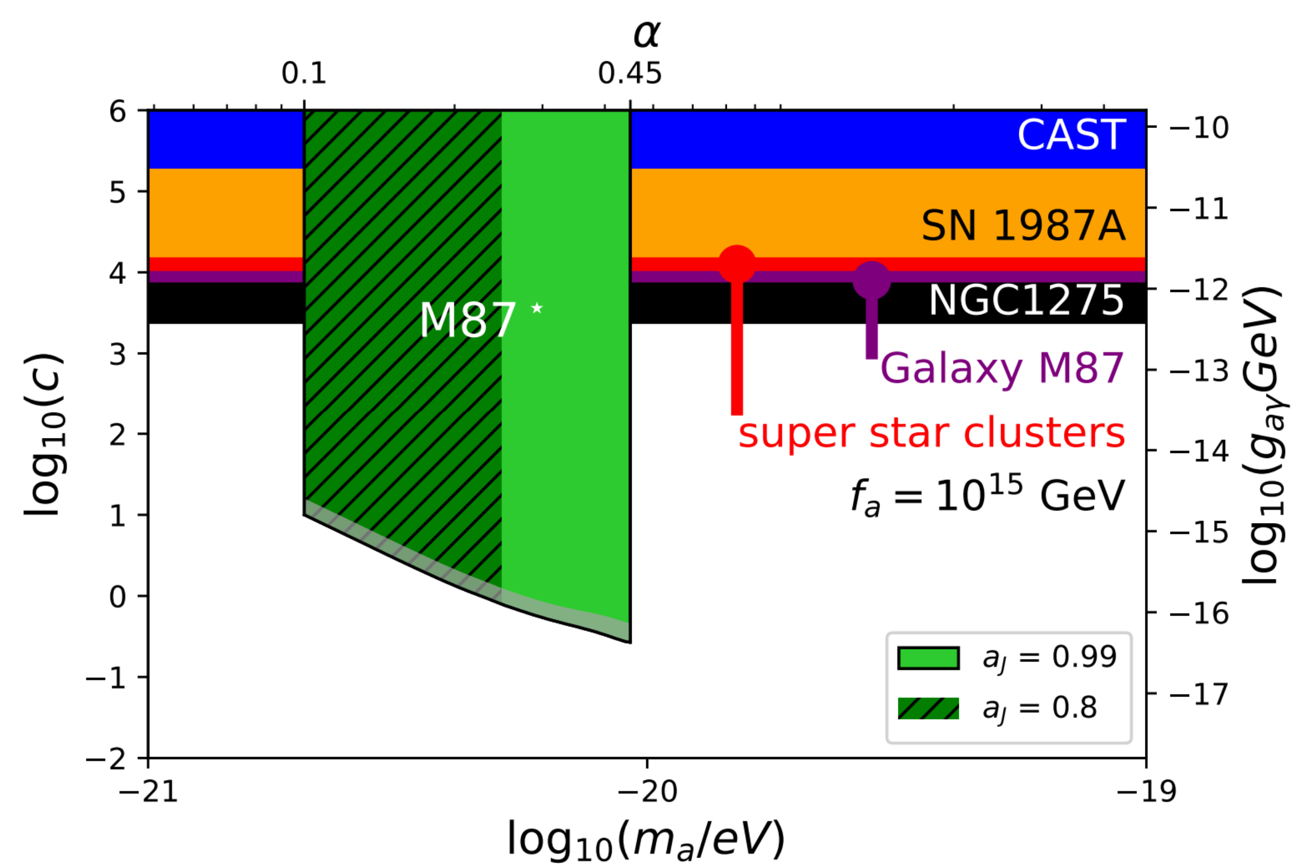

Illustration of the *IPOLE* simulation of polarized emission from a Kerr black hole surrounded by an axion cloud.

Guan-Wen Yuan, et al, Testing the ALP-photon coupling with polarization measurements of Sagittarius A*, JCAP 03(2021)018, [arXiv:2008.13662]
Yifan Chen, et al, Stringent axion constraints with Event Horizon Telescope polarimetric measurements of M87*, Nat.Astro. 6(2022)5,592-598, [arXiv:2105.04572]

Part II: Searching for ULDM and WIMP Spike with S-star Kinematics Observed by Keck/VLT

- Constraining properties of ULDM with Keck Observations of S2's Orbit
  A. The Black Hole-Scalar Field System
  B. ULDM Interacting with SM and Frequency Shift
  C. Constraints on ULDM
- Exploring WIMP-spike distribution around GC with S-stars
  A. Dark Matter Spike Around SMBH
  B. Joint Analysis with S-stars' Orbit Measurements
  C. Constraint on gNFW/Einasto Spike Distribution

VLT/Keck Observatory Monitoring the Stellar Orbits around GC

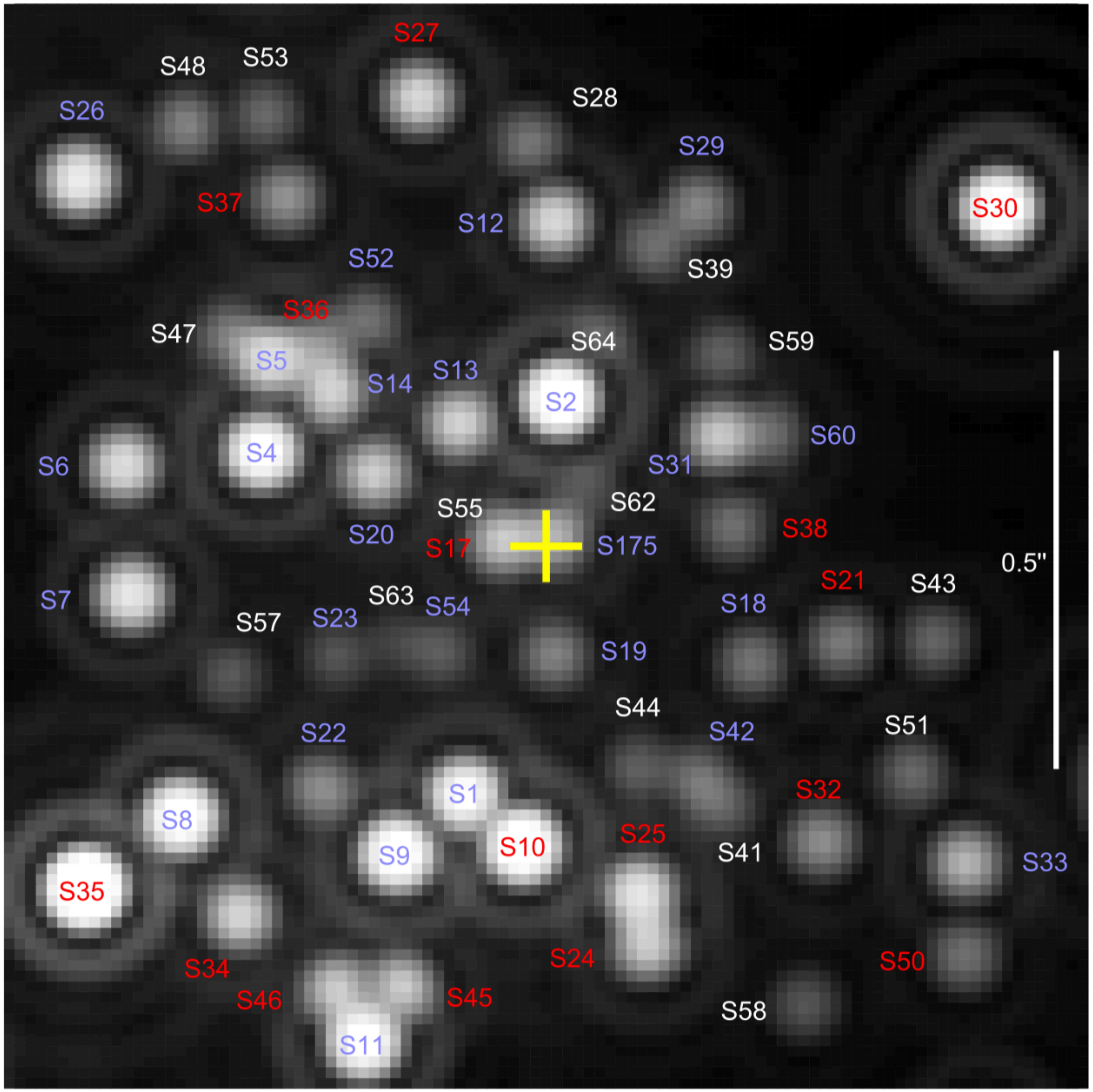

Very Large Telescope@MPE

Keck Observatory@UCLA

VLT/Keck Observatory Monitoring the Stellar Orbits around GC

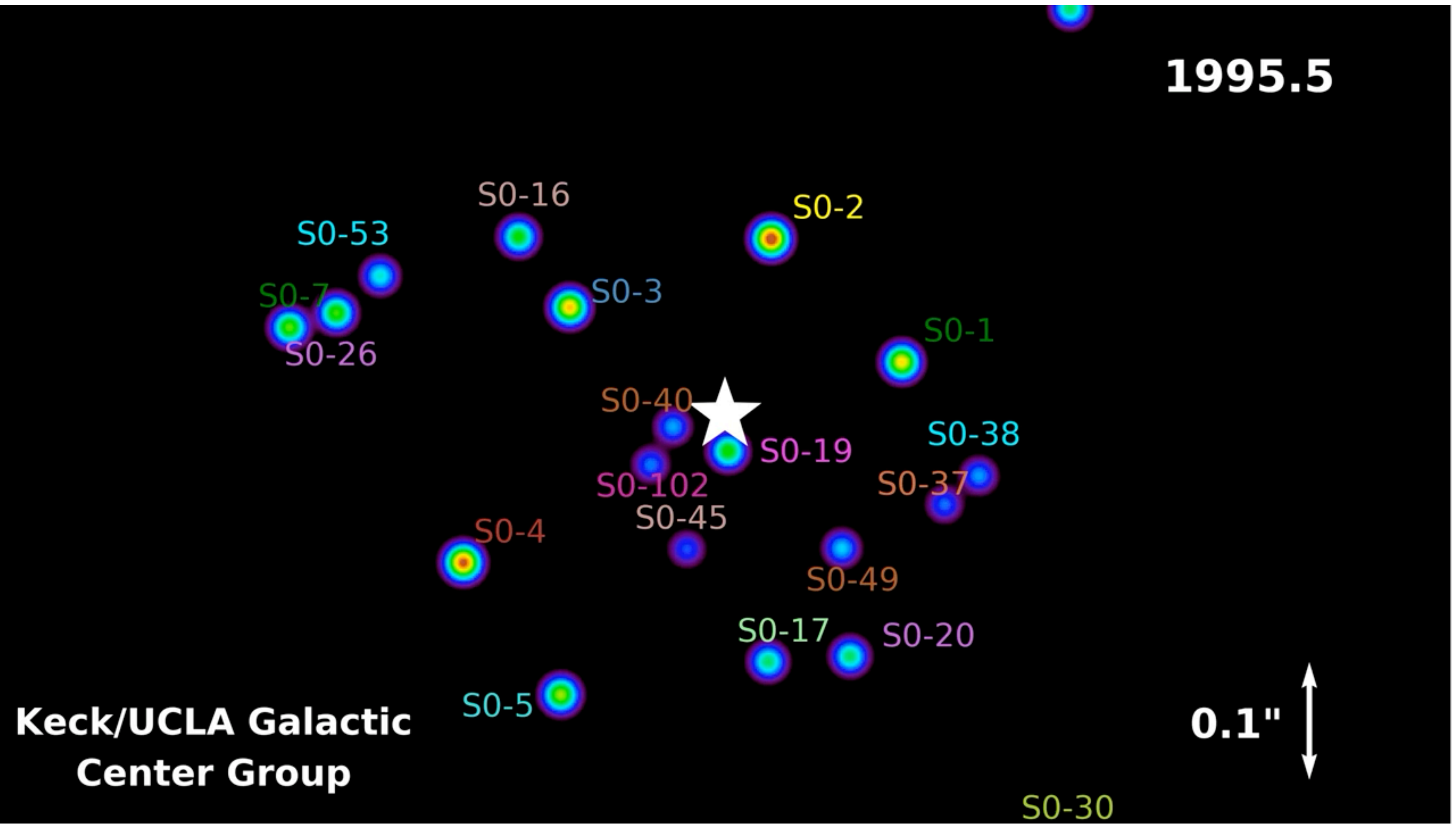

Very Large Telescope@MPE

Keck Observatory@UCLA

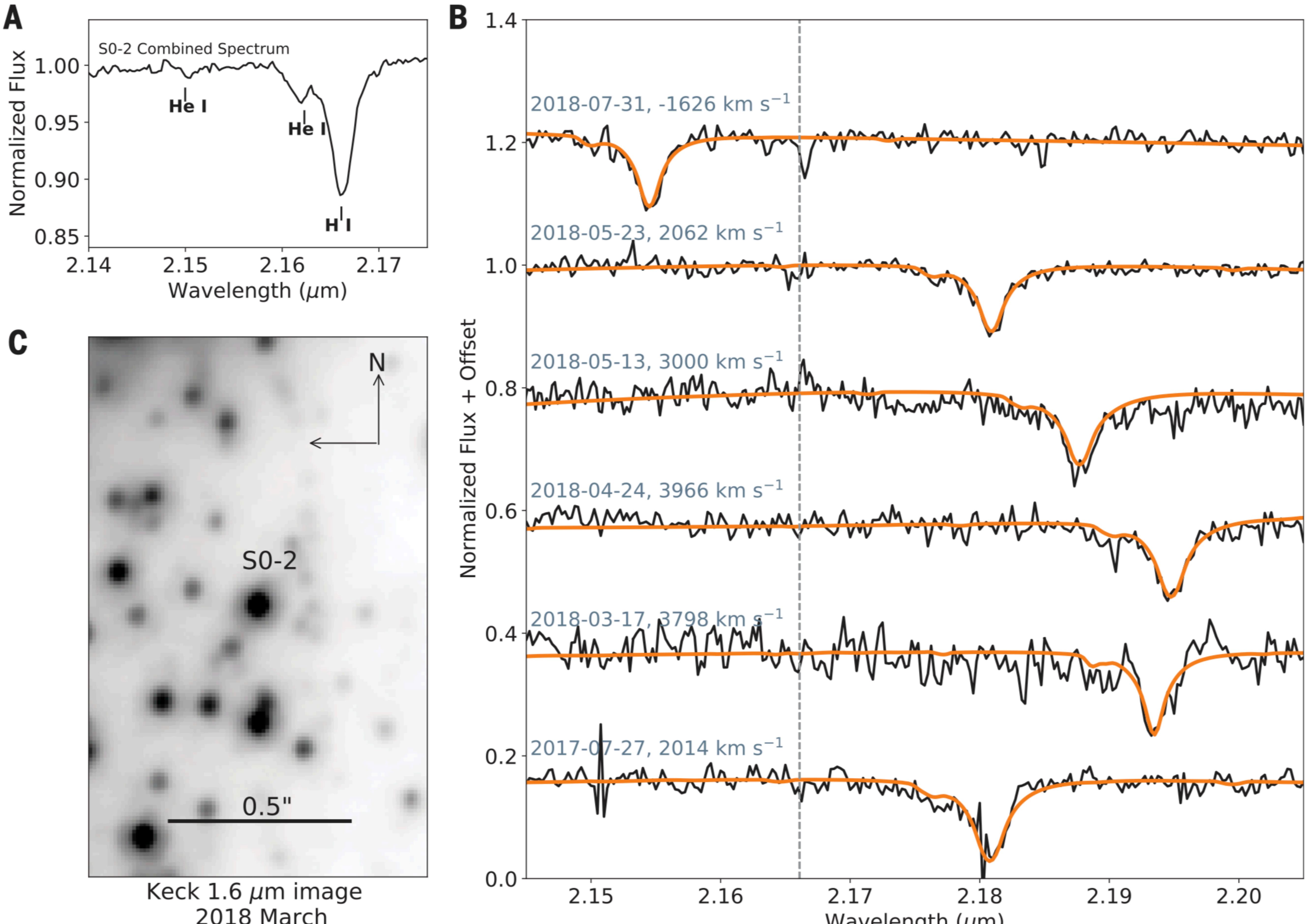

Tuan Do, et al, Science (2019)

Project3—Ultralight Scalar Dark Matter around SMBH

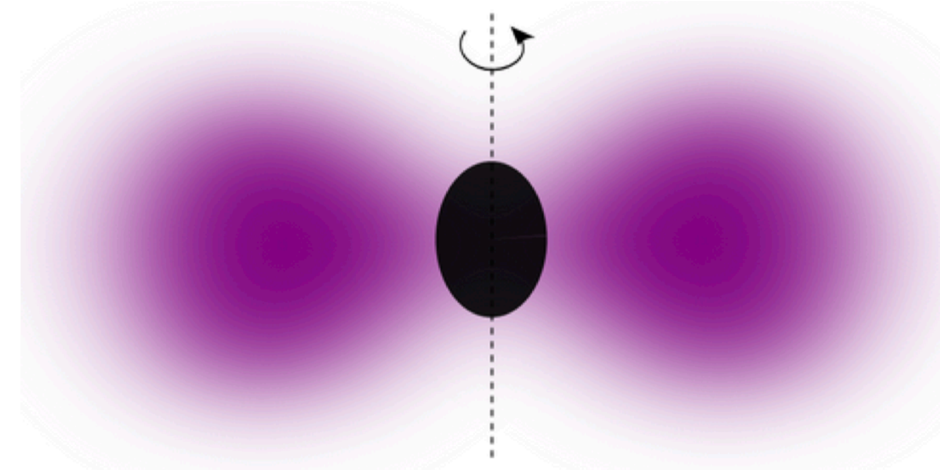

Solving the Klein-Gordon equation at the Kerr metric:

$$\nabla_\alpha \nabla^\alpha \Phi = \mu_s^2 \Phi,$$
$$\Phi_{\ell m}(t, r, \theta, \varphi) = e^{-i\omega t + im\varphi} S_{\ell m}(\theta) R_{\ell m}(r), \qquad (1)$$

Spheroidal harmonics function:

$$\frac{1}{\sin\theta}\frac{d}{d\theta}\left(\sin\theta \frac{dS_{\ell m}}{d\theta}\right) - \left[a^2 q^2 \cos^2\theta + \frac{m^2}{\sin^2\theta}\right] S_{\ell m} = A_{\ell m} S_{\ell m} \qquad (2)$$

Radial function:

$$\frac{d}{dr}\left(\Delta \frac{dR_{\ell m}}{dr}\right) + \left[\frac{K^2}{\Delta} - a^2\omega^2 + 2ma\omega - \mu_s^2 r^2\right] R_{\ell m} = A_{\ell m} R_{\ell m} \qquad (3)$$

Solution with Legendre and generalized Laguerre polynomials:

$$\begin{cases} S_{\ell m}(\theta) &= P_\ell^m(\cos\theta), \\ R_{\ell n}(r) &= A_{\ell n} v^\ell \mathrm{e}^{-v/2} L_n^{2\ell+1}(v), \end{cases} \quad \text{With} \quad v = \frac{2rM_\bullet \mu_s^2}{\ell + n + 1}, \qquad (4)$$

Specific mode ($n = 0, l = m = 1$)will grow more efficiently due to the super radiance mechanism:

GRAVITY Collaboration, Scalar field effects on the orbit of S2 star, MNRAS(2019)

Ultralight Scalar Dark Matter around SMBH

The mass coupling in Scalar field-Black hole system:

$$\zeta = \frac{r_g}{\lambda_C} = \mu_s M_\bullet \sim \mathcal{O}(10^{-3}) \qquad (5)$$

$$\begin{cases} \bar{\omega}_R \sim \zeta - \zeta\left(\frac{\zeta}{\ell+n+1}\right)^2 \\ \bar{\omega}_I \sim \left(\frac{a}{M_\bullet}\mu_s - 2\zeta\bar{r}_+\right)\frac{\zeta^{4\ell+5}}{\sigma_\ell} \end{cases} \qquad (6)$$

$\tau_I \sim \zeta^{-9}$ and $\tau_R \sim \zeta^{-1}$, hence $\tau_R \ll \tau_I$

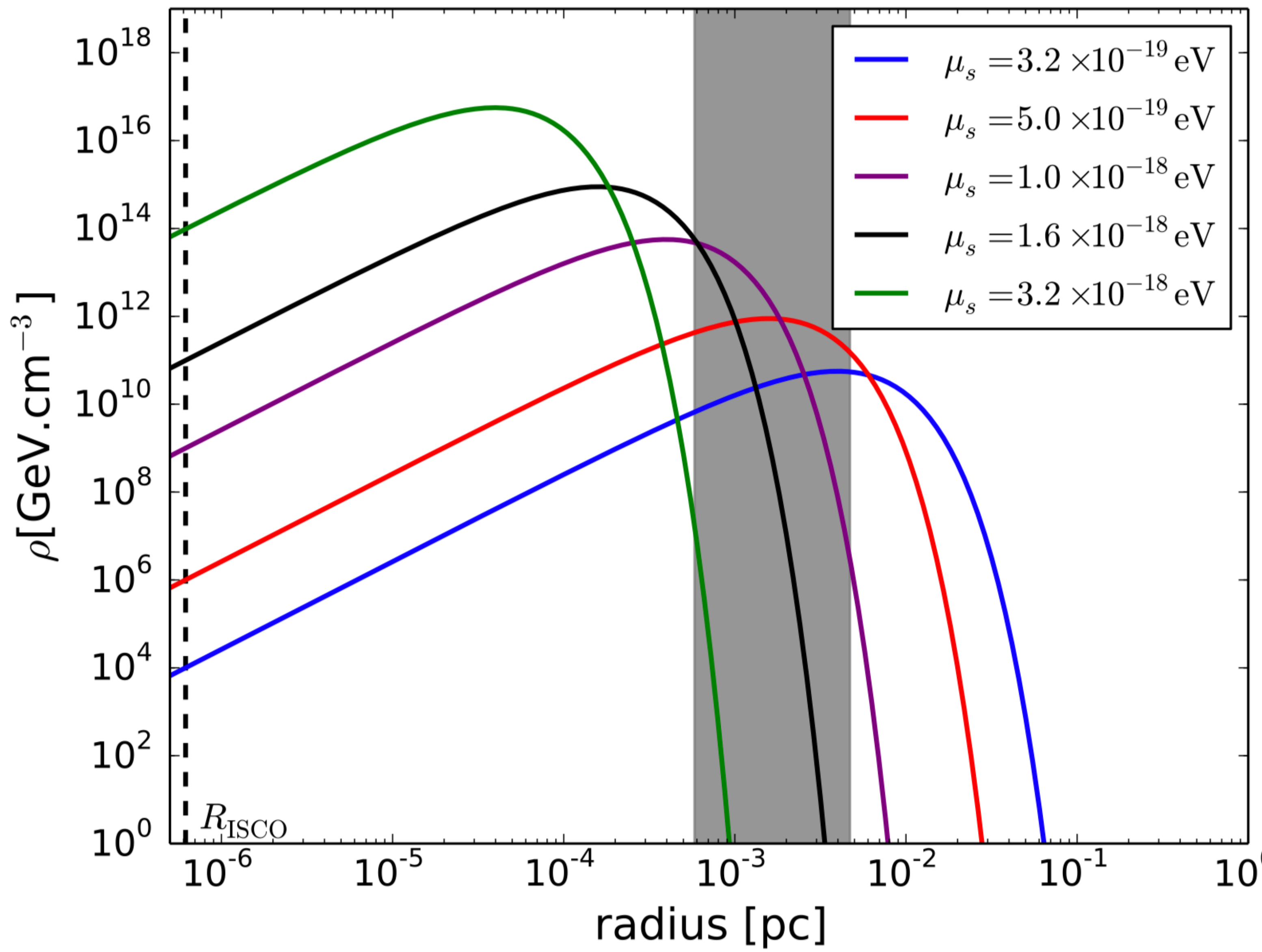

$$\Phi = C_0 e^{-i(\bar{\omega}_R \bar{t} - \varphi)} \bar{r}\zeta^2 e^{-\frac{\bar{r}\zeta^2}{2}} \sin\theta. \qquad (7)$$

$$\rho = \frac{1}{2}\mu_s^2|\Phi|^2 = \frac{1}{2}\mu_s^2\left(C_0^2\zeta^4 e^{-\zeta^2\bar{r}}\bar{r}^2\sin^2\theta\right). \qquad (8)$$

$$\kappa = \frac{M_{\rm cloud}}{M_\bullet} = \frac{\int \rho r^2 \sin\theta dr d\theta d\varphi}{M_\bullet}. \qquad (9)$$

Frequency Shift Induced by SM-DM Interaction

$$\boxed{E_n = -\frac{\mu e^4}{2\left(4\pi\epsilon_0\right)^2 \hbar^2}\frac{1}{n^2} \simeq -\frac{m_e c^2}{2}\frac{\alpha^2}{n^2}}$$

Higgs portal interaction:

$$\mathcal{L}_{\Phi H} = \beta|\Phi|^2|H|^2,$$

The Higgs vacuum expectation value:

$$v = v_{\rm ew}\sqrt{1-\frac{2\beta}{m_H^2}\frac{\rho(r)}{2\mu_s^2}} \approx v_{\rm ew}\left(1-\frac{\beta}{m_H^2}\frac{\rho(r)}{2\mu_s^2}\right),$$

$$m_e \approx m_e^{\rm bare}\left(1-\frac{\beta}{m_H^2}\frac{\rho(r)}{2\mu_s^2}\right),$$

Photon portal interaction:

$$\mathcal{L}_{\Phi\gamma} = \frac{g}{4}|\Phi|^2 F^2,$$

The fine structure constant:

$$\alpha = \alpha_0\left(\frac{1}{1-gv_\Phi^2}\right) \approx \alpha_0(1+g\frac{\rho}{2\mu_s^2}).$$

Energy shift and radial velocity:

$$\left[\frac{\delta V_{mn}}{V_{mn}}(r)\right]_{\Phi H} \approx \frac{\delta m_e}{m_e} \approx \frac{\beta}{m_H^2}\frac{\rho(r)}{2\mu_s^2}.$$

$$\left[\frac{\delta V_{mn}}{V_{mn}}(r)\right]_{\Phi\gamma} \approx \frac{2\delta\alpha}{\alpha} \approx 2g\frac{\rho(r)}{2\mu_s^2}.$$

Orbital Model and Initial Conditions

Stellar orbit around SMBH is unstable, the orbital parameters have a drift by strong gravitation. Considering GR, the orbit dynamics of star is determined by integrating the post-Newtonian EoM.

$$\boxed{\frac{\mathrm{d}^2\boldsymbol{r}}{\mathrm{d}t^2} = -\frac{GM}{r^3}\boldsymbol{r} + \frac{GM}{c^2r^3}\left(4\frac{GM}{r} - v^2\right)\boldsymbol{r} + 4\frac{GM(\boldsymbol{r}\cdot\boldsymbol{v})}{c^2r^3}\boldsymbol{v},}$$

$$\begin{aligned}
X(t_p) &= -r_p \sin\omega\cos I\sin\Omega + r_p\cos\omega\cos\Omega,\\
Y(t_p) &= r_p \sin\omega\cos I\cos\Omega + r_p\cos\omega\sin\Omega,\\
Z(t_p) &= -r_p \sin\omega\sin I,\\
V_X(t_p) &= -v_p \cos\omega\cos I\sin\Omega - v_p\sin\omega\cos\Omega,\\
V_Y(t_p) &= v_p \cos\omega\cos I\cos\Omega - v_p\sin\omega\sin\Omega,\\
V_Z(t_p) &= -v_p \cos\omega\sin I.
\end{aligned}$$

$$t_{\mathrm{em}} = t_{\mathrm{obs}} + \frac{Z(t_{\mathrm{obs}})}{c}. \tag{5}$$

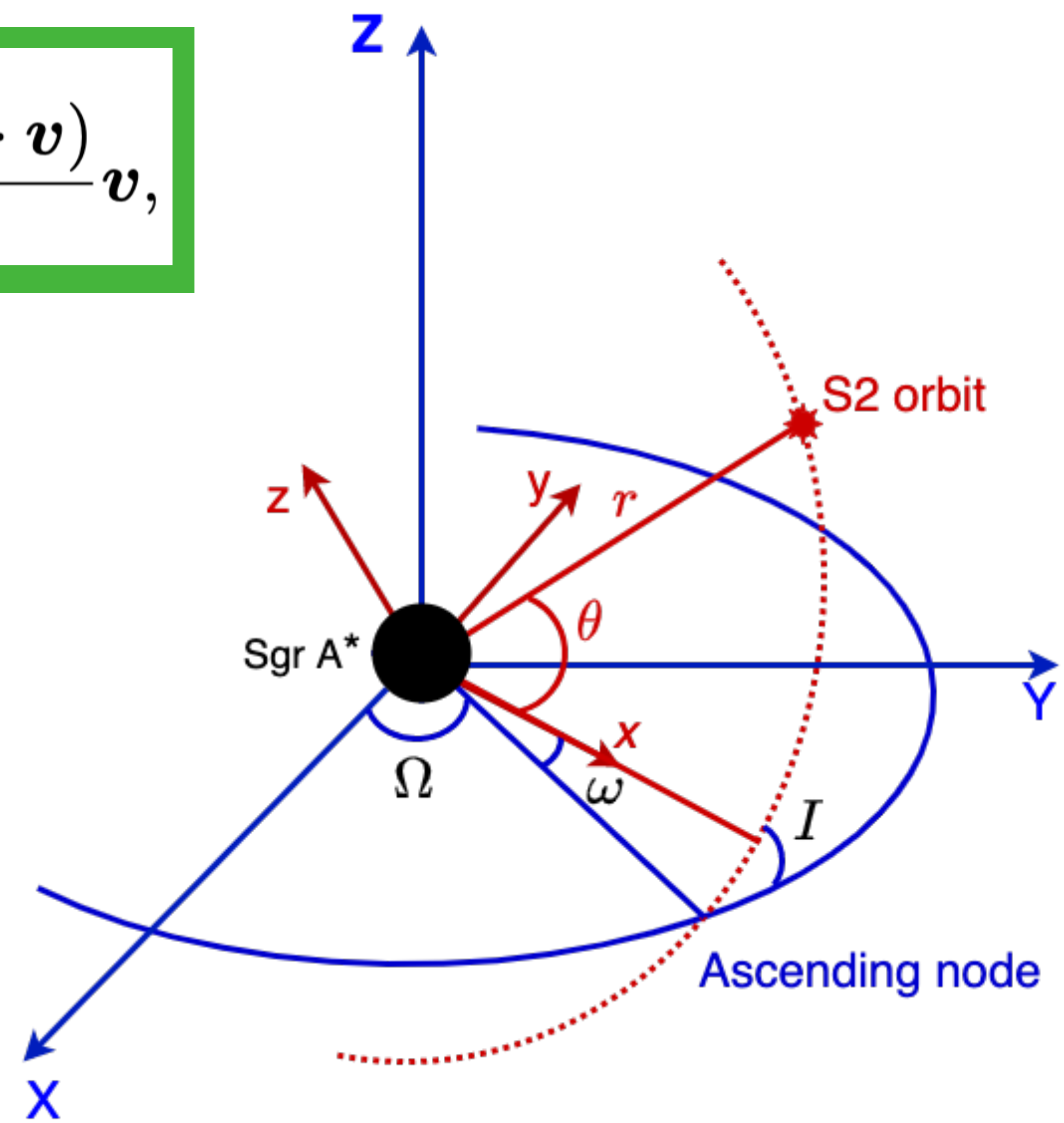

$$\begin{aligned}
\alpha_*(t_{\mathrm{obs}}) &= \frac{Y(t_{\mathrm{em}})}{R_0} + \alpha_{\mathrm{BH}} + v_\alpha\cdot(t_{\mathrm{em}} - t_{\mathrm{J2000}}),\\
\delta_*(t_{\mathrm{obs}}) &= \frac{X(t_{\mathrm{em}})}{R_0} + \delta_{\mathrm{BH}} + v_\delta\cdot(t_{\mathrm{em}} - t_{\mathrm{J2000}}),\\
v_r(t_{\mathrm{obs}}) &= V_Z(t_{\mathrm{em}}) + v_{r0} + \boxed{\left[\frac{V_Z^2(t_{\mathrm{em}})}{2c} + \frac{GM}{c\,r(t_{\mathrm{em}})}\right]} + \underline{\Delta V_r},
\end{aligned}$$

v_p, r_p are the velocity and radius at time t_p :

$$(a, e, P, I, \Omega, \omega) \longrightarrow (r_p, v_p, t_p, I, \Omega, \omega)$$

Scalar Filed Mass Model

Case I: the SMBH + scalar field

$$M(r) = M_\bullet + 2\pi \int_{r_{\rm ISCO}}^{r} r'^2 \mathrm{d}r' \int_0^\pi \sin\theta' \mathrm{d}\theta' \rho(r', \theta'),$$

Case II: the SMBH + scalar field
+ astrophysical background

$$M(r) = M_\bullet + A r^{1.6} + 2\pi \int_{r_{\rm ISCO}}^{r} r'^2 \mathrm{d}r' \int_0^\pi \sin\theta' \mathrm{d}\theta' \rho(r', \theta'),$$

Mass distribution of scalar field:

$$\rho = \frac{1}{2}\mu_s^2 |\Phi|^2 = \frac{1}{2}\mu_s^2 \left(C_0^2 \zeta^4 \mathrm{e}^{-\zeta^2 \bar{r}} \bar{r}^2 \sin^2\theta \right).$$

$$\kappa = \frac{M_{\rm cloud}}{M_\bullet} = \frac{\int \rho r^2 \sin\theta dr d\theta d\varphi}{M_\bullet}.$$

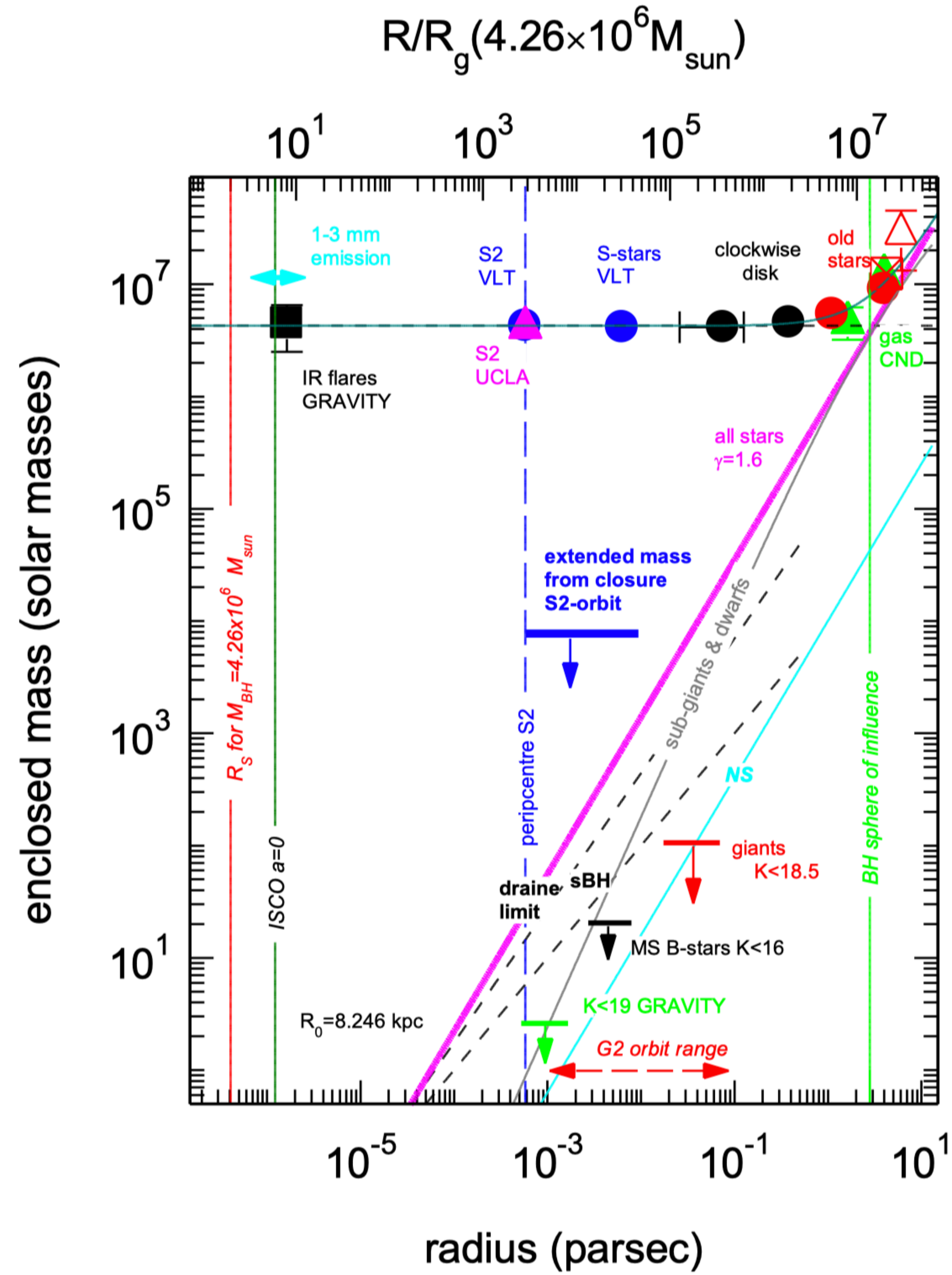

Astrophysical background around Galactic center credited by *GRAVITY A&A(2020)*

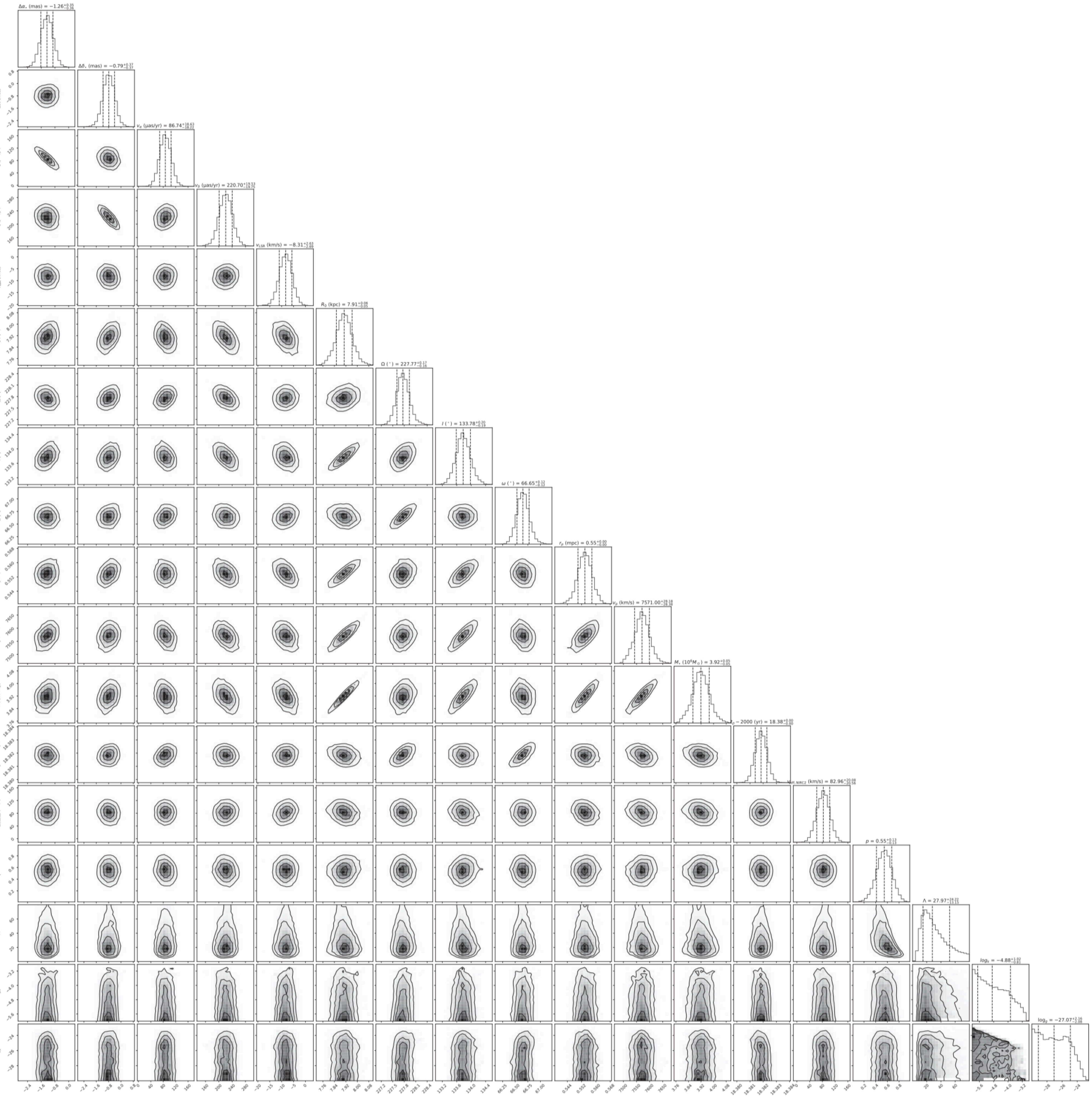

Priors and Fitting Results of All Parameters

		Case I		Case II	
Parameter	Prior	Best fit	Posterior mean $\pm 1\sigma$	Best fit	Posterior mean $\pm 1\sigma$
$M_\bullet$ ($10^6\ M_\odot$)	4.0 ± 1.1	3.91	3.92 ± 0.05	3.90	3.92 ± 0.05
R_0 (kpc)	8.15 ± 0.15	7.90	7.90 ± 0.05	7.89	7.91 ± 0.05
$\alpha_{\rm BH}$ (mas)	$(-10, 10)$	-1.38	$-1.27^{+0.35}_{-0.36}$	-1.28	-1.22 ± 0.33
$\delta_{\rm BH}$ (mas)	$(-10, 10)$	-0.75	$0.79^{+0.38}_{-0.37}$	-0.87	-0.75 ± 0.37
v_α (mas yr^{-1})	$(-500, 500)$	94	87^{+19}_{-18}	86	85 ± 18
v_δ (mas yr^{-1})	$(-500, 500)$	220	221 ± 20	231	218 ± 19
v_{r0} (km s^{-1})	$(-100, 100)$	-6.3	-8.3 ± 2.7	-8.1	-8.7 ± 2.8
r_p (10^{-3} pc)	$(0.01,\ 1)$	0.554	0.554 ± 0.004	0.552	0.554 ± 0.003
v_p (km s^{-1})	$(-10^5, 10^5)$	7559	7571^{+28}_{-29}	7559	7573^{+27}_{-26}
t_p (yr)	$(2010,\ 2030)$	2018.3818	2018.3818 ± 0.0004	2018.3819	2018.3818 ± 0.0004
I (°)	$(0,\ 360)$	133.80	133.78 ± 0.20	133.70	133.80 ± 0.18
ω (°)	$(0,\ 360)$	66.70	66.66 ± 0.12	66.65	66.66 ± 0.12
Ω (°)	$(0,\ 360)$	227.83	227.77 ± 0.16	227.73	227.79 ± 0.17
offset (km s^{-1})	$(-300, 300)$	77	83^{+20}_{-21}	81	83^{+19}_{-20}
p	$(0.01,\ 0.99)$	0.70	0.54 ± 0.13	0.62	$0.54^{+0.14}_{-0.13}$
Λ (mas)	$(1,\ 100)$	13	32^{+20}_{-17}	16	31^{+19}_{-17}
$\log_{10}\kappa$	$(-6, -1)$	-4.45	$-4.79^{+0.96}_{-0.90}$	-5.51	$-4.82^{+0.95}_{-0.89}$
$\log_{10}\beta$	$(-30, -20)$	-24.89	$-27.0^{+2.1}_{-2.2}$	-24.88	$-26.81^{+2.11}_{-2.20}$
μ_s (eV)	…	10^{-18}	…	10^{-18}	…
$-2\ln\mathcal{L}_{\rm tot}$	…	-14.77	…	-14.21	…

Orbit Fitting and Results

45 astrometric measurements (1995-2018) and 115 radial velocity measurements (2000-2018) from Keck.

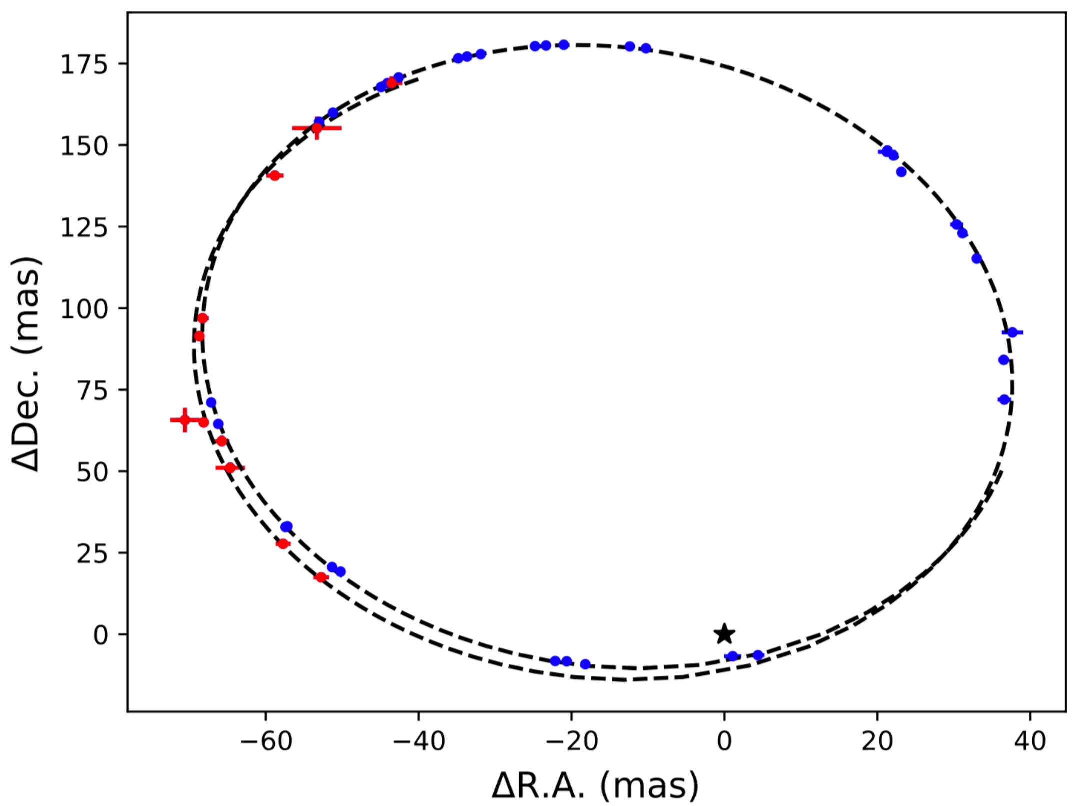

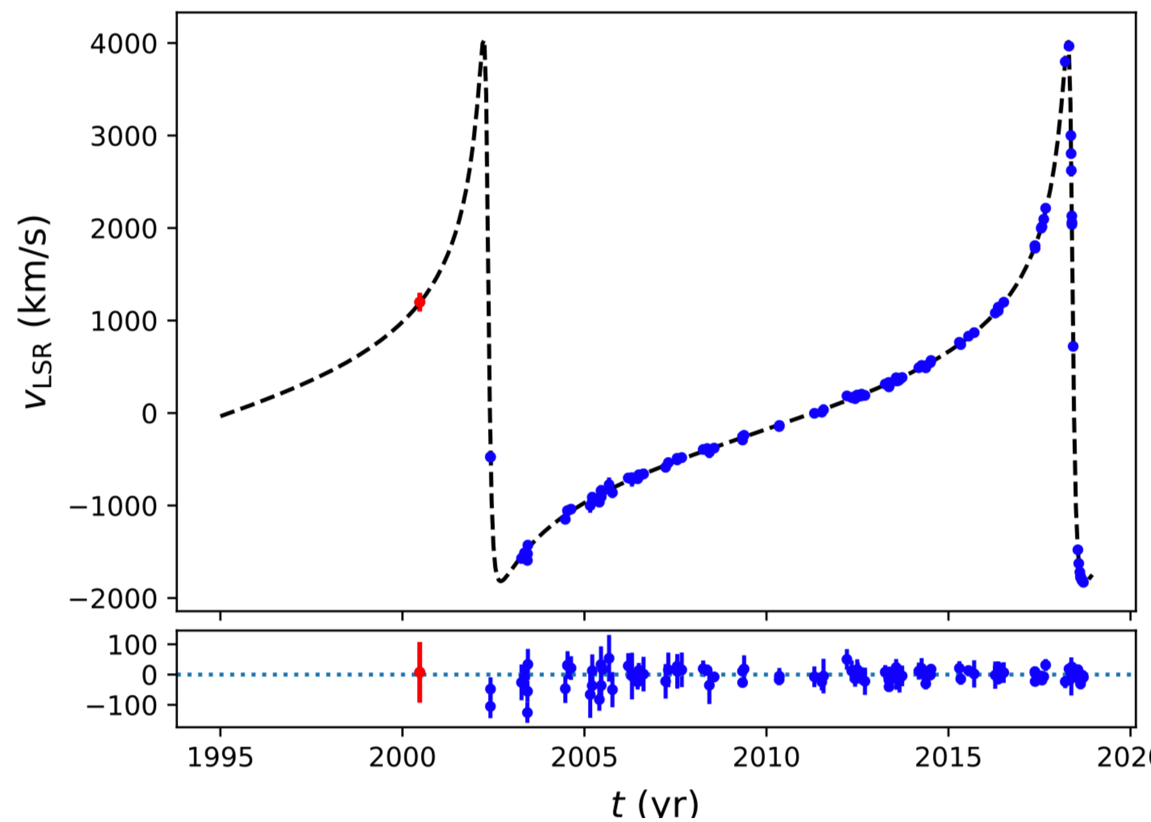

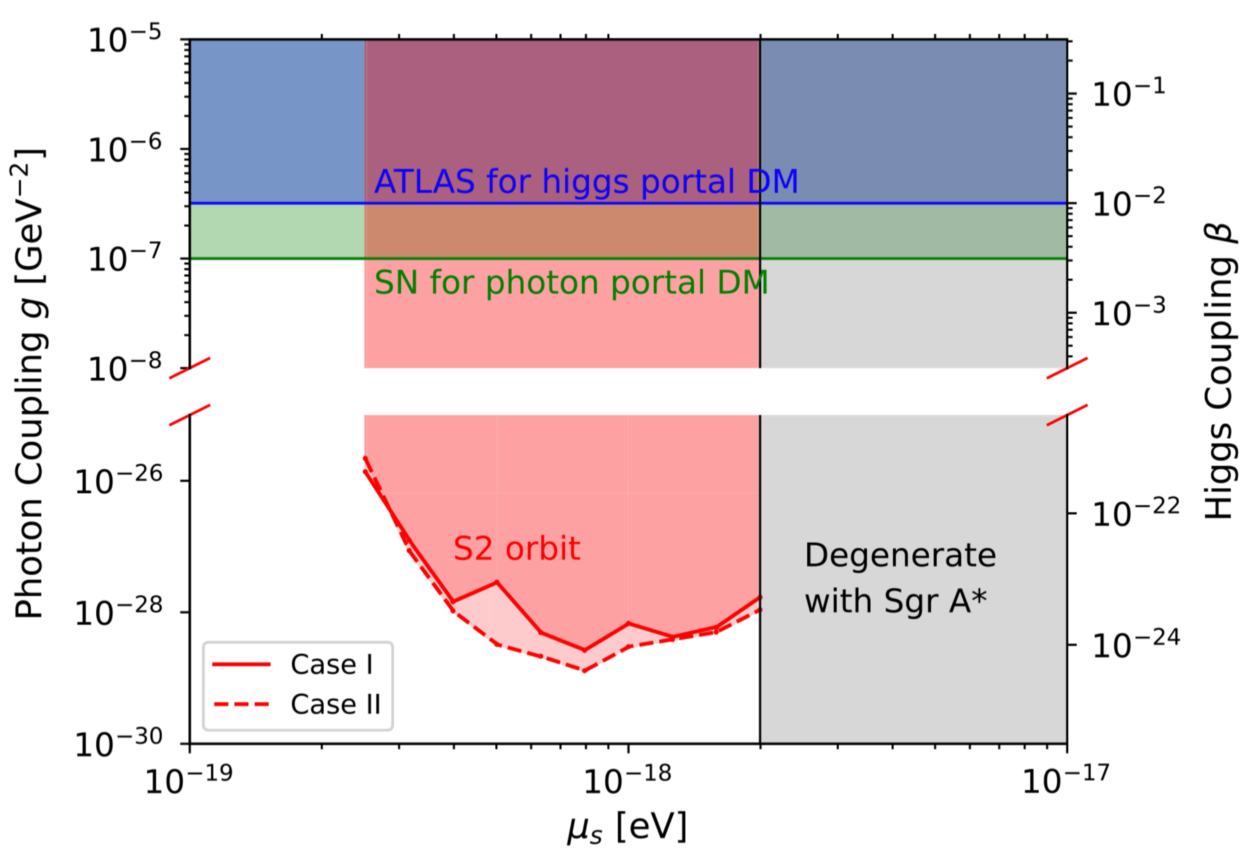

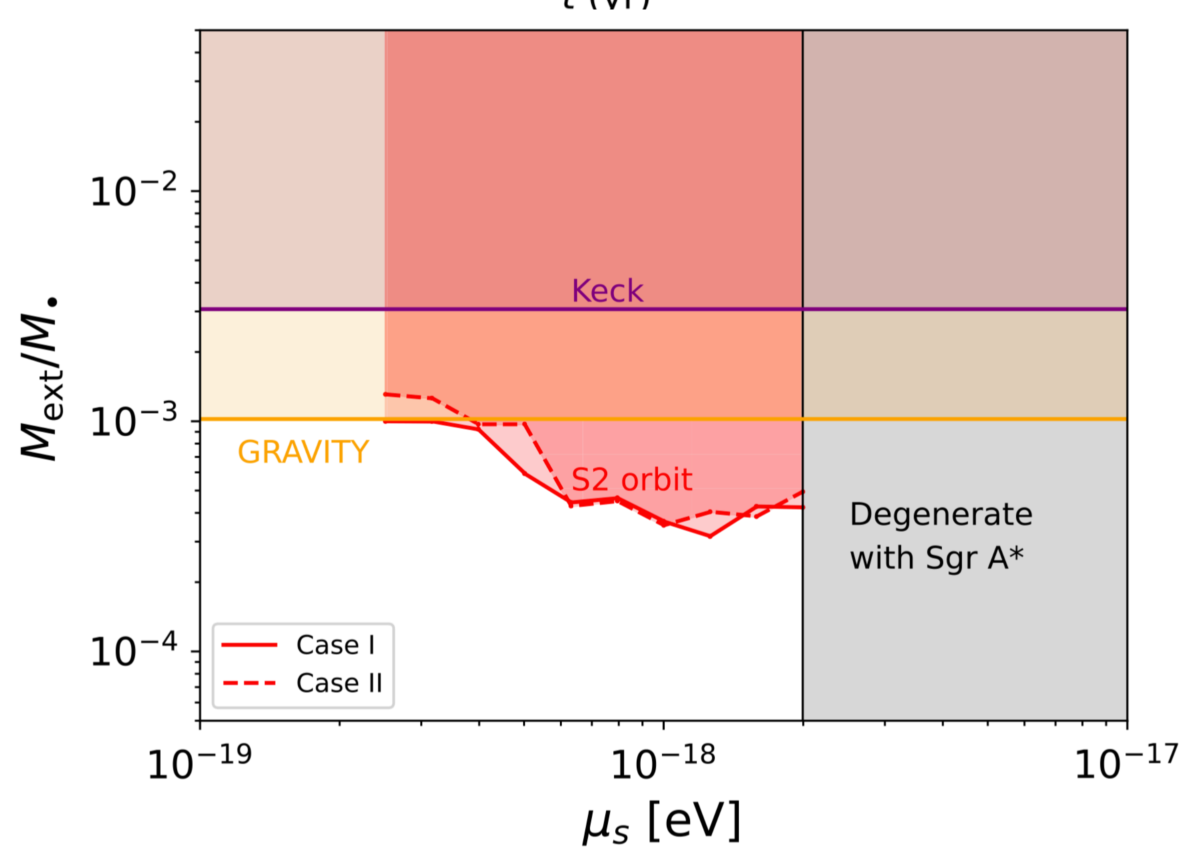

<u>*Guan-Wen Yuan*</u>, et al, Constraining ultralight bosonic dark matter with Keck observations of S2's orbit and kinematics, Phys.Rev.D 106 (2022) 10, 103024, [arXiv: 2205.04970]

Project4—DM spike is formed along with the growth of SMBH

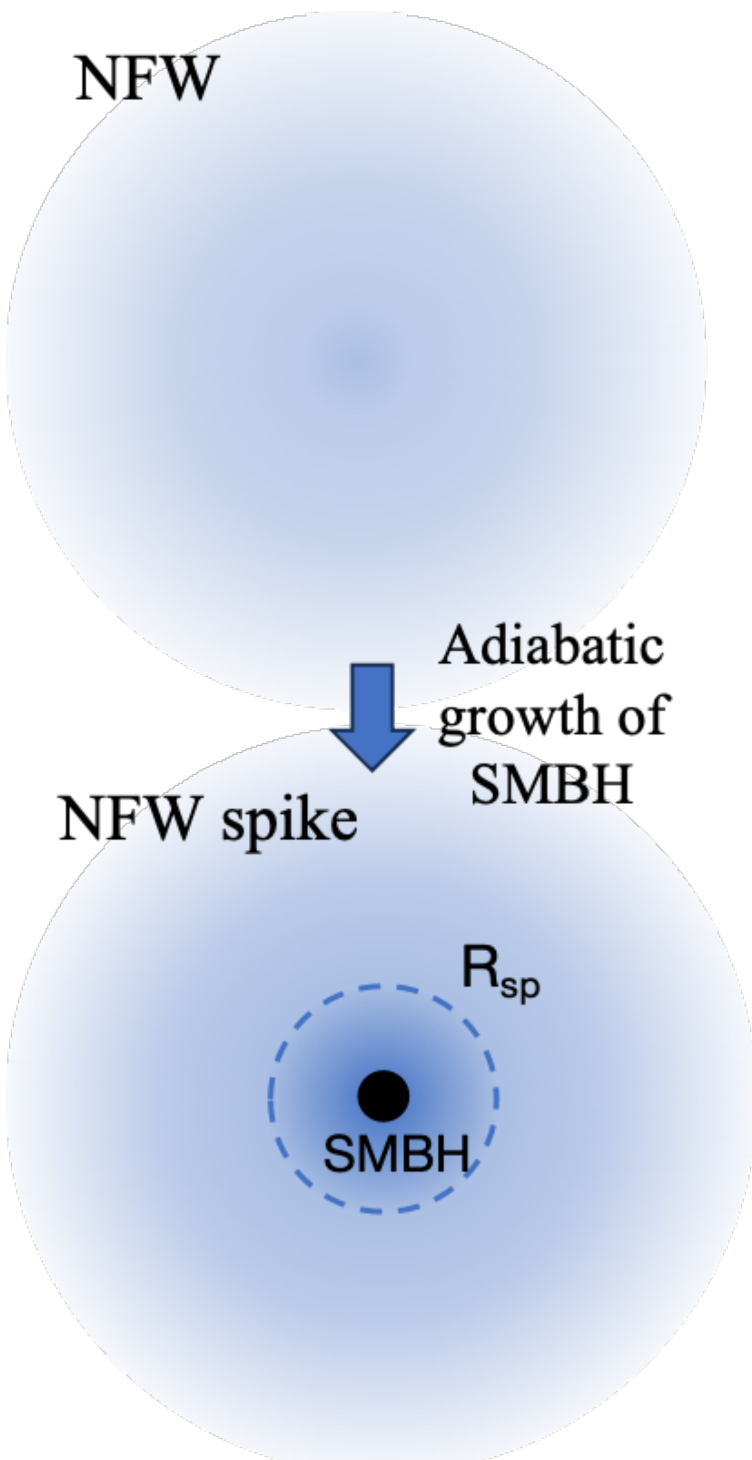

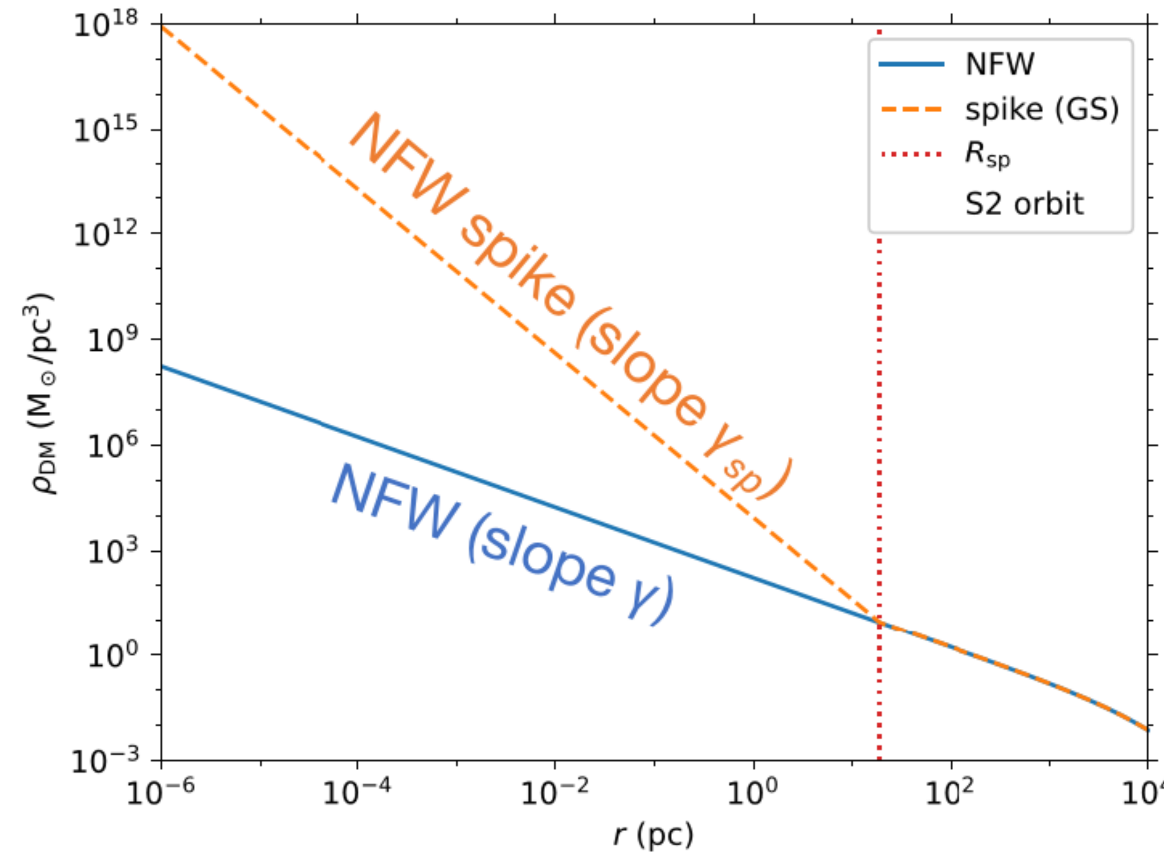

NFW:

$$\rho_{NFW}(r) = \frac{\rho_0}{(r/r_0)\,(1+r/r_0)^2}$$

Spike:

$$\rho(r) = \begin{cases} 0 & r < 2R_S \\ \rho_{halo}(R_{sp})\left(\frac{r}{R_{sp}}\right)^{-\gamma_{sp}} & 2R_S \leqslant r < R_{sp} \\ \rho_{halo}(r) & r \geqslant R_{sp}, \end{cases}$$

Direct Constraint on the DM spike

Dynamical equation (1PN; Rubilar&Eckart 2001):

$$\frac{d^2\boldsymbol{r}}{dt^2} = -\frac{GM_{\rm tot}(r)}{r^3}\boldsymbol{r} - \frac{GM_{\rm tot}(r)}{c^2r^3}\left[(4\phi(r)+v^2)\boldsymbol{r} - 4\boldsymbol{v}(\boldsymbol{v}\cdot\boldsymbol{r})\right]$$

where $M_{tot}(r) = M_{BH} + M_{DM}(r)$ and $M_{DM}(r) = \int 4\pi r^2 dr\, \rho_{DM}(r)$,

$$\rho_{DM}(r) = \begin{cases} 0 & r < 2R_S \\ \rho_{\rm halo}(R_{\rm sp})\left(\frac{r}{R_{\rm sp}}\right)^{-\gamma_{\rm sp}} & 2R_S \leqslant r < R_{\rm sp} \\ \rho_{\rm halo}(r) & r \geqslant R_{\rm sp}, \end{cases}$$

We set two types of constraints:

- Constrain the spike radius R_{sp}
- Constrain the spike slope γ_{sp}

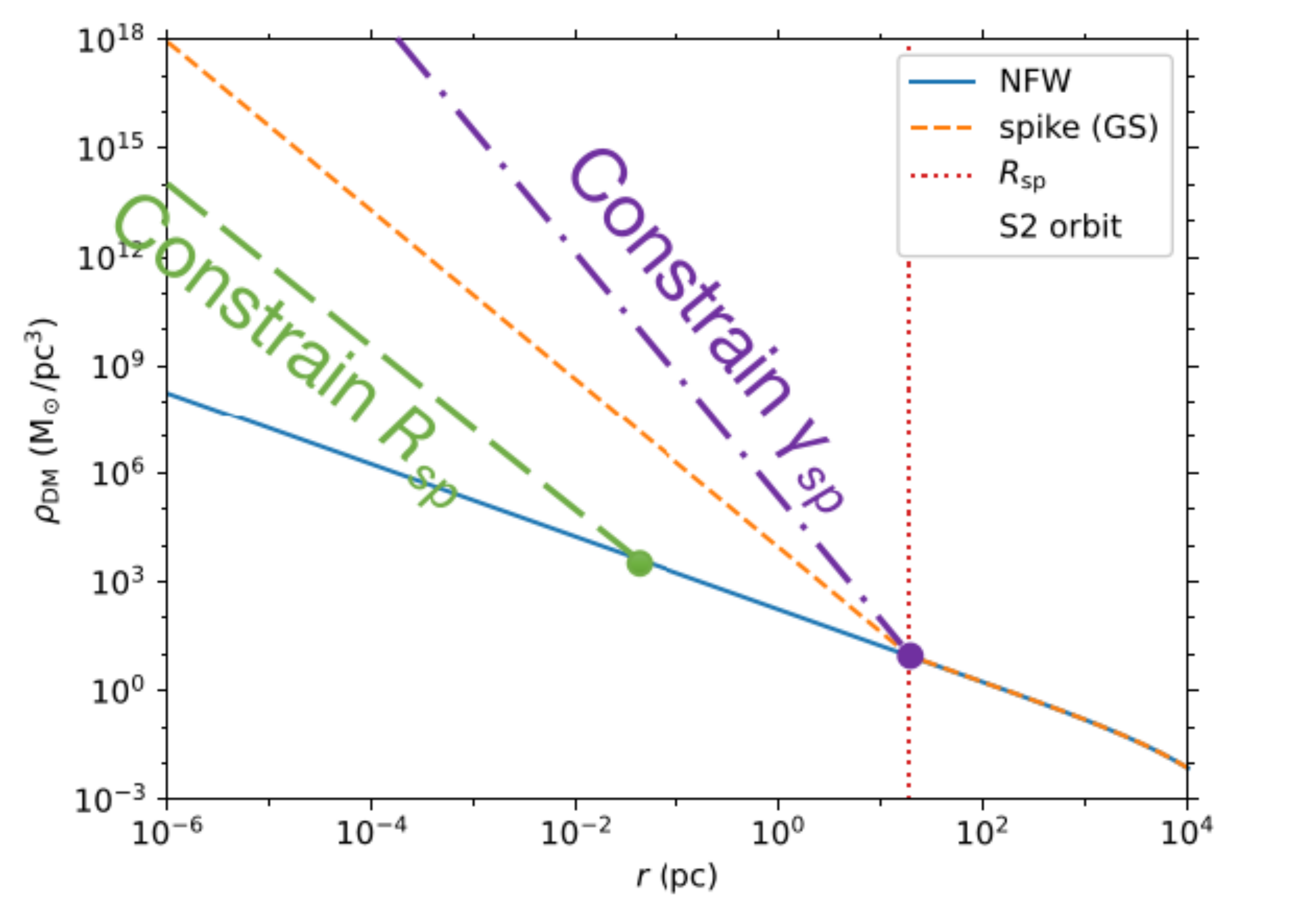

Result1: Constraint the generalized NFW spike profile with S2

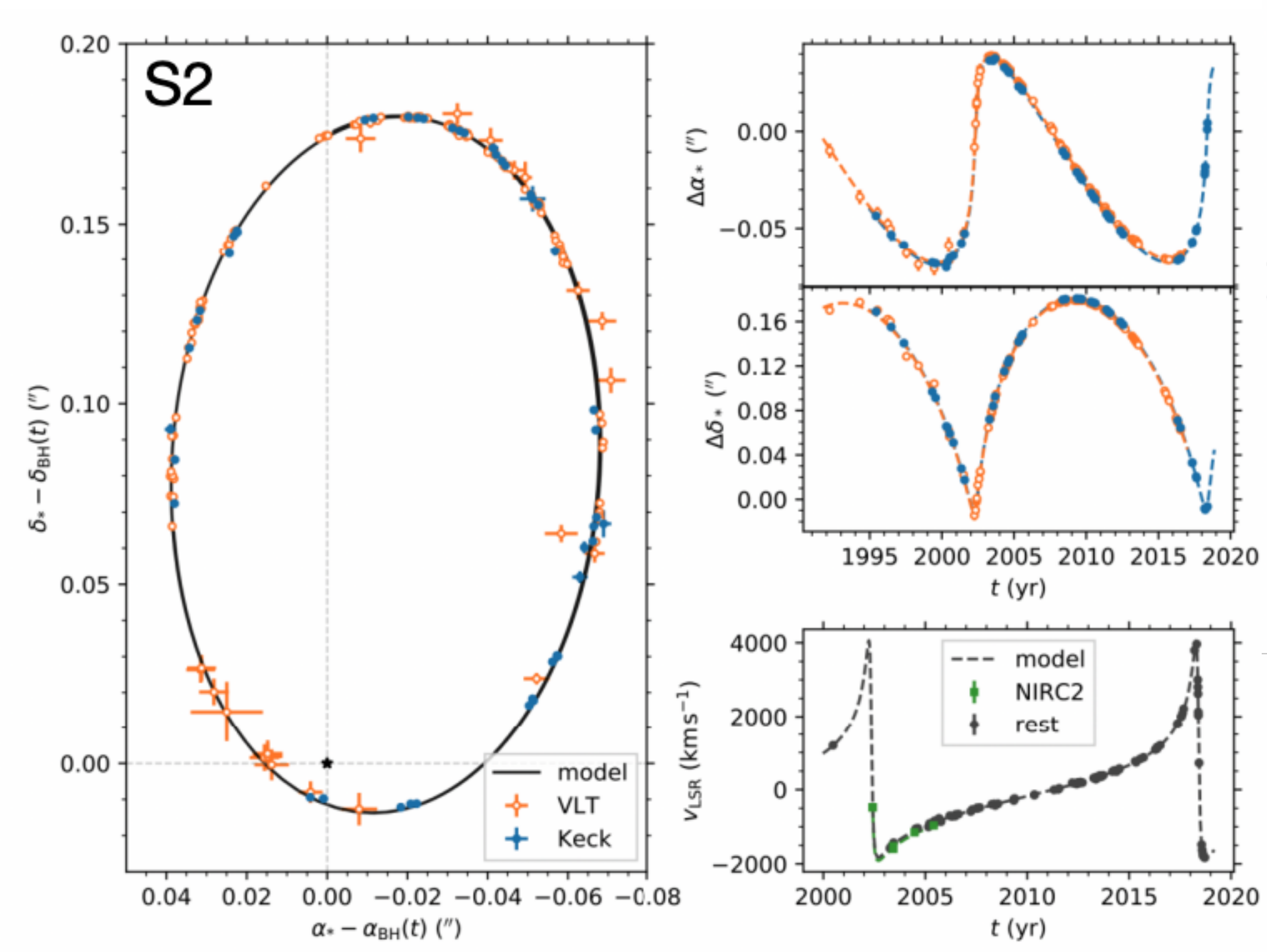

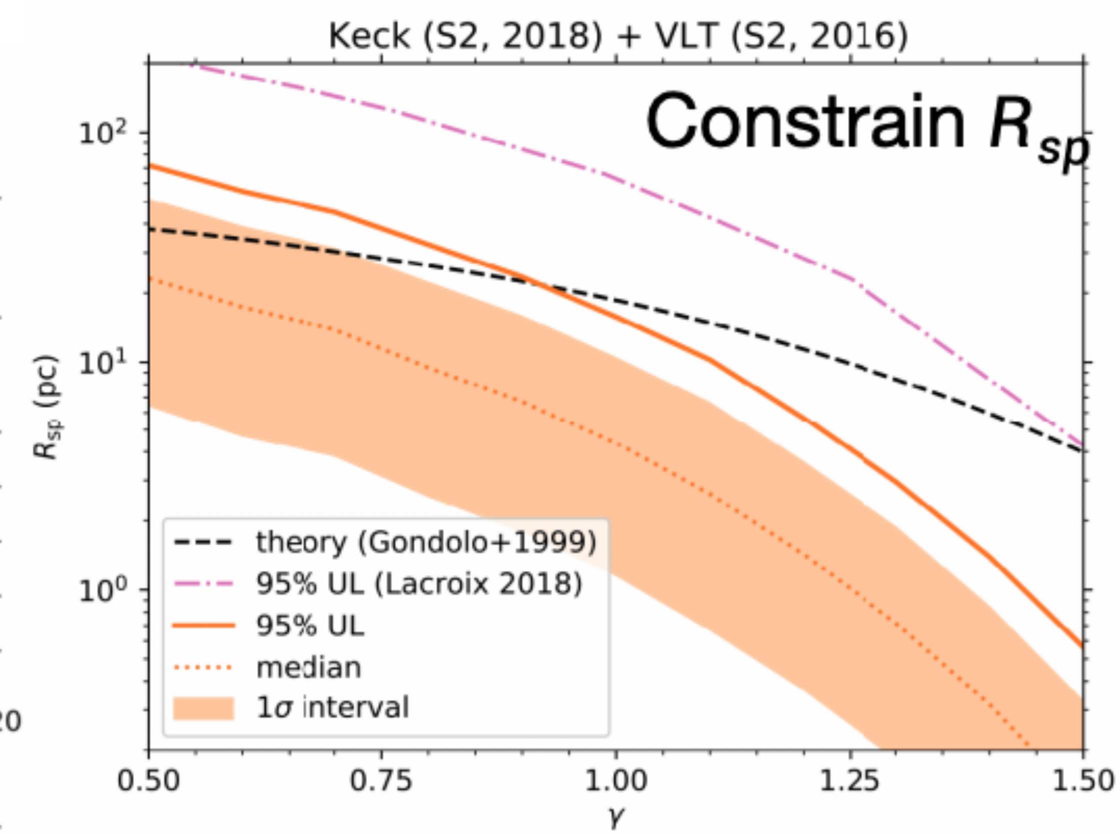

- $R_{sp} < 15.7$ pc for NFW spike at 95% CL
- $\gamma_{sp} < 2.32$ for NFW spike at 95% CL
- The GS spike model is disfavoured at 95% when the initial slope $\gamma > 0.92$

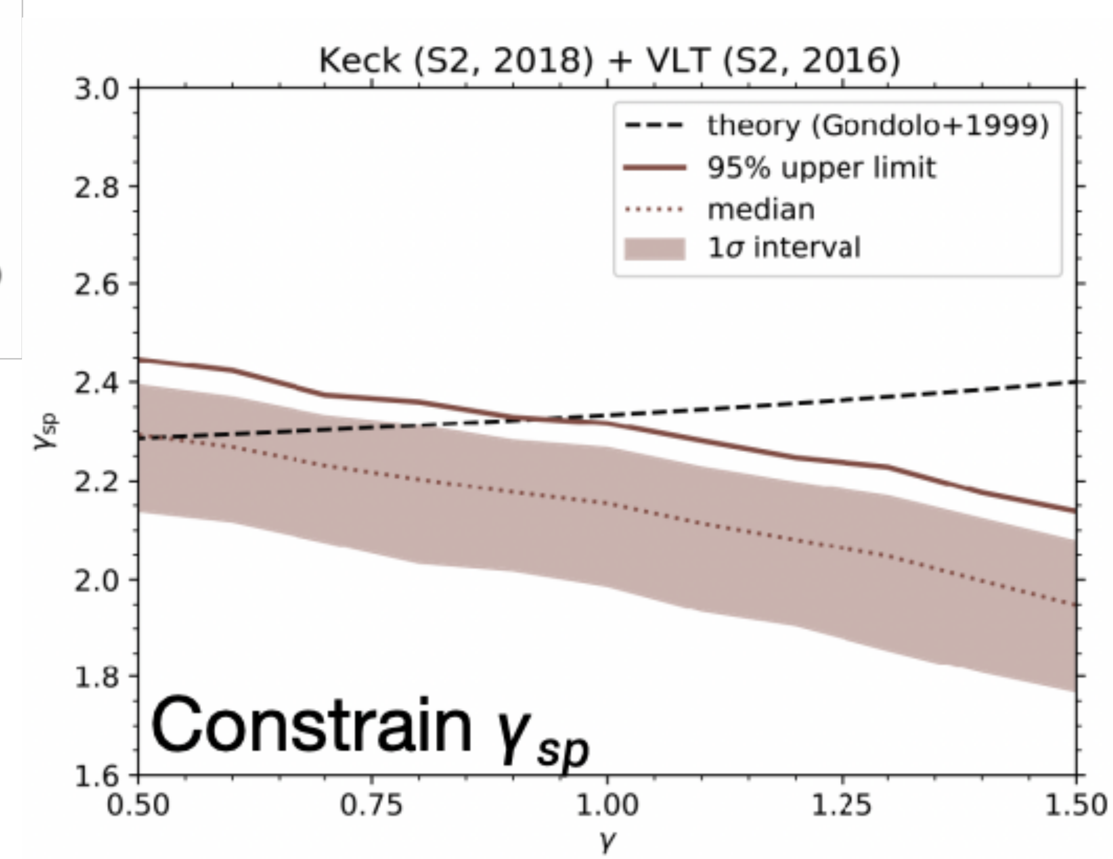

Results II. Other Cases

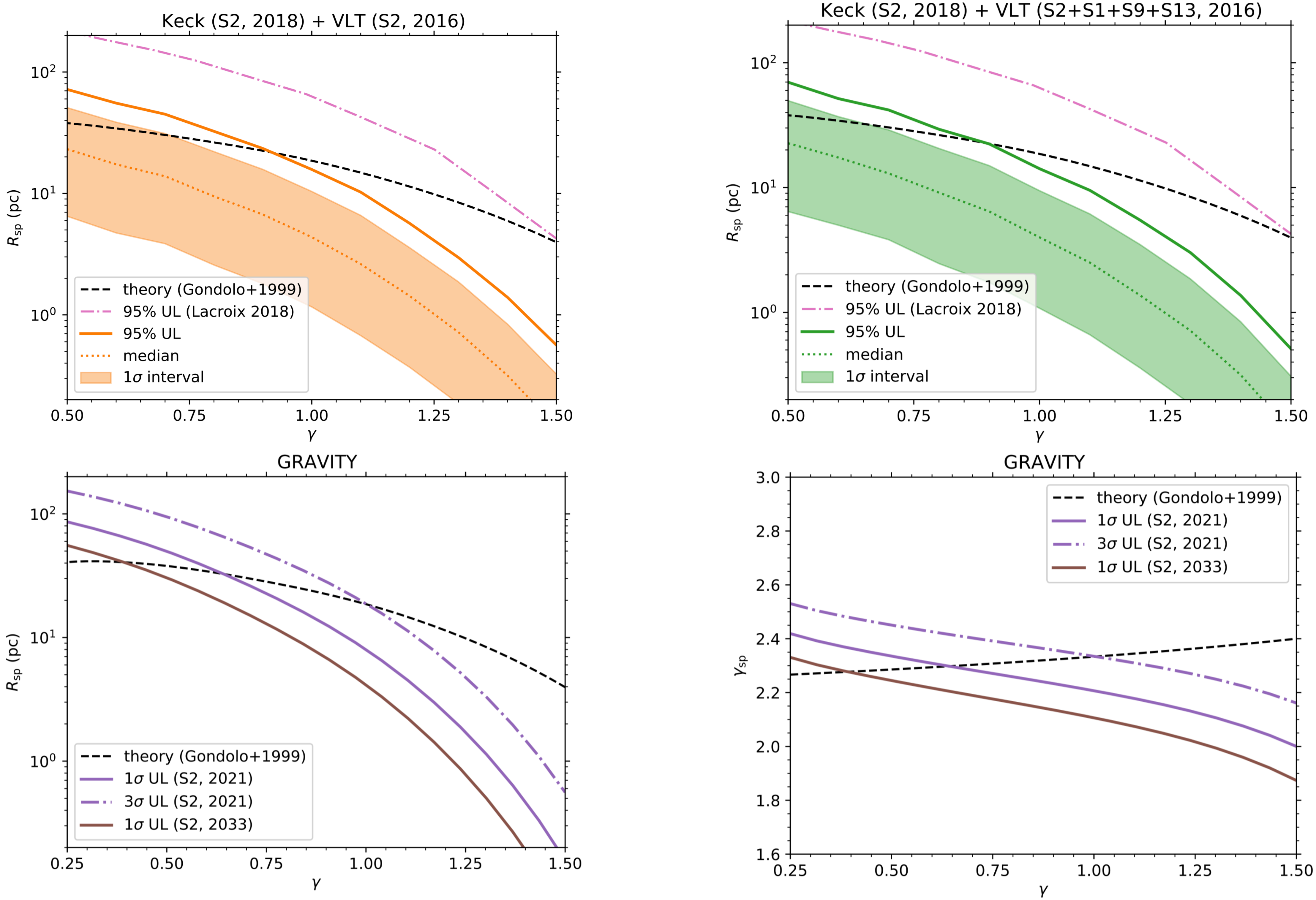

(1) The upper limits on the spike radius $R_{\rm sp}$ between S2 only and the four S-stars are negligible.

(2) We estimate the GRAVITY constraining power for the gNFW/Einasto spike.

(3) We also consider the effect of dark matter annihilation, and find that the surviving NFW spike infer the 95% lower limit of $\langle \sigma v \rangle \gtrsim 7.7 \times 10^{-27} \mathrm{cm^3 s^{-1}} \times (m_{\rm DM}/100\mathrm{GeV})(10\mathrm{Gyr}/\tau_{\rm BH})$

Zhao-Qiang Shen, Guan-Wen Yuan, et al, Exploring dark matter spike distribution around the Galactic centre with stellar orbits, Mon.Not.Roy.Astron.Soc. 527 (2024) 3196, [arXiv:2303.09284].

Fermionic Dark Matter@ICRANet

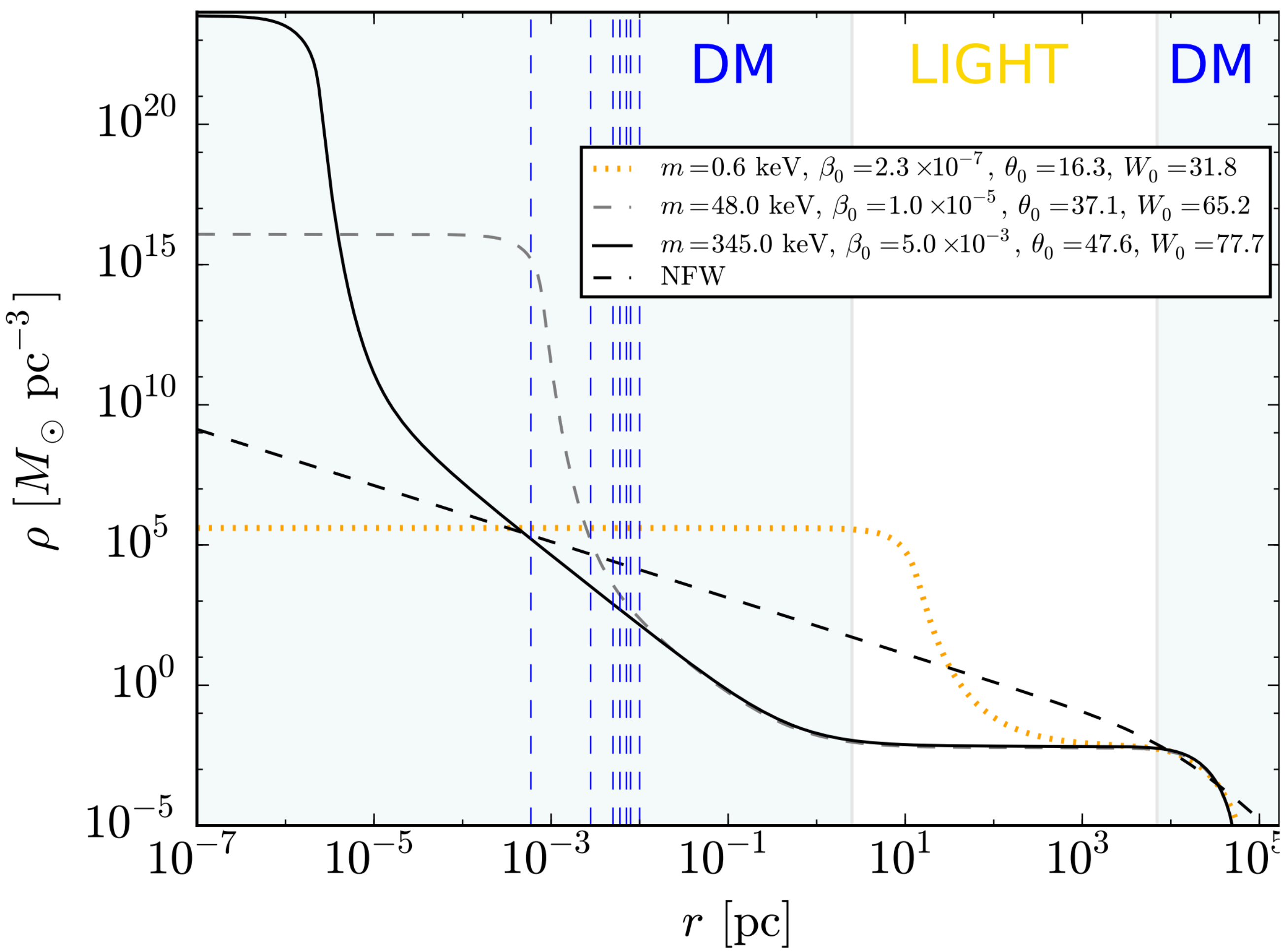

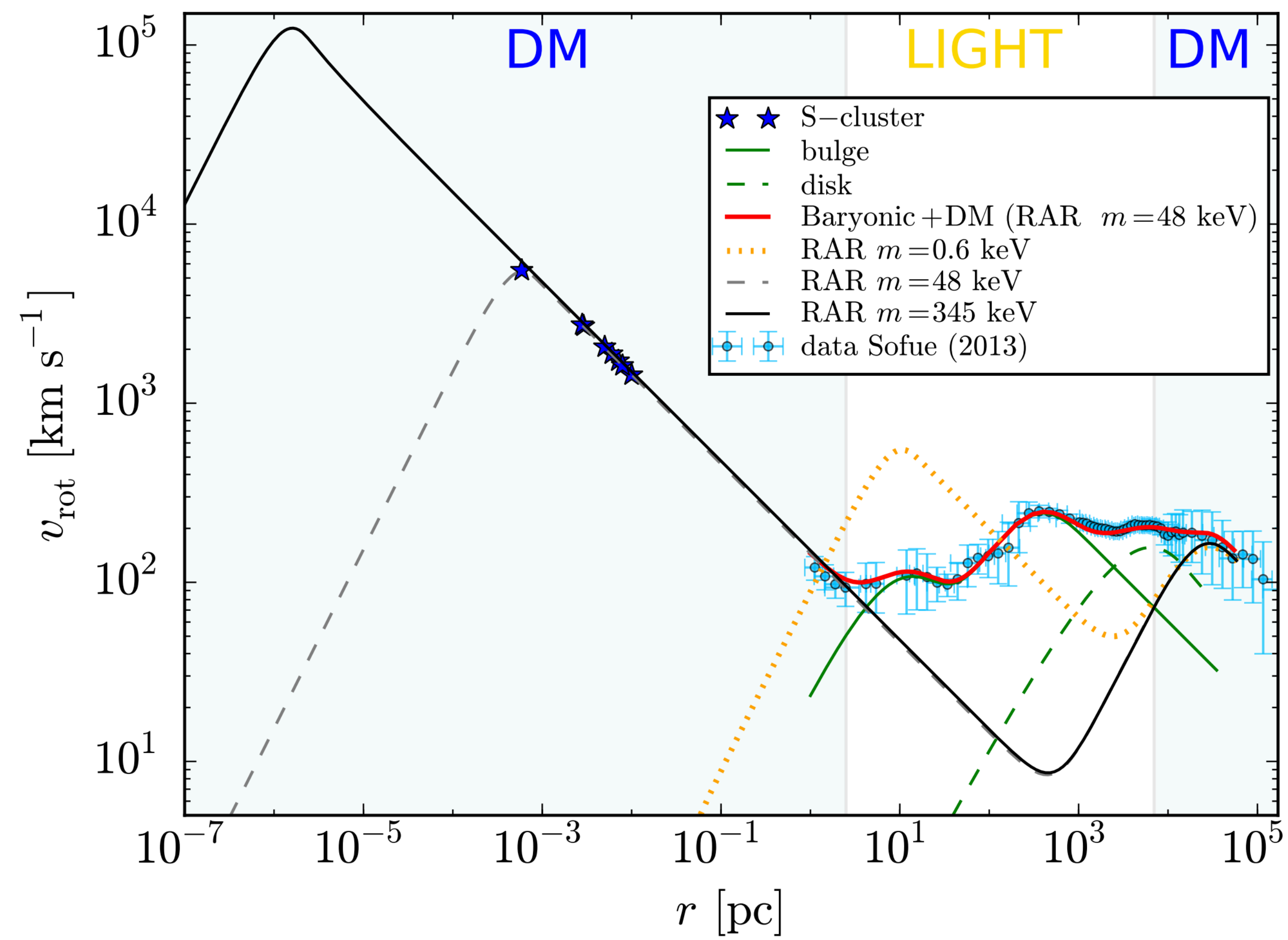

e.g

Argüelles, Carlos Raúl, et al. "Novel constraints on fermionic dark matter from galactic observables I: The Milky Way." *Physics of the Dark Universe* 21 (2018): 82-89.

Argüelles, Carlos Raúl, et al. "Novel constraints on fermionic dark matter from galactic observables II: Galaxy scaling relations." *Physics of the Dark Universe* 24 (2019): 100278.

Part III: Rapidly Growing PBHs as Seeds of the Massive High-Redshift JWST Galaxies

- Bondi Accretion of PBHs
- PBH Mass Functions
- JWST Observations and Hierarchical Bayesian Inference

The Challenge of SMBH Formation processes

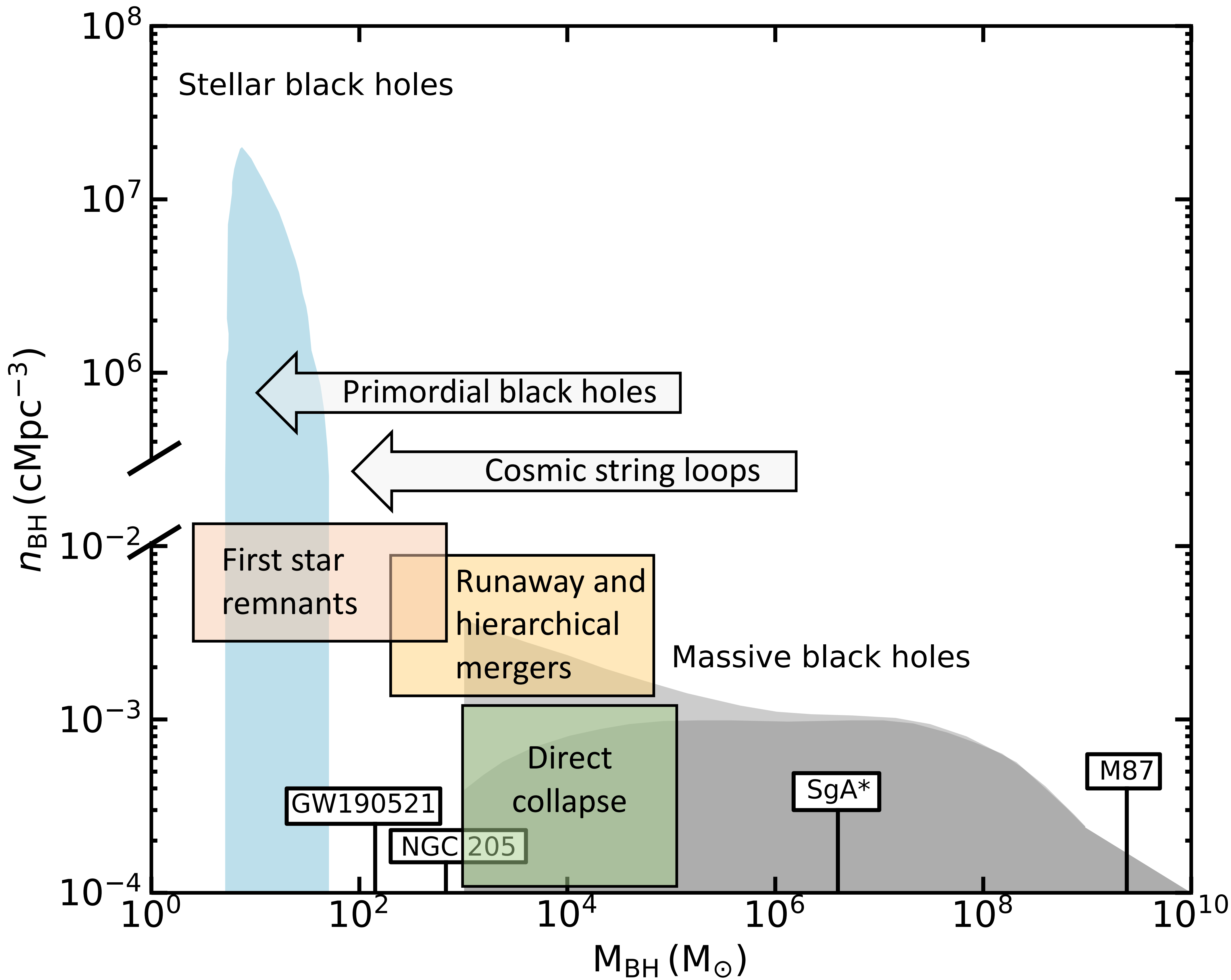

Marta Volonteri, Melanie Habouzit, and Monica Colpi, the origins of massive black holes, Nature Review Physics.(2022)

Source ID	R.A. (deg)	Decl. (deg)	$z_{\rm spec}$	$\log(M_\star/M_\odot)$	Reference
CEERS-61419	214.897232	52.843854	$8.998^{+0.001}_{-0.001}$	$7.78^{+0.30}_{-0.30}$	Fu23
CEERS-61381	214.901252	52.846997	$8.881^{+0.001}_{-0.001}$	$7.30^{+0.30}_{-0.30}$	Fu23
CEERS-7078	215.011708	52.988303	$8.876^{+0.002}_{-0.002}$	$8.08^{+0.24}_{-0.30}$	Fu23
CEERS-4702	214.994404	52.989378	$8.807^{+0.003}_{-0.003}$	$8.08^{+0.22}_{-0.30}$	Fu23
CEERS-4774	215.005185	52.996577	$8.005^{+0.001}_{-0.001}$	$8.30^{+0.27}_{-0.22}$	Fu23
CEERS-4777	215.005365	52.996697	$7.993^{+0.001}_{-0.001}$	$8.94^{+0.24}_{-0.31}$	Fu23
CEERS-23084	214.830685	52.887771	$7.769^{+0.003}_{-0.003}$	$9.49^{+0.22}_{-0.24}$	Fu23
CEERS-43725	214.967532	52.932953	$8.715^{+0.001}_{-0.001}$	$9.05^{+0.03}_{-0.02}$	He23
CEERS-81061	215.035392	52.890667	$8.679^{+0.001}_{-0.001}$	$10.0^{+0.01}_{-0.01}$	He23
EGS-11855	215.218762	53.069862	$8.610^{+0.001}_{-0.001}$	$9.47^{+0.04}_{-0.06}$	He23
EGS-34697	215.089714	52.966183	$8.175^{+0.001}_{-0.001}$	$9.04^{+0.10}_{-0.11}$	He23
CEERS-59920	214.882994	52.840416	$7.820^{+0.001}_{-0.001}$	$9.07^{+0.01}_{-0.01}$	He23
EGS-8901	215.188413	53.033647	$7.776^{+0.001}_{-0.001}$	$8.85^{+0.07}_{-0.06}$	He23
EGS-33634	215.150862	52.989562	$7.752^{+0.001}_{-0.001}$	$9.84^{+0.44}_{-0.66}$	J23
EGS-36986	214.999053	52.941977	$7.546^{+0.001}_{-0.001}$	$9.77^{+0.51}_{-0.69}$	J23
CEERS-16943	214.943152	52.942442	$11.416^{+0.005}_{-0.005}$	$8.6^{+0.3}_{-0.3}$	AH23
CEERS-11384	214.906640	52.945504	$11.043^{+0.003}_{-0.003}$	$8.7^{+0.1}_{-0.1}$	AH23
GS-z10-0	53.15884	-27.77349	$10.38^{+0.07}_{-0.06}$	$7.58^{+0.19}_{-0.20}$	La23
GS-z11-0	53.16476	-27.77463	$11.58^{+0.05}_{-0.05}$	$8.67^{+0.08}_{-0.13}$	La23
GS-z12-0	53.16634	-27.82156	$12.63^{+0.24}_{-0.08}$	$7.64^{+0.66}_{-0.39}$	La23
GS-z13-0	53.14988	-27.77650	$13.20^{+0.04}_{-0.07}$	$7.95^{+0.19}_{-0.29}$	La23
GN-z11	189.10608333	62.2420556	$10.603^{0.001}_{0.001}$	$8.73^{+0.06}_{-0.06}$	Bu23
Gz9p3	3.617193	-30.4255352	$9.3127^{+0.0002}_{-0.0002}$	$9.40^{+0.11}_{-0.10}$	Bo23

Table 1. (1) Source ID corresponds to galaxies. (2) Right Ascension (R.A.) in J2000 coordinates, (3) Declination (Decl.) in J2000 coordinates; (4)Spectroscopic redshift values obtained from measurements of emission lines. (5) Mass of galaxies.(6) Literatures reporting these sources. Fu23 (Fujimoto et al. 2023), He23 (Heintz et al. 2023), J23 (Jung et al. 2023), AH23 (Arrabal Haro et al. 2023), La23 (Curtis-Lake et al. 2023), Bu23 (Bunker et al. 2023), and Bo23 (Boyett et al. 2023).

JWST observed a large number of high-redshift galaxies, prompting us to question how such massive and numerous galaxies (and their central massive black holes) could have formed just ~500 Myr after the Big Bang.

The empirical relationship between the galaxy mass $M_\star$ and its central M_{BH} is $M_{BH} = \alpha + \beta \log(M_\star/M_0) + \epsilon \log(1+z)$

Project5—Bondi Accretion of Naked/DM Clothing PBHs

Bondi-Hoyle mass accretion rate: $$\dot{M}_{\rm B} = 4\pi\lambda m_H n_{\rm gas} v_{\rm eff} r_{\rm B}^2,$$

The accretion parameter λ takes into account the effects of the Hubble expansion, the gas viscosity, and the coupling of the CMB radiation to the gas through Compton scattering.

$$\lambda = \exp\left(\frac{9/2}{3+\hat{\beta}^{0.75}}\right) x_{\rm cr}^2,$$

Dark halo around each PBH as $\rho \sim r^{\alpha}$, is a dominant DM component. While direct accretion of DM is negligible for PBH evolution, the effect of this DM clothing is to enhance the gas accretion rate, acting in this way as a catalyst.

$$M_h(z) = 3M\left(\frac{1+z}{1000}\right)^{-1},$$

$$r_h = 0.019\ \mathrm{pc}\left(\frac{M}{M_\odot}\right)^{1/3}\left(\frac{1+z}{1000}\right)^{-1},$$

$$\kappa \equiv \frac{r_{\rm B}}{r_h} = 0.22\left(\frac{1+z}{1000}\right)\left(\frac{M_h}{M_\odot}\right)^{2/3}\left(\frac{v_{\rm eff}}{\mathrm{km\ s^{-1}}}\right)^{-2}.$$

$$\hat{\beta}^h \equiv \kappa^{\frac{p}{1-p}}\hat{\beta}, \quad \lambda^h \equiv \bar{\Upsilon}^{\frac{p}{1-p}}\lambda(\hat{\beta}^h), \quad r_{\rm cr}^h \equiv \left(\frac{\kappa}{2}\right)^{\frac{p}{1-p}} r_{\rm cr},$$

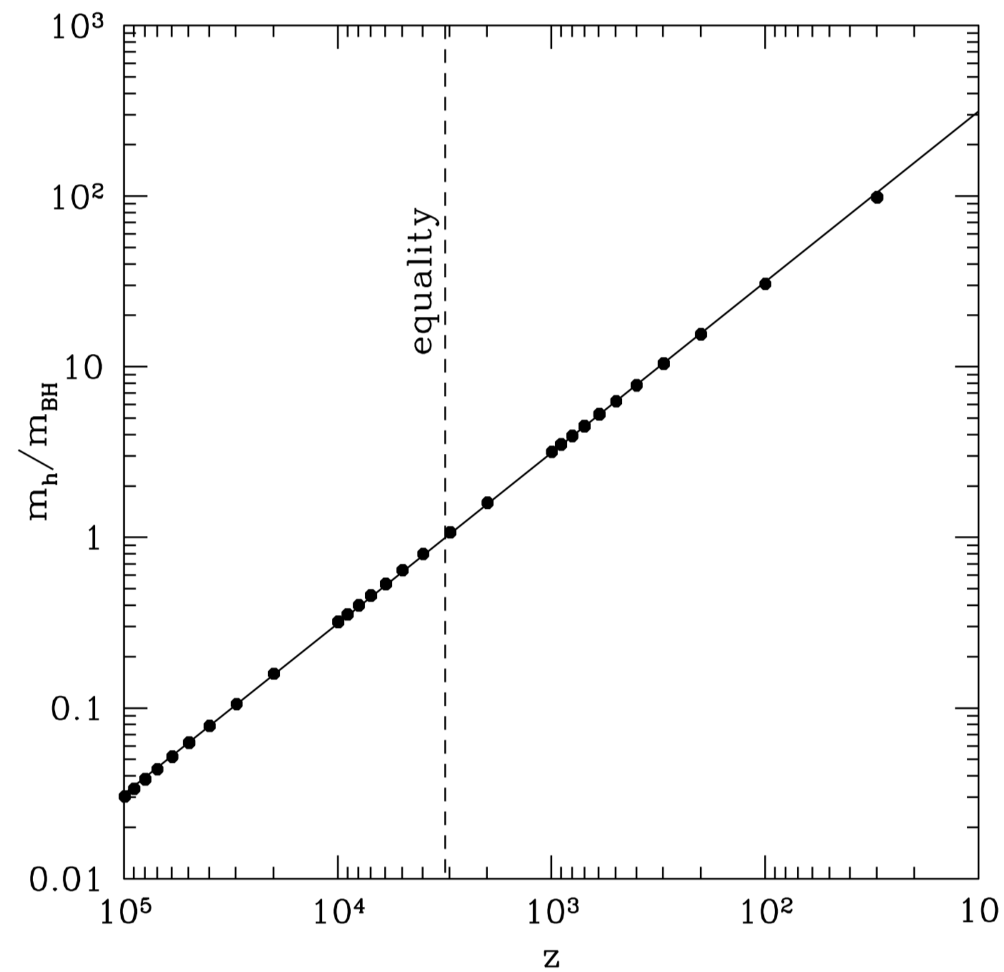

Fig. 1.—Accreted halo mass vs. redshift. The halo radius is defined at an overdensity of $\delta = 2$. We include a dashed line to indicate the redshift of matter-radiation equality.

[1]Massimo Ricotti, Bondi accretion in the early universe, ApJ(2007)
[2]Katherine J. Mack, Jeremiah P. Ostriker, Growth of structure seeded by primordial black holes, ApJ(2007)
[3]Massimo Ricotti, Katherine J. Mack, Jeremiah P. Ostriker, Effect of primordial black holes on the cosmic microwave background and cosmological parameter estimates, ApJ(2008).
[4] Yacine Ali-Haimoud, Marc Kamionkowski, Cosmic microwave background limits on accreting PBHs, PRD(2017).

Mechanical Feedback in Accretion

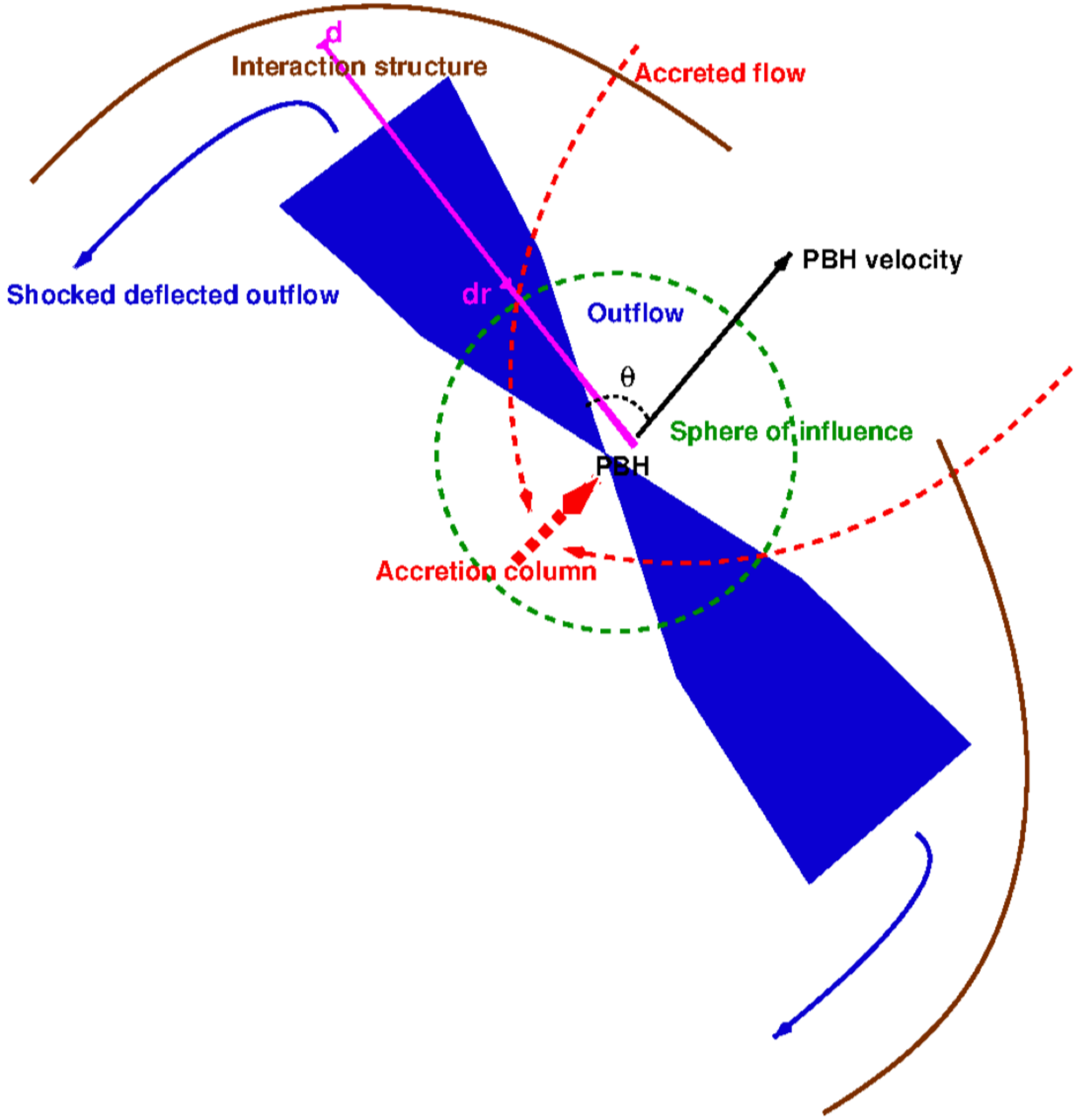

$$\dot{M}_{\rm acc} = f_{\rm MF} \times 4\pi\lambda m_H n_{\rm gas} v_{\rm eff} r_{\rm B}^2$$

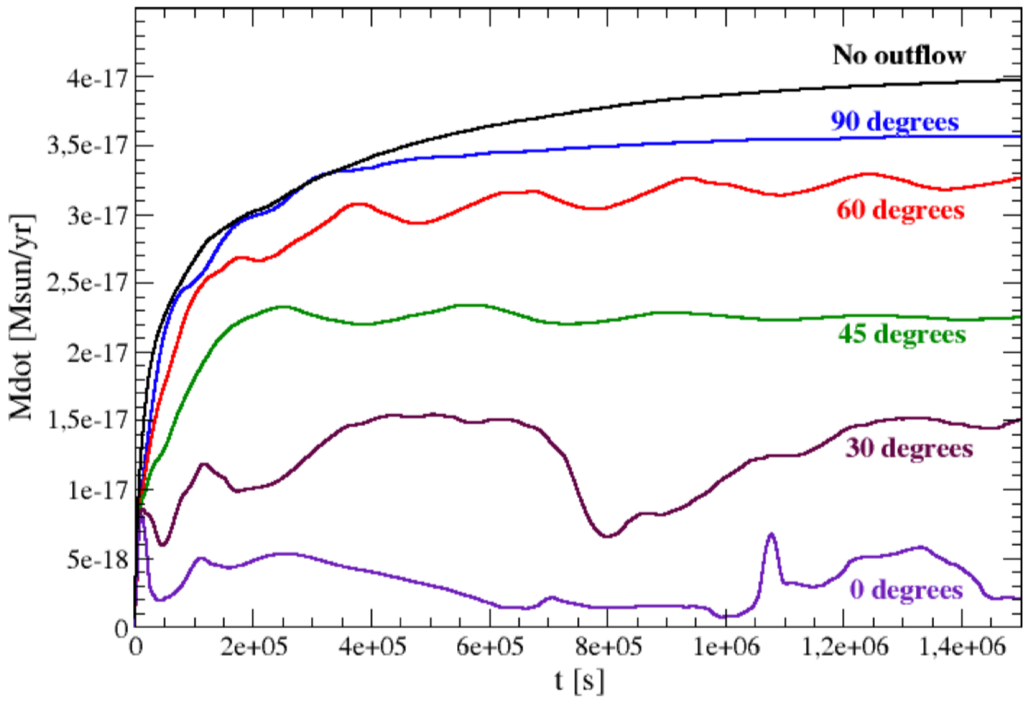

Fig. 8: Accretion rate for the reference cases (from top to bot-

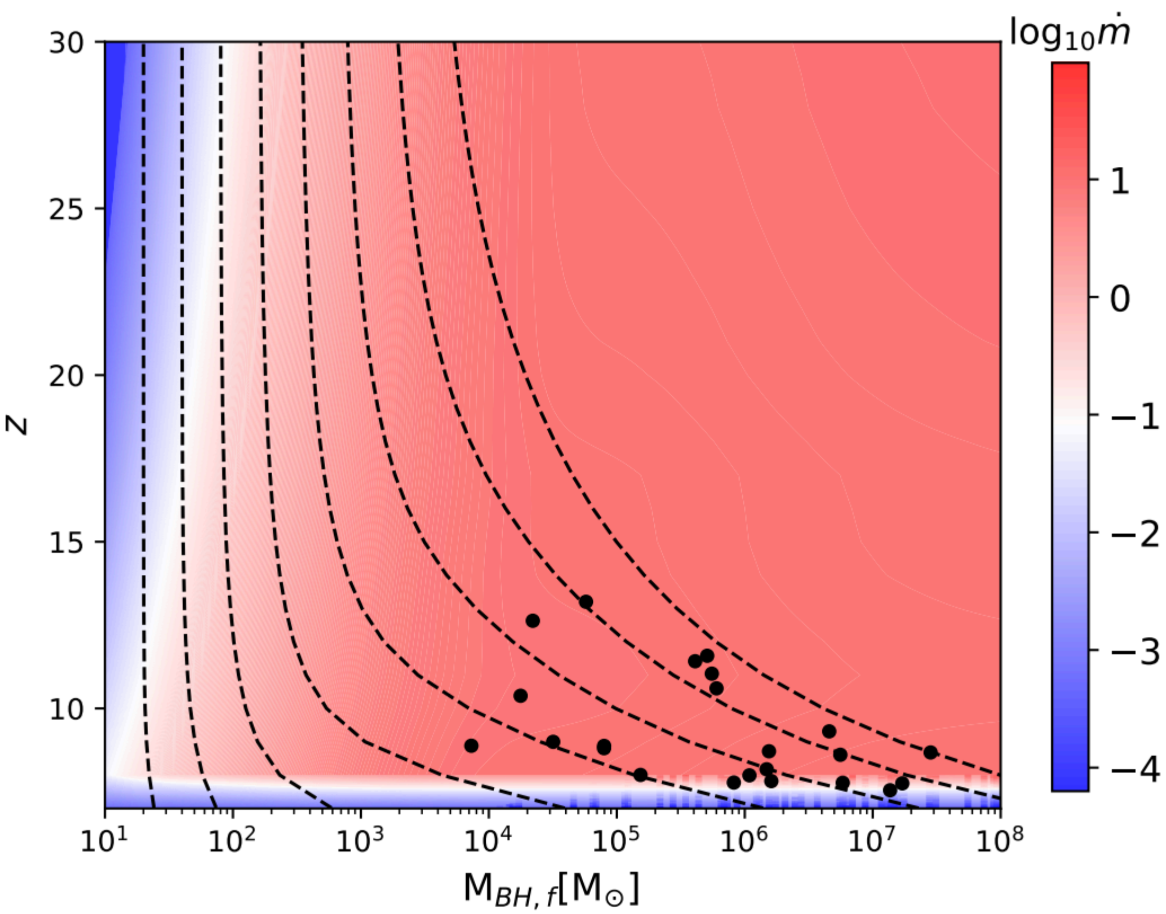

[1]Valenti Bosch-Ramon, Nicola Bellomo, Mechanical feedback effects on primordial black hole accretion , A&A(2020)
[2]Valenti Bosch-Ramon, 3D hydrodynamical simulations of the impact of mechanical feedback on accretion in supersonic stellar-mass black hole, A&A(2022)

$M_\star - M_{BH}$ Relation

An empirical relationship between M_{BH} and the galaxy mass $M_\star$ is

$$M_{BH} = \alpha + \beta \log(M_\star/M_0) + \epsilon \log(1+z)$$

we take the best-fit intercept for early-type galaxies, $\alpha = 7.89 \pm 0.09$, $\beta = 1.33 \pm 0.12$ and $\epsilon = 0.2$

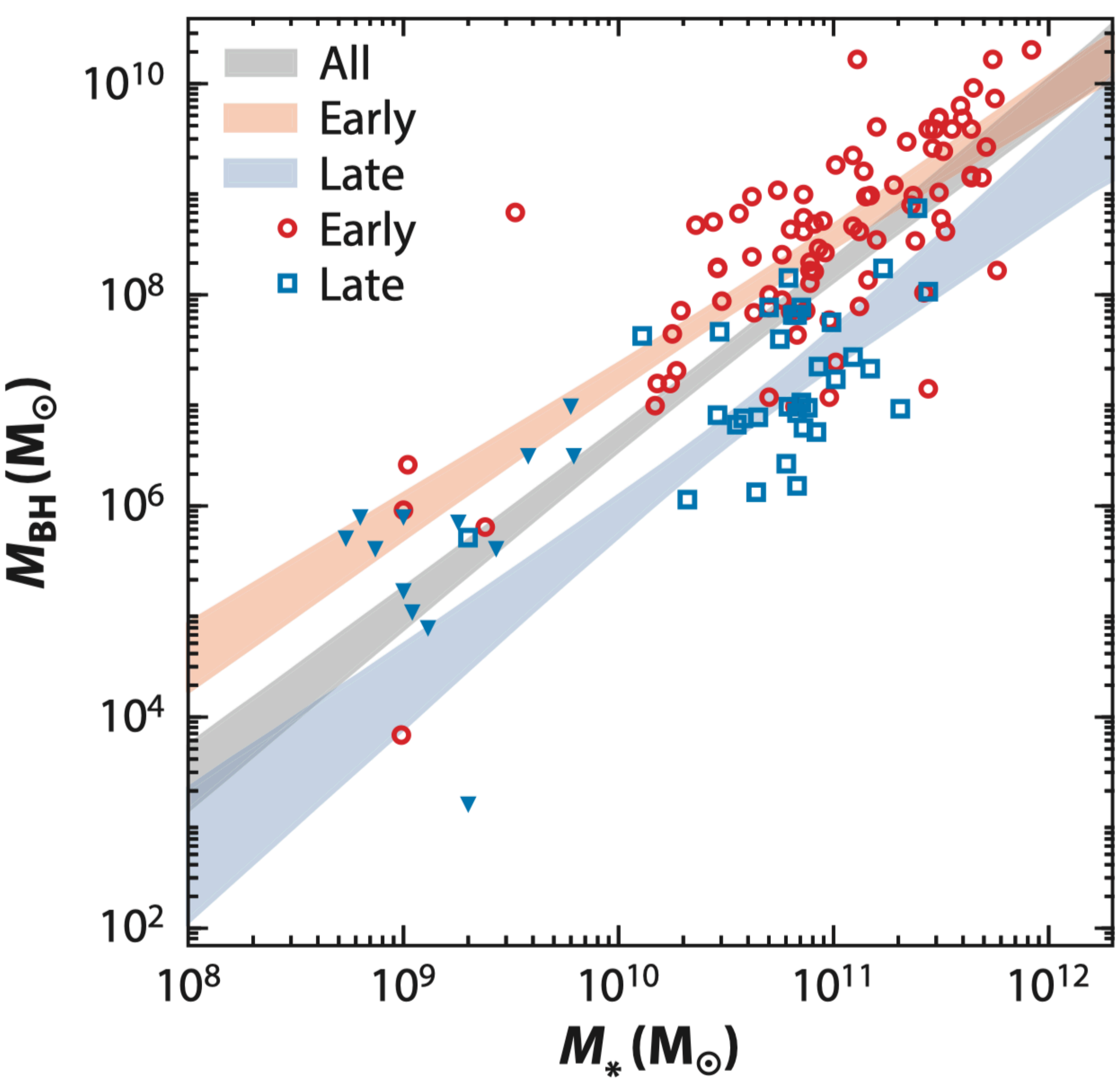

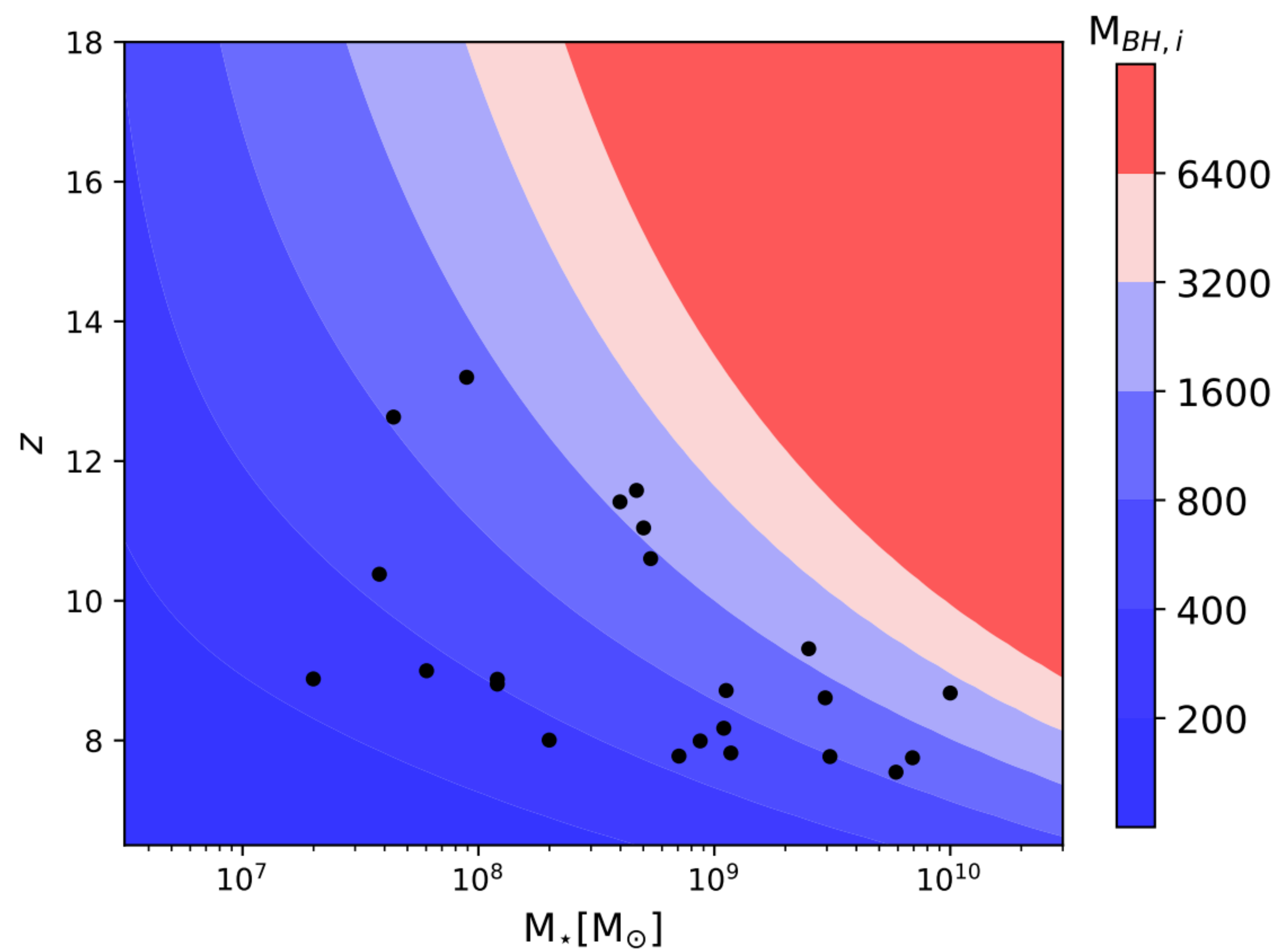

Jenny E. Greene, Jay Strader and Luis C. Ho, Intermediate-Mass Black Holes, Ann. Rev. Astro. Astrophys.(2020)

Exploring PBH Mass Distribution with JWST Observations

The Bondi accretion will affect the mass distribution of PBHs with redshift, and the evolution of an initial PBH's mass function $\psi(M, z_i)$ at formation redshift z_i is governed by:

$$\psi(M_f(M,z),z)dM_f = \psi(M,z_i)dM.$$

To distinguish various forms of theoretically predicted PBH mass functions, we consider the following typical PBH mass functions that arise in PBH formation models,

$$\psi_M = \begin{cases} \frac{1}{\sqrt{2\pi}\sigma M}\exp(-\frac{\log^2(\mathrm{M}/\mathrm{M_c})}{2\sigma^2}) & \textbf{Lognormal}, \\ \sum_{n=1} A_n \delta(M - M_{cn}) & \textbf{Multipeak}, \\ \frac{1}{2}\frac{M_c^{1/2}}{M^{3/2}}\Theta(M - M_c) & \textbf{Powerlaw}, \\ \frac{1}{\sqrt{2\pi}\sigma}\exp(-\frac{(\mathrm{M}-\mathrm{M_c})^2}{2\sigma^2}) & \textbf{Gaussian}, \\ \frac{3.2}{M}\left(\frac{M}{M_c}\right)^{3.85}\exp^{-\left(\frac{M}{M_c}\right)^{2.85}} & \textbf{Critical}. \end{cases}$$

Where $\Theta(M - M_c)$ is the step function, and the M_c, M_{cn} and σ are parameters in these distributions. For the Multipeak model, we use two normalized Gaussian distribution with the same width in our analysis, as the evolution of $\delta(M - M_{cn})$.

Hierarchical Bayesian Inference

We use the masses of high-redshift galaxies observed by JWST to constrain the hyper-parameters $\boldsymbol{\lambda}$ of each initial PBH mass function though hierarchical Bayesian inference. For a series of N independent observations, the posterior distribution for $\boldsymbol{\lambda}$ is given by

$$p(\boldsymbol{\lambda} \mid \boldsymbol{d}) = \pi(\boldsymbol{\lambda}) \prod_{i}^{N} \int \mathcal{L}(d_i \mid \theta_i) p_{\mathrm{pop}}(\theta_i \mid \boldsymbol{\lambda}) \mathrm{d}\theta_i,$$

- $\mathscr{L}(d_i \mid \theta_i)$ is the likelihood of the JWST data given a galaxy's properties θ_i (mass and redshift).
- the distribution of θ_i satisfies $p_{\mathrm{pop}}(\theta_i \mid \boldsymbol{\lambda}) = p(m)p(z)$;
- $p(z)$ is the mass distribution of galaxies, which is calculated from the initial PBH mass function;
- the galaxies are assumed distributing uniformly in the co-moving frame of the Universe;
- we assign Uniform priors $\pi(\boldsymbol{\lambda})$ for all of the hyper-parameters.

Models	x_e	M_c	σ	M_{c2}	f_{M_c}	N_{dof}	$\Delta \ln \mathcal{B}$	ΔAIC
Lognormal	$0.54^{+0.32}_{-0.36}$	$748.39^{+130.50}_{-111.08}$	$0.74^{+0.14}_{-0.11}$	-	-	2	16.25	0.00
Powerlaw	$0.60^{+0.28}_{-0.36}$	$242.65^{+34.43}_{-34.83}$	-	-	-	1	14.28	8.36
Multipeak	$0.45^{+0.37}_{-0.31}$	$675.16^{+167.36}_{-152.24}$	$457.38^{+173.04}_{-116.23}$	$1956.69^{+505.87}_{-420.64}$	$0.77^{+0.13}_{-0.16}$	4	13.20	8.22
Gaussian	$0.42^{+0.37}_{-0.29}$	$947.99^{+155.29}_{-150.46}$	$692.58^{+141.08}_{-105.48}$	-	-	2	9.78	10.68
Critical	$0.18^{+0.27}_{-0.13}$	$1142.07^{+94.12}_{-80.16}$	-	-	-	1	0.00	31.26

- According to Jeffreys' scale criterion, a Bayes factor larger than $(10, 10^{1.5}, 10^2)$ or $(e^{2.30}, e^{3.45}, e^{4.61})$ would imply a strong, very strong, or decisive Bayesian evidence.
- We also calculate the Akaike information criterion (AIC) to compare models with different numbers of parameters. The AIC penalizes models with more parameters, and a difference of ΔAIC of 2 or more indicates strong evidence against the model with the higher AIC value.

The posterior population distribution of PBH models

- The presence of some $\sim 500 M_\odot$ PBHs act as seeds for early galaxies formation with mass of $\sim 10^7 - 10^{10} M_\odot$ at $z \sim 8$, hence accounting for the JWST observations.
- We find the observations of JWST could distinguish the various PBH mass functions, and the Lognormal model with the $M_c \sim 750 M_\odot$ is strongly preferred over other hypotheses.
- Our analysis also highlights the importance of statistical analysis in making conclusion about the PBHs population and their implications for early cosmology.

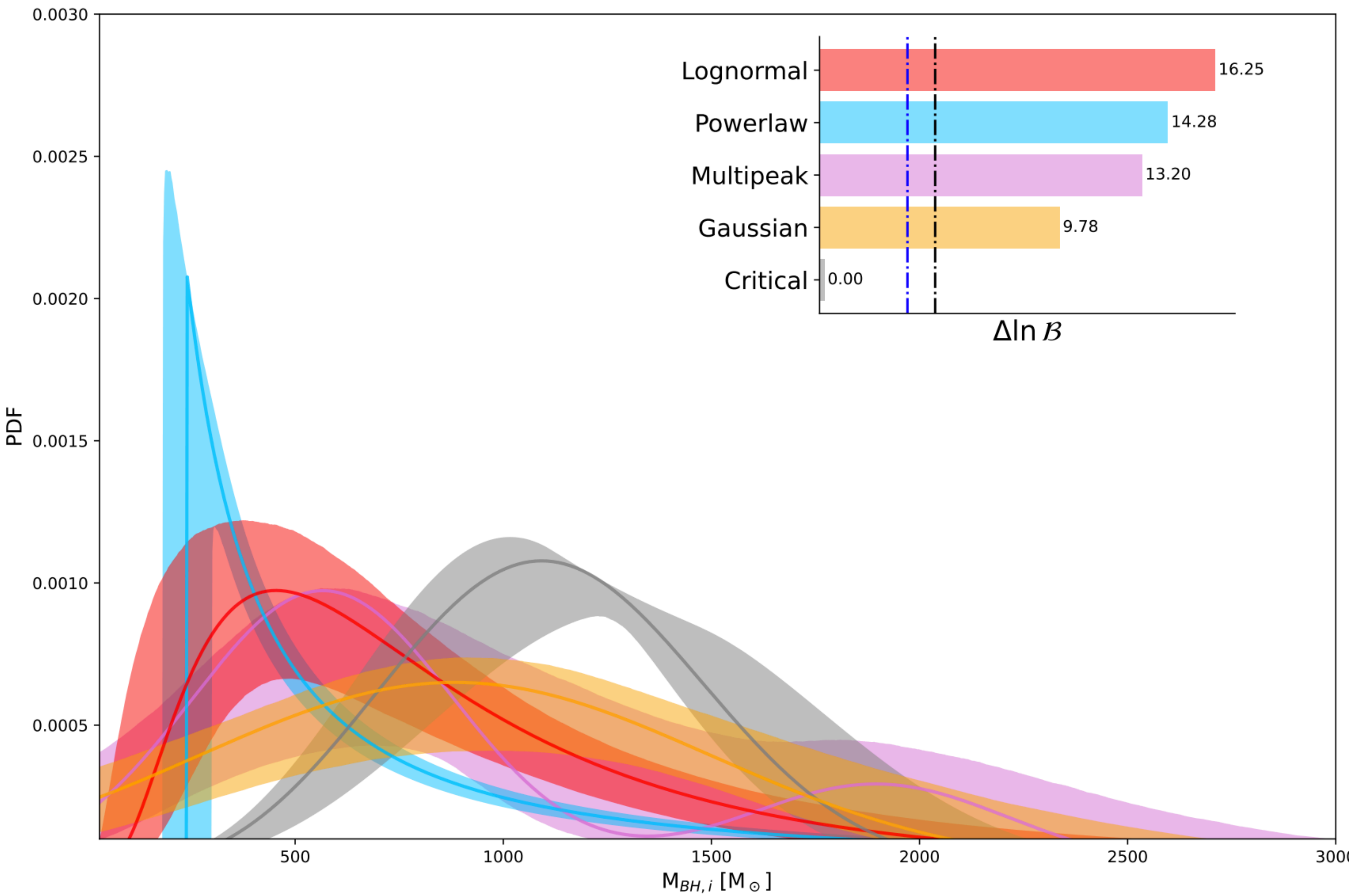

Guan-Wen Yuan, et al, Rapidly growthing primordial black holes as seeds of the massive high-redshift JWST Galaxies, Sci.China Phys.Mech.Astron. 67 (2024) 10, 109512, [arXiv: 2306.17143].

Part IV: Exploring DM distribution with stochastic gravitational wave background

A New Milestone in GW Astronomy@2023

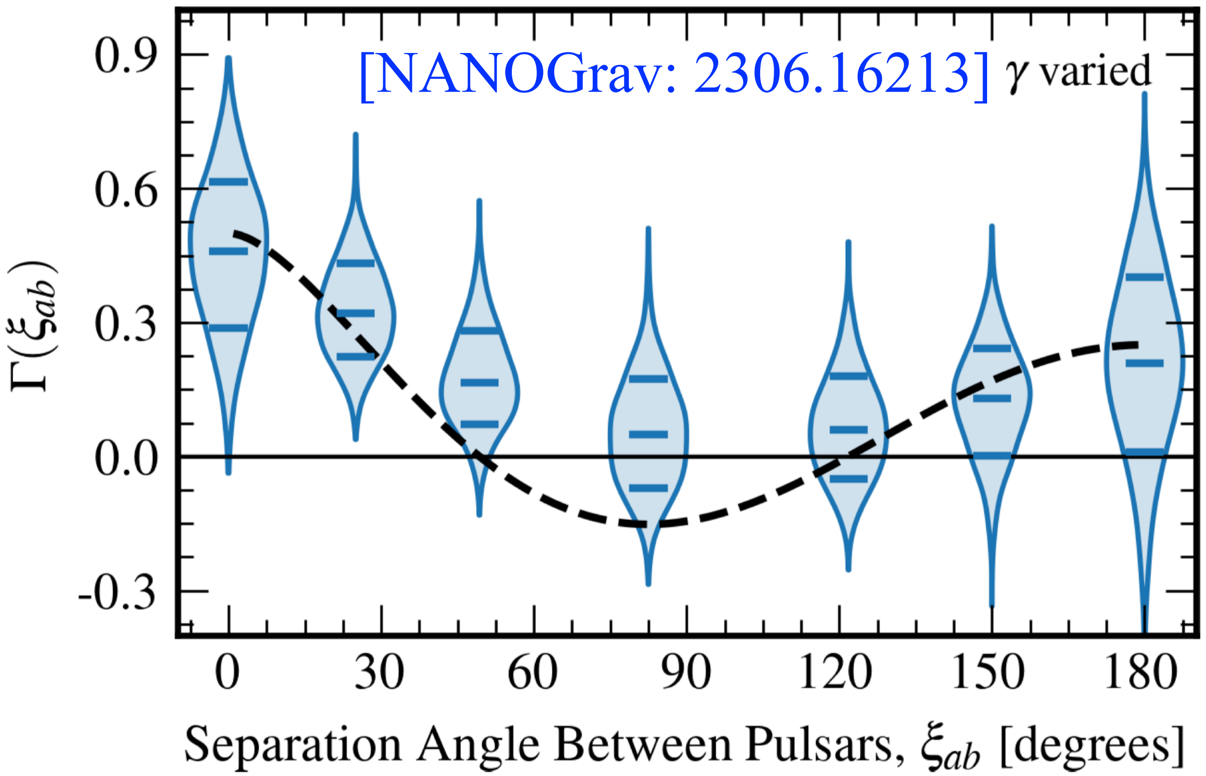

NANOGrav 15yr > 3.5σ

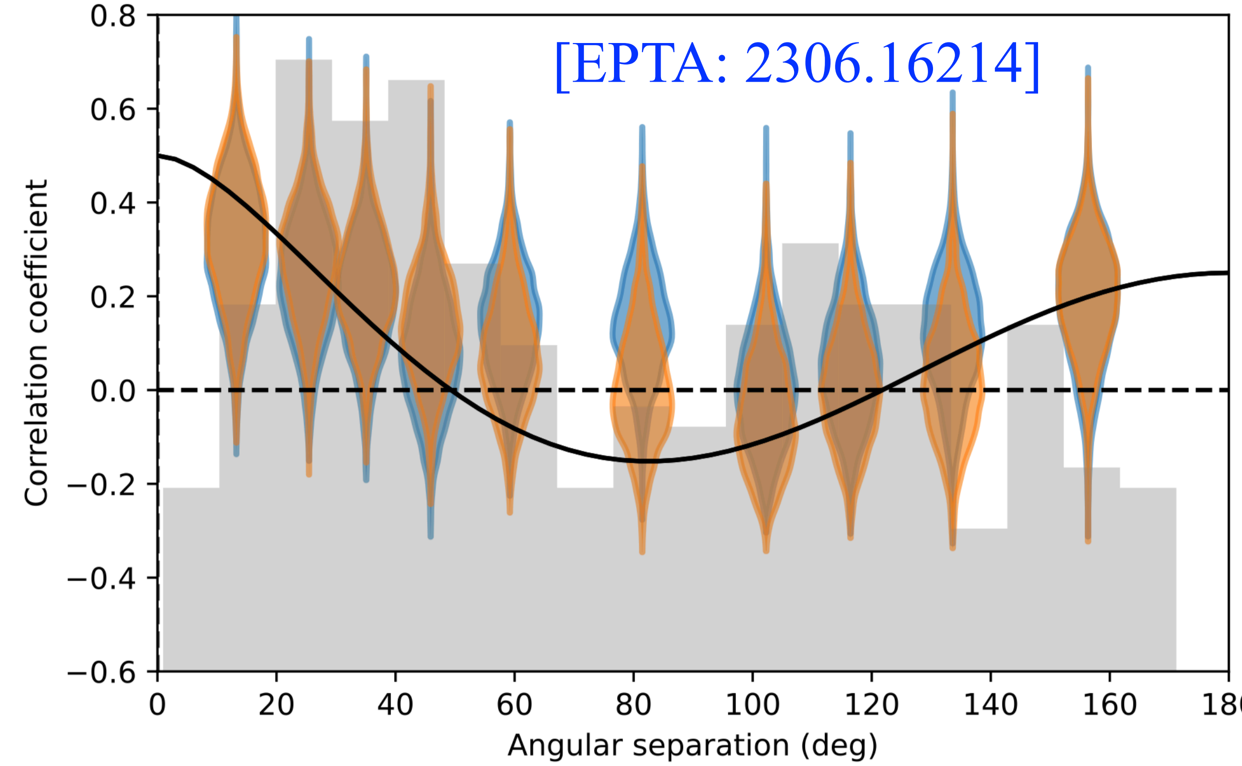

EPTA DR2 > 3σ

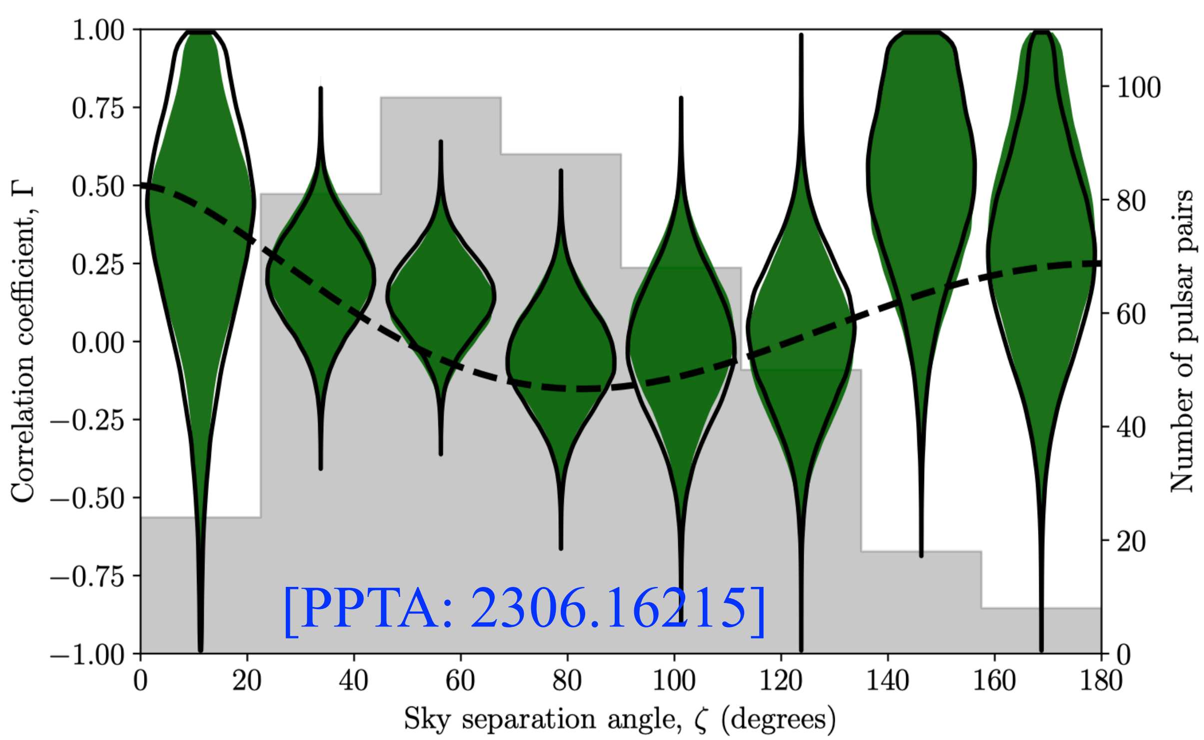

PPTA DR3~2σ

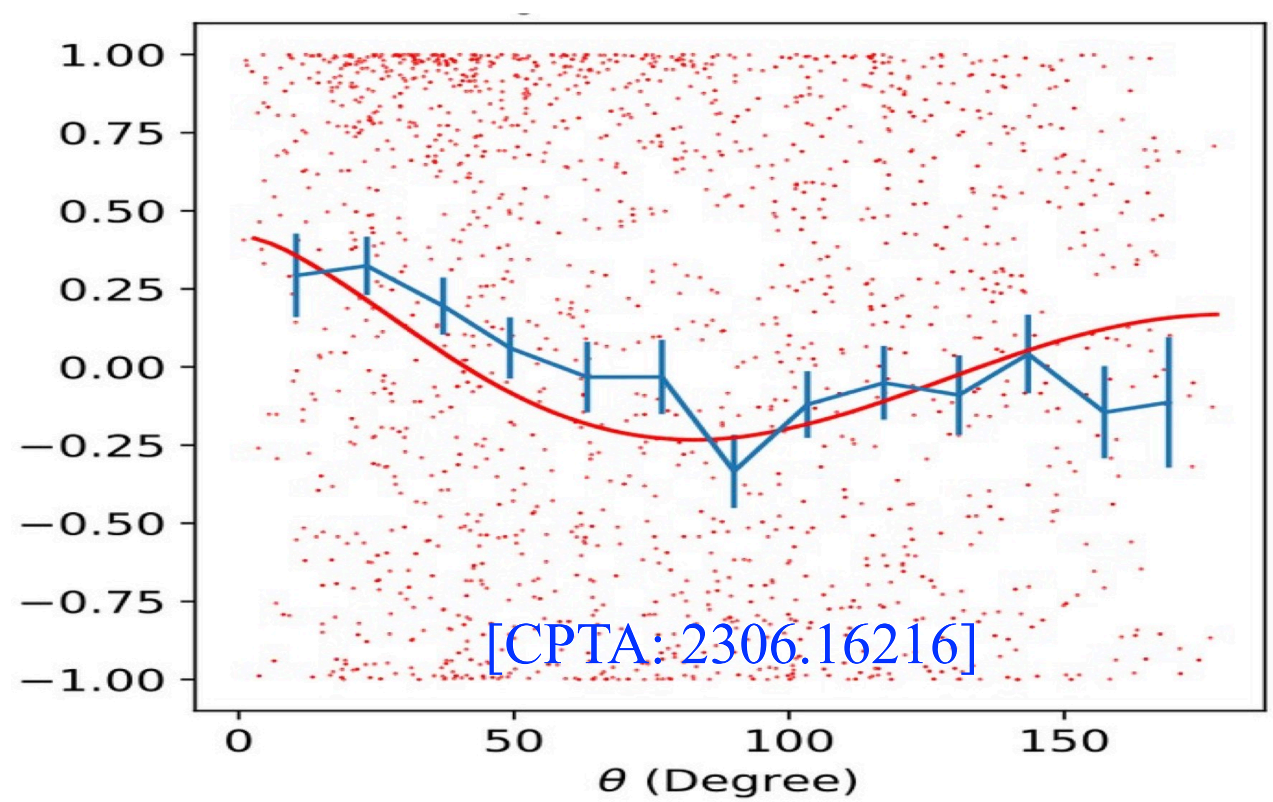

CPTA DR1~4.6σ

Orbital Evolution of SMBH Binary

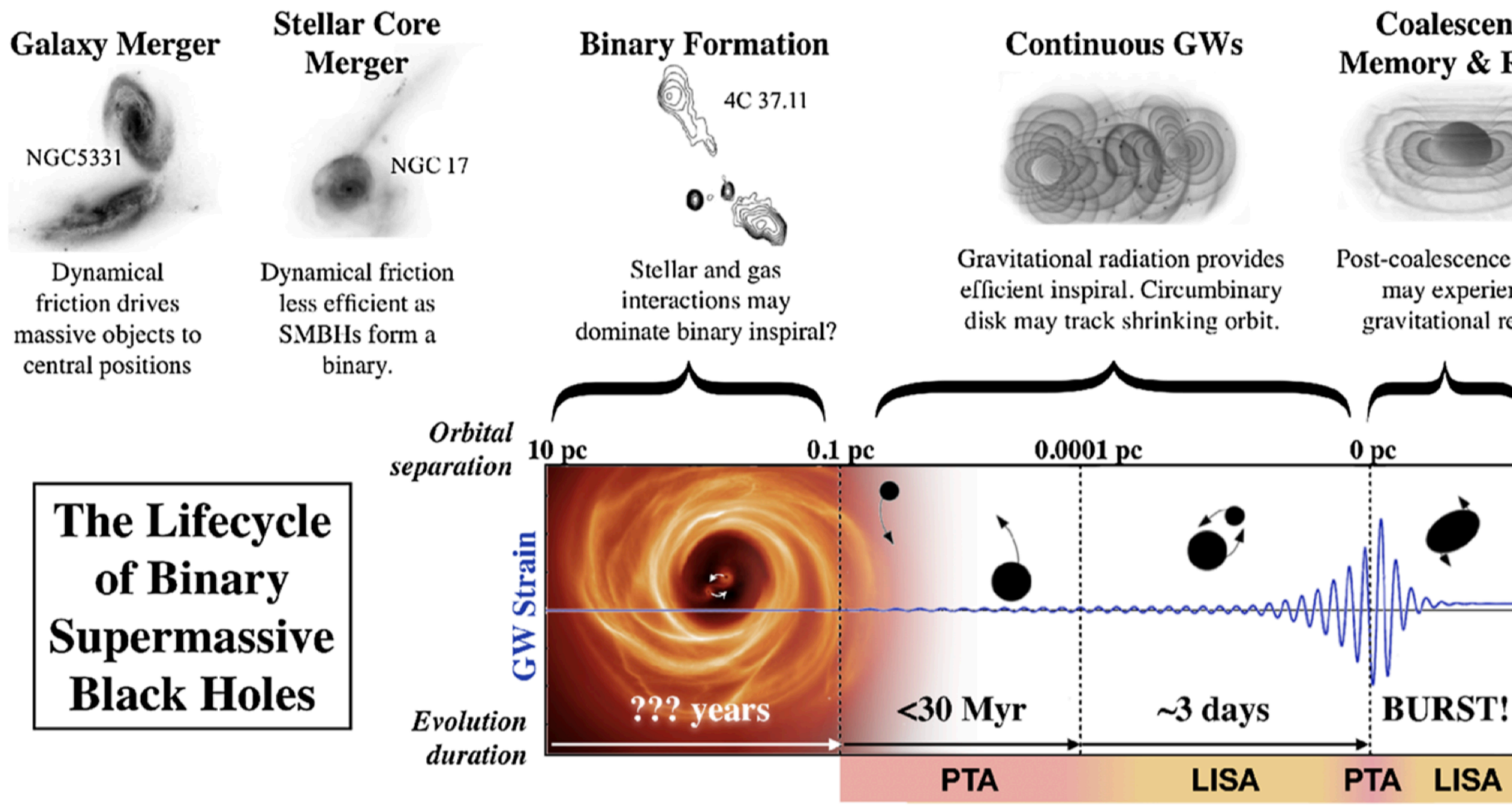

Sarah Burke-Spolaor et al, The astrophysics of nanohertz gravitational wave, The Astronomy and Astrophysics Review(2019).

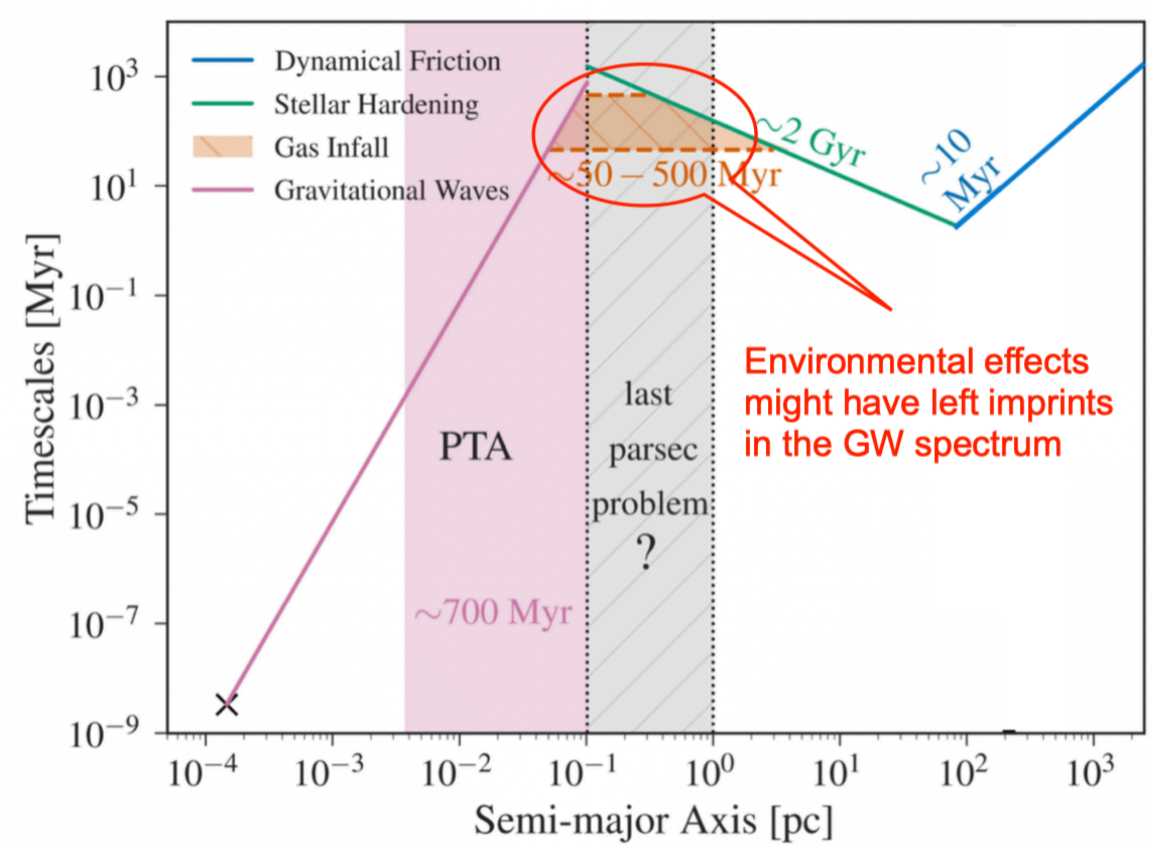

[J. Weaver: Astrobites (2019)]

- Dynamical friction
  - Drag force
- Stellar Hardening
  - Stellar loss-cone scattering
- Gas infall
  - Viscous circum-binary disk interaction
- GW inspiral
  - Decouple from astro environment
  - GW-driven orbital evolution

Lose energy and angular momentum

Time

Theoretical Analysis

typical time scale associated with the viscous circumbinary gas and disk interaction on GW spectrum can be parametrized as [8, 9]

$$t_{\rm env} \equiv -\frac{R}{\dot{R}} \propto R^{\beta} \propto f_r^{-2\beta/3} \,, \tag{16}$$

where β is determined by the environment model and in general well below the benchmark value 4, as shown below Eq. (14). Since

$$\frac{{\rm d}E_{\rm GW}}{{\rm d}\ln f_r} = \frac{{\rm d}E_{\rm GW}}{{\rm d}t}\frac{{\rm d}t}{{\rm d}\ln f_r} = \frac{{\rm d}E_{\rm GW}}{{\rm d}t}\frac{{\rm d}t}{{\rm d}\ln R}\frac{{\rm d}\ln R}{{\rm d}\ln f_r} = \frac{2}{3}\frac{{\rm d}E_{\rm GW}}{{\rm d}t}t_{\rm env} \,, \tag{17}$$

where $\frac{{\rm d}E_{\rm GW}}{{\rm d}t}$ is calculated by Eq. (11), which is only determined by GW dynamics. We also used Kepler's law, $f_r \sim R^{-\frac{3}{2}}$ and the definition of t_{env}. The energy spectrum of GWs is calculated by

$$\begin{aligned} \Omega_{\rm gw}(f_r) \sim h_c^2(f_r) &\sim \int dz dm_1 dm_2 \frac{\partial n}{\partial m_1 \partial m_2 \partial z}\frac{1}{1+z}\frac{dE_{gw}}{d\ln f_r} \\ &= \int dz dm_1 dm_2 \frac{\partial n}{\partial m_1 \partial m_2 \partial z}\frac{1}{1+z}\frac{2}{3}\frac{dE_{gw}}{dt}t_{env} \\ &= \int dz dm_1 dm_2 \frac{\partial n}{\partial m_1 \partial m_2 \partial z}\frac{1}{1+z}\frac{2}{3}\frac{dE_{gw}}{dt}t_{GW}\frac{t_{env}}{t_{GW}} \end{aligned} \tag{18}$$

If we don't consider the impact of the environment, the energy spectrum

$$\Omega_0 \sim \int dz dm_1 dm_2 \frac{\partial n}{\partial m_1 \partial m_2 \partial z}\frac{1}{1+z}\frac{2}{3}\frac{dE_{gw}}{dt}t_{GW}$$

$$-\frac{{\rm d}E_{\rm orb}}{{\rm d}t} = \frac{{\rm d}E_{\rm GW}}{{\rm d}t} + \frac{{\rm d}E_{\rm env}}{{\rm d}t}$$

The emitted power $\frac{dE_{GW}}{dt}$ is solely determined by the masses of the objects involved and the geometry of their orbit, thus $\Omega_{gw}(f_r)$ can be expressed as [9]

$$\Omega_{\rm gw}(f_r) = \Omega_0(f_r)\frac{t_{\rm env}}{t_{\rm GW}} \,, \tag{20}$$

where $\Omega_0(f_r)$ refers to the pure GW case, given by $\Omega_0(f_r) = A_{gw}^2 \frac{2\pi^2}{3H_0^2}\left(\frac{f_r}{f_{ref}}\right)^{\frac{2}{3}}$.

Project6—Dark Matter Surrounding SMBHB enhance SGWB

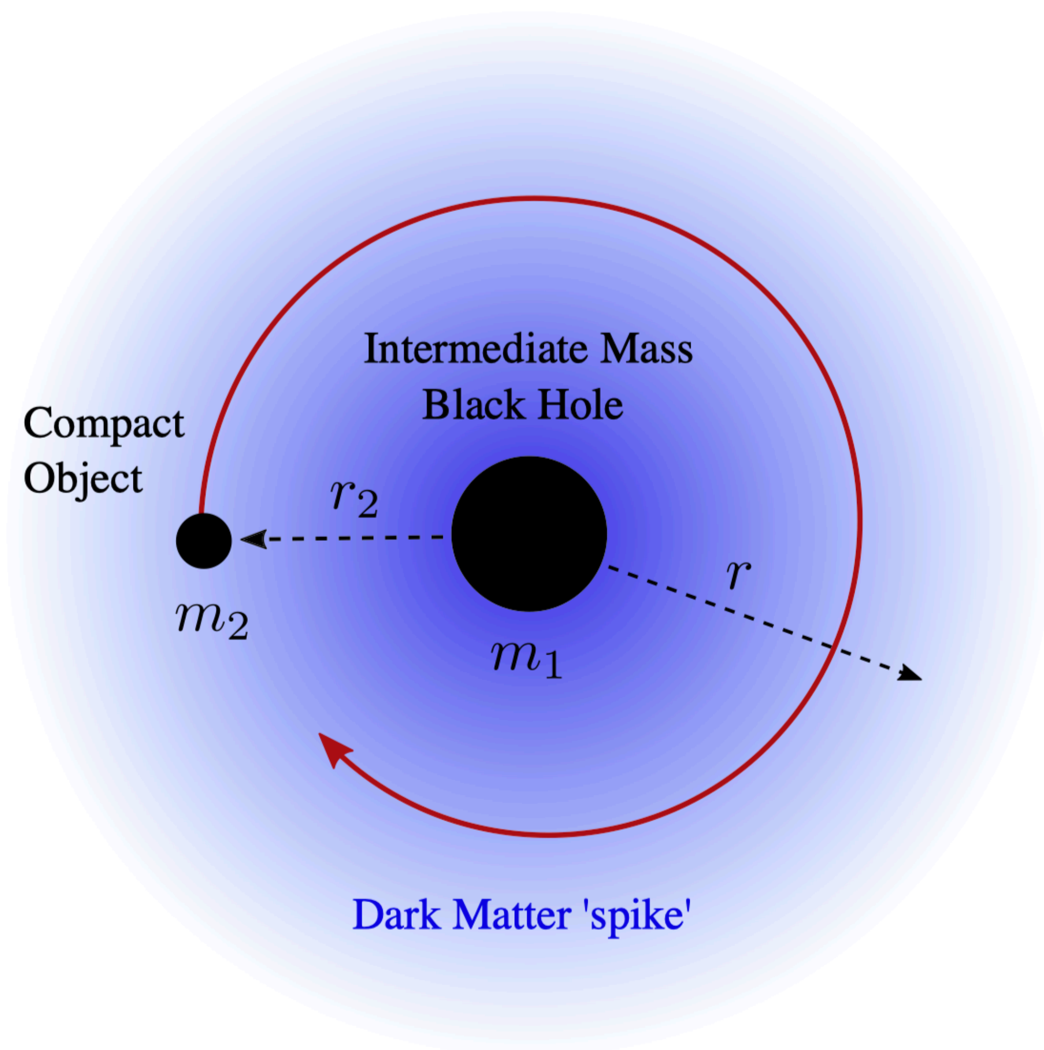

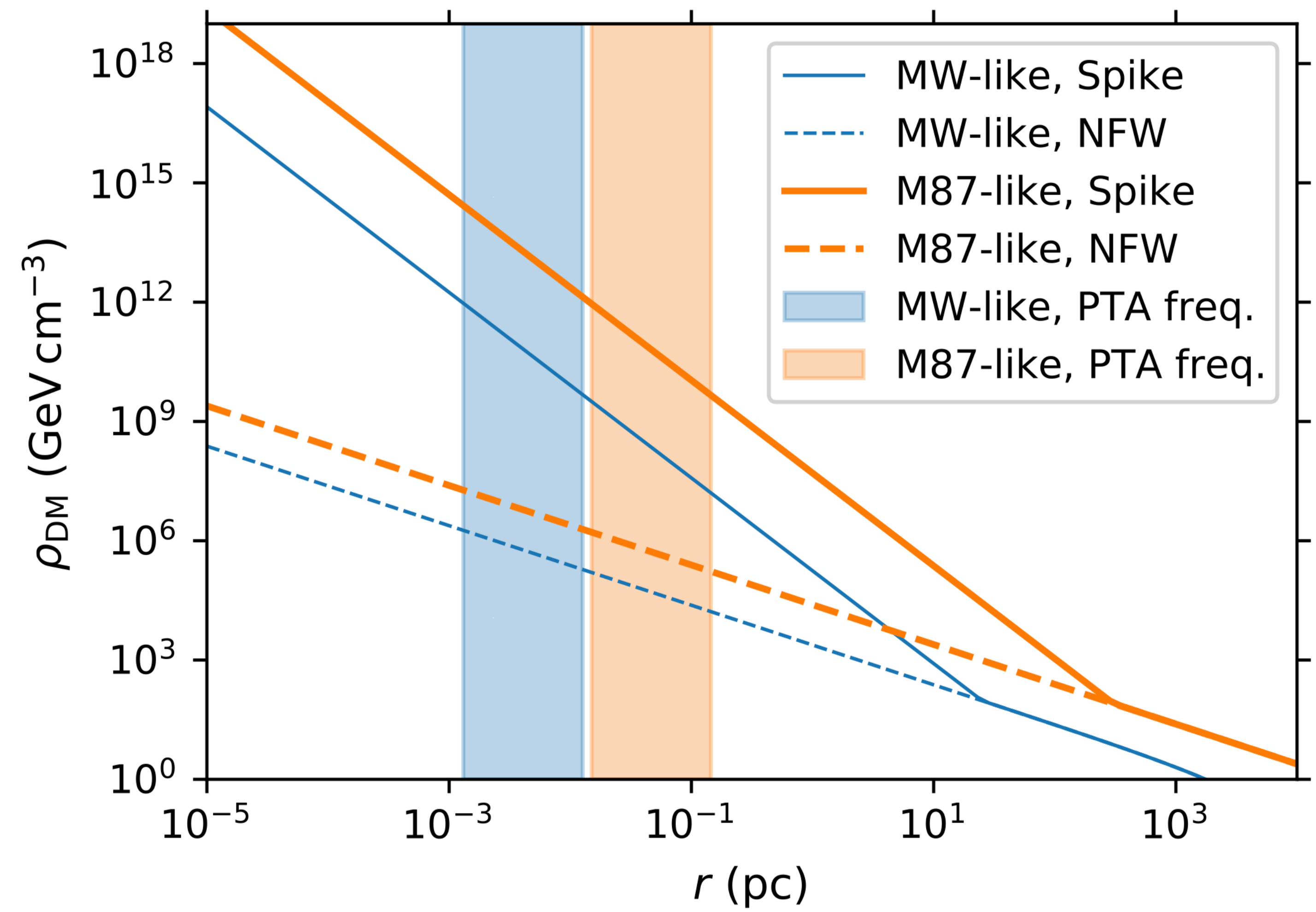

Braadly Kavanagh, et al, PRD(2020)

$$-\frac{\mathrm{d}E_{\rm orb}}{\mathrm{d}t}=\frac{\mathrm{d}E_{\rm GW}}{\mathrm{d}t}+\frac{\mathrm{d}E_{\rm env}}{\mathrm{d}t}$$

$$\rho(r)=\begin{cases}0 & r<R_{Sch}\\ \frac{\rho_{sp}(r)\rho_{\rm sat}}{\rho_{\rm sp}(r)+\rho_{\rm sat}} & R_{Sch}\le r<R_{\rm sp}\\ \frac{\rho_0}{(r/r_0)(1+r/r_0)^2} & r\ge R_{\rm sp}\end{cases}$$

$$\left|\tilde{h}_+(f)\right|=\frac{1}{2d_{\rm L}}\frac{4G\mu\omega_s^2(t)R^2(t)}{c^4}\sqrt{\frac{2\pi}{\ddot{\Phi}(t)}}\frac{1+\cos^2\iota}{2},$$

$$\left|\tilde{h}_\times(f)\right|=\frac{1}{2d_{\rm L}}\frac{4G\mu\omega_s^2(t)R^2(t)}{c^4}\sqrt{\frac{2\pi}{\ddot{\Phi}(t)}}\cos\iota,$$

$$\Omega_{\rm gw}(f)\equiv\frac{1}{\rho_{\rm c}}\frac{\mathrm{d}\rho_{\rm gw}(f)}{\mathrm{d}\ln f}=\frac{\pi}{4}\frac{f^2h_c^2(f)}{G\rho_{\rm c}}$$

$$\frac{\mathrm{d}E_{\rm gw}}{\mathrm{d}f_r}=\frac{2\pi^2c^3}{G}d_{\rm M}^2f^2\left\langle\left|\tilde{h}_+(f)\right|^2+\left|\tilde{h}_\times(f)\right|^2\right\rangle_{\Omega_s}=\frac{\pi}{3G}\frac{(G\mathscr{M})^{5/3}}{(\pi f_r)^{1/3}}\frac{\mathrm{d}E_{\rm gw}/\mathrm{d}t}{\mathrm{d}E_{\rm gw}/\mathrm{d}t+\mathrm{d}E_{\rm df}/\mathrm{d}t}$$

Dark Matter Surrounding SMBHB enhance SGWB

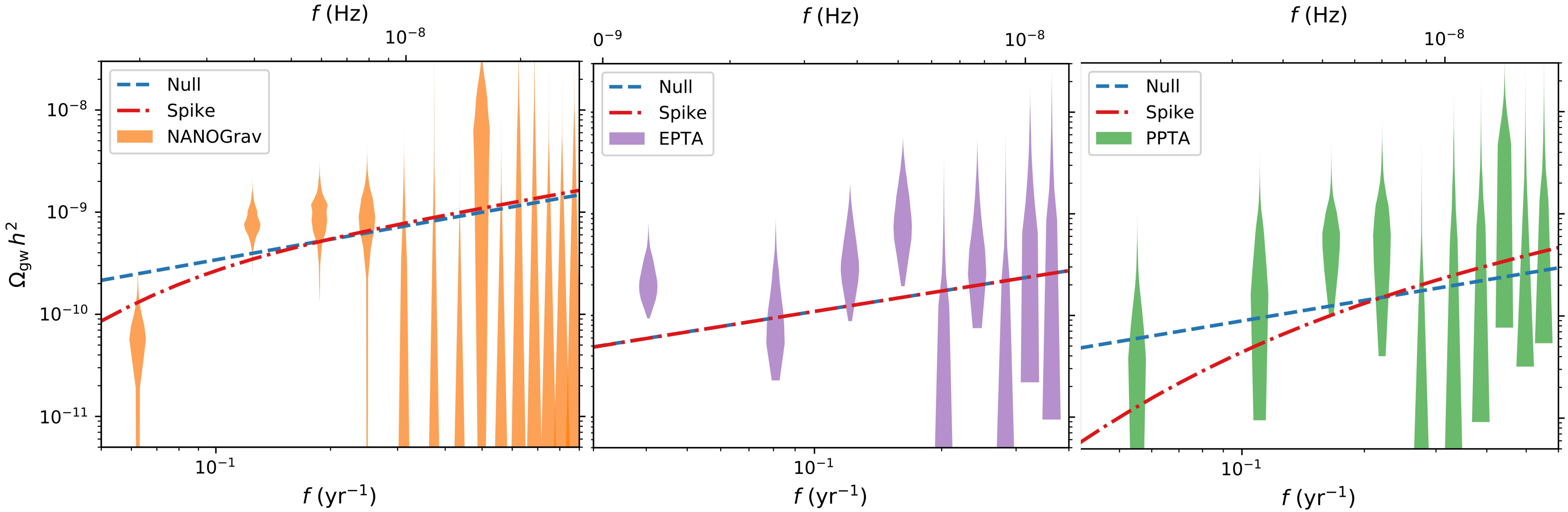

$$h_c^2(f) = \frac{4G}{\pi f c^2} \iiint \mathrm{d}z \mathrm{d}M_{\rm tot} \mathrm{d}\mu \, \frac{\mathrm{d}^2 n}{\mathrm{d}z \mathrm{d}\mathscr{M}} \, \frac{\mathrm{d}E_{\rm gw}(f; M_{\rm tot}, \mu, z)}{\mathrm{d}f_r}$$

$$\frac{\mathrm{d}^2 n}{\mathrm{d}z \ \mathrm{d}\lg \mathscr{M}} = \dot{n}_0 \left[\left(\frac{\mathscr{M}}{10^7 M_\odot} \right)^{-\alpha} e^{-\mathscr{M}/\mathscr{M}_*} e^{-z/z_0} \right] \times (1+z)^{\beta_z} \frac{\mathrm{d}t_R}{\mathrm{d}z}$$

Parameter	Prior	NANOGrav		EPTA		PPTA	
		Null	Spike	Null	Spike	Null	Spike
$\lg(\dot{n}_0/(\mathrm{Mpc}^{-3}\,\mathrm{Gyr}^{-1}))$	$\mathcal{U}(-13, 7)$	$-3.0^{+1.8}_{-3.8}$	$-4.3^{+2.7}_{-4.9}$	$-3.3^{+1.7}_{-3.4}$	$-5.0^{+2.6}_{-4.4}$	$-3.4^{+1.8}_{-3.5}$	$-3.6^{+2.1}_{-5.7}$
$\lg(\mathcal{M}_\star/M_\odot)$	$\mathcal{U}(6, 10)$	$8.0^{+1.4}_{-1.4}$	$8.5^{+1.0}_{-1.6}$	$7.9^{+1.4}_{-1.3}$	$8.4^{+1.0}_{-1.2}$	$7.9^{+1.4}_{-1.3}$	$7.9^{+1.3}_{-1.0}$
z_0	$\mathcal{U}(0.1, 4)$	$2.1^{+1.3}_{-1.3}$	$2.1^{+1.4}_{-1.6}$	$2.0^{+1.3}_{-1.3}$	$2.1^{+1.2}_{-1.3}$	$2.0^{+1.3}_{-1.3}$	$2.1^{+1.3}_{-1.2}$
α	$\mathcal{U}(-3, 3)$	$0.0^{+2.1}_{-1.9}$	$-1.4^{+2.2}_{-1.2}$	$0.2^{+1.9}_{-2.1}$	$-0.8^{+1.7}_{-1.5}$	$0.1^{+2.0}_{-2.0}$	$-0.2^{+1.9}_{-1.8}$
β_z	$\mathcal{U}(-2, 7)$	$2.5^{+3.1}_{-3.1}$	$3.2^{+2.1}_{-2.9}$	$2.5^{+3.0}_{-3.0}$	$3.4^{+2.6}_{-3.7}$	$2.5^{+3.0}_{-3.0}$	$2.5^{+2.7}_{-3.0}$
$\gamma_{\rm sp}$	$\mathcal{U}(0, 3)$	$\cdots$	$0.7^{+0.4}_{-0.4}$	$\cdots$	$0.5^{+0.4}_{-0.3}$	$\cdots$	$0.8^{+0.7}_{-0.5}$
$-2\ln\mathcal{L}$		-527.86	-532.11	-366.71	-366.72	-403.70	-405.01

Five popular model parameters $\{\dot{n}_0, \mathscr{M}_*, z_0, \alpha, \beta_z\}$, and dark matter spike model $\gamma_{\rm sp}$.

Zhao-Qiang Shen, *Guan-Wen Yuan**, et al, Dark Matter Spike surrounding Supermassive Black Holes Binary and the nanohertz Stochastic Gravaitational Wave Background, Phys.Dark Univ. 48 (2025), [arXiv: 2306.17143].

Future: The Evolution of Massive Black Hole Binaries

$$\rho(r) = \rho_{\rm inf}\left(\frac{r}{r_{\rm inf}}\right)^{-\gamma} \qquad r < r_{\rm inf}$$
$$\rho(r) = \frac{\sigma^2}{2\pi G r^2} \qquad r > r_{\rm inf}.$$

$$\frac{da}{dt} = \sum_i \frac{da}{dt}\Big|_i$$
$$\frac{de}{dt} = \sum_i \frac{de}{dt}\Big|_i,$$

Bound Cusp Erosion

$$\frac{da}{dt}\Big|_b = -\frac{2a^2}{GM_1M_2}\int_0^\infty \Delta\mathcal{E}\frac{d^2N_{\rm ej}}{da_*dt}da_*,$$

$$\frac{de}{dt}\Big|_b = \int_0^\infty \Delta e\frac{d^2N_{\rm ej}}{da_*dt}da_*.$$

Slingshot of Unbound Stars

$$\frac{da}{dt}\Big|_u = -\frac{a^2G\rho}{\sigma}H,$$

$$\frac{de}{dt}\Big|_u = \frac{aG\rho}{\sigma}HK.$$

Gravitational Wave Emission

$$\frac{da}{dt}\Big|_{\rm GW} = -\frac{64}{5}\frac{G^3}{c^5}\frac{M_1M_2M}{a^3(1-e^2)^{7/2}}\left(1+\frac{73}{24}e^2+\frac{37}{96}e^4\right)$$
$$= -\frac{64}{5}\frac{G^3}{c^5}\frac{M_1M_2M}{a^3}F(e)$$
$$\frac{de}{dt}\Big|_{\rm GW} = -\frac{304}{15}\frac{G^3}{c^5}\frac{M_1M_2M}{a^4(1-e^2)^{5/2}}e\left(1+\frac{121}{304}e^2\right)$$

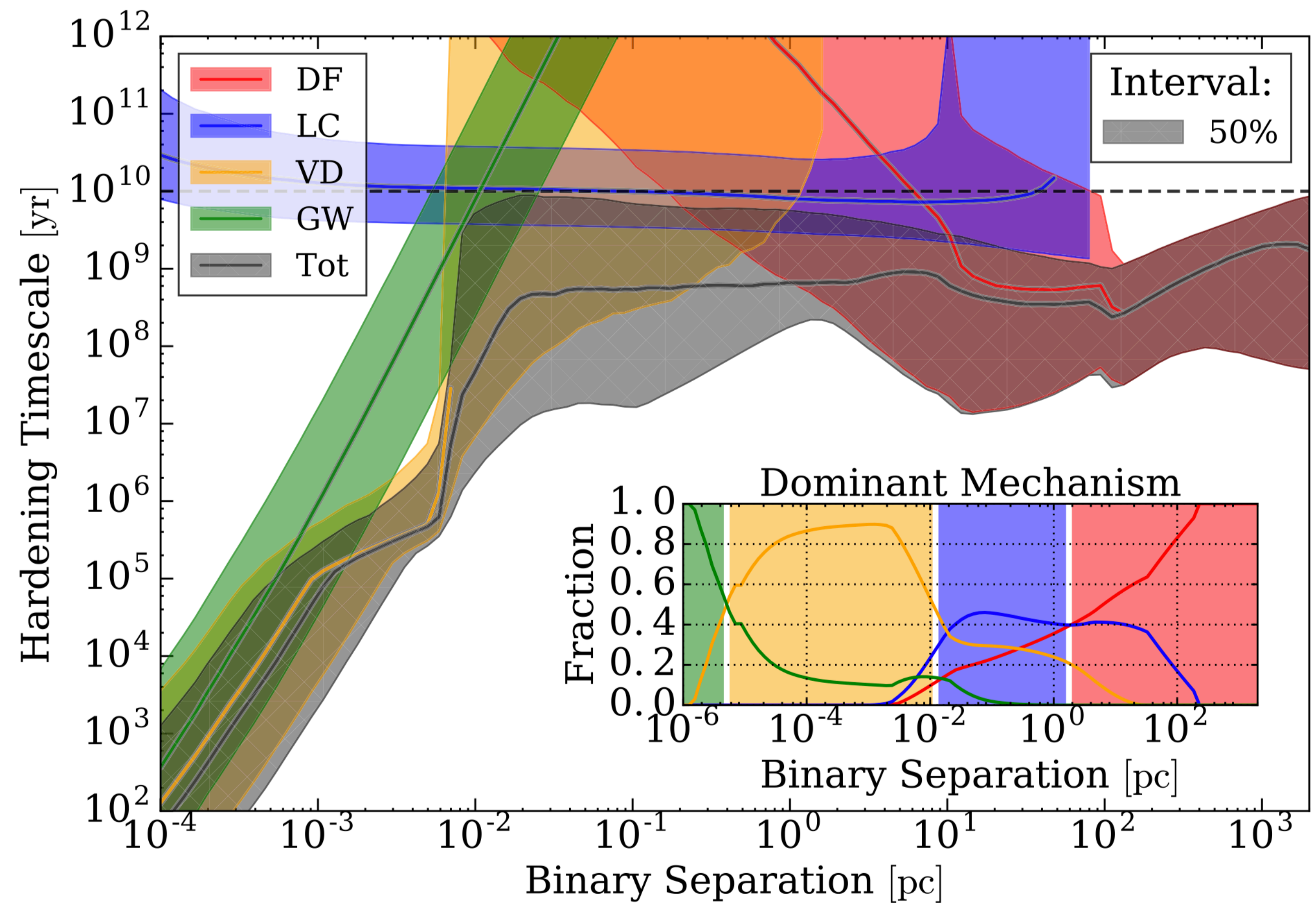

[1] Alberto Sesana, Self consistent model for the evolution of eccentric massive black hole binaries in stellar environments: implications for gravitational wave observations, ApJ(2010)

[2] Luke Kelley, Laura Blecha, Lars Hernquist, Massive black hole binary mergers in dynamical galactic environments, MNRAS(2017)

Summary

Combine two important things

Observations involved SMBH— EHT/GRAVITY(Keck)/JWST/PTA

Dark Matter Detection— WIMP/ALP/ULDM/PBH

Muti-messenger era
BH Physics
Formation&Evolution

Annihilation
Oscillation
Accretion
Density

Searching for the possible signals of DM candidates in the observations of SMBH

+

Analyze the phenomenological behavior of **different DM candidates** in **SMBH observations** by **Statistical Analysis**

Our findings can not only shed light on the role that dark matter played in the formation and evolution of SMBH, but they can also offer fresh physical motivation of future multi-messenger observations of SMBH.

Thanks for Your Attention!